

NASA CR-836

A GRAVITY INDEPENDENT
VAPOR ABSORPTION REFRIGERATOR

By J. R. Blutt and S. E. Sadek

Distribution of this report is provided in the interest of information exchange. Responsibility for the contents resides in the author or organization that prepared it.

Issued by Originator as Report No. 695

Prepared under Contract No. NASw-1372 by
DYNATECH CORPORATION
Cambridge, Mass.

for

NATIONAL AERONAUTICS AND SPACE ADMINISTRATION

For sale by the Clearinghouse for Federal Scientific and Technical Information
Springfield, Virginia 22151 - CFSTI price \$3.00

ABSTRACT

Vapor absorption refrigerator systems were designed to operate independent of gravity. The weights of these systems were determined and were found to be competitive with the weights of semi-passive and vapor compression systems of the same ratings.

A critical design evaluation of all major components was conducted in order to determine the feasibility of operating independent of gravity. Analog and/or model component tests were conducted to demonstrate the lack of dependence on gravity.

Two reference systems were designed. A portable thermal control system for cooling a spacesuit during extravehicular activities resulted in an 89-pound system with a total radiator area of 27 ft² for a 2500 Btu/hr. cooling capacity. The second reference design was a refrigerator for cooling a thermal radiation shield protecting cryogenic storage tanks. The system has 1 KW cooling capacity at -40°F and weighs 242 pounds.

TABLE OF CONTENTS

<u>Section</u>		<u>Page</u>
	ABSTRACT	iii
1	INTRODUCTION AND SUMMARY	1
2	CYCLE ANALYSIS AND FLUID SELECTION	8
	2.1 Introduction	8
	2.2 Sources of Inefficiency in the Absorption Refrigerator	12
	2.3 Operational Limits of an Absorption Refrigeration Cycle	12
	2.4 Cycle Analysis	15
	2.5 Heat Fluxes in an Absorption Refrigeration System	16
	2.6 Fluids Selection	18
3	CRITICAL COMPONENT DESIGNS	29
	3.1 Condenser	31
	3.2 Evaporator	34
	3.3 Absorber	37
	3.3.1 Electrohydrodynamic Absorber-Radiator	39
	3.3.2 Ejector Absorber-Radiator	41
	3.3.3 Conclusions	44
	3.4 Vapor Generator	44
	3.5 Liquid-Vapor Separator	45
	3.5.1 Electrohydrodynamic Separator	45
	3.5.2 Surface Tension Separator	48
	3.5.3 Vortex Separator	50
	3.5.4 Wick'Generator/Separator' Concept	50
	3.5.5 Conclusions	53
4	SYSTEMS COMPARISON	55
	4.1 Semi-Passive Thermal Control System	56
	4.2 Vapor Compression Refrigeration Systems	56
	4.3 Vapor Absorption Refrigeration Systems	56
	4.4 Comparison and Conclusions	61
5	REFERENCE SYSTEMS DESIGNS	68
	5.1 Radiator Shield Refrigerator	70
	5.2 Portable Thermal Control System	75

Table of Contents (continued)

<u>Section</u>		<u>Page</u>
6	CONCLUSIONS AND RECOMMENDATIONS	83
	REFERENCES	85
<u>Appendix</u>		
A		
	A.1 Cycle Analysis	87
	A.2 Penalties Caused by Solvent Carryover	91
B		
	B.1 Experimental Determination of Vapor-Liquid Equilibrium	94
	B.2 Viscosity	99
C	COMPONENT DESIGN AND WEIGHT ANALYSES	104
	C.1 Radiators	104
	C.2 Heat Exchangers	108
	C.3 Liquid/Vapor Separator	110
	C.4 Pumps and Compressors	110
	C.5 High Voltage Power Supply	111
	C.6 Power Weight Penalty	111
D	ANALYSIS AND TESTS OF AN ELECTROHYDRODYNAMIC LIQUID/VAPOR SEPARATOR	114
E	SEMI-PASSIVE SYSTEMS	124
F	VAPOR COMPRESSION SYSTEMS	127
G	WICK-TYPE LIQUID/VAPOR SEPARATOR	130
	G.1 Introduction	130
	G.2 Laboratory Demonstrations	131
	G.3 Failure Analysis	141
	G.4 Weight Analysis	146

LIST OF ILLUSTRATIONS

<u>Figure</u>		<u>Page</u>
1.1	Systems Weight Comparison (vs. Capacity)	5
1.2	Systems Weight Comparison (vs. Radiator Temperature)	6
2.1	Schematic - Ideal Refrigerator	9
2.2	Schematic - Vapor Absorption Refrigerator	9
2.3	Flow Diagram - Simple Vapor Absorption Cycle	11
2.4	Cycle Operation Limits	14
2.5	Flow Diagram - Improved Vapor Absorption Cycle	17
2.6	Component Heat Fluxes ($T_E = -40^\circ\text{F}$)	19
2.7	Component Heat Fluxes ($T_E = 40^\circ\text{F}$)	20
2.8	Flow Rates ($T_E = -40^\circ\text{F}$)	21
2.9	Flow Rates ($T_E = 40^\circ\text{F}$)	22
3.1	Condenser-Radiator	32
3.2	Radiator Weights	33
3.3	Twisted Tape Evaporator	35
3.4	Evaporator Weight	36
3.5	EHD Absorber-Radiator	38
3.6	Ejector Absorber-Radiator	43
3.7	Vapor Generator Weight	46
3.8	EHD Separator	47
3.9	Wick Separator	49
3.10	Wick Separator Weight	51
3.11	Vortex Separator	52
3.12	Wick Generator/Separator	54
4.1	Flow Diagram - Semi-Passive System	57
4.2	Semi-Passive System Weight	58
4.3	Flow Diagram - Vapor Compression Refrigerator	59
4.4	Vapor Compression System Weight	60
4.5	Two-Stage Vapor Absorption Cycle	62
4.6	Vapor Absorption Refrigerator Weight (vs. Capacity)	63
4.7	Vapor Absorption Refrigerator Weight (vs. Radiator Temperature)	64

List of Illustrations (continued)

<u>Figure</u>	<u>Page</u>
1.1	Systems Weight Comparison (vs. Capacity) 65
1.2	Systems Weight Comparison (vs. Radiator Temperature) 66
5.1	Generator Temperature Optimization (a and b) 71 & 72
5.2	Radiator Temperature Optimization (a and b) 73 & 74
5.3	Radiation Shield Refrigerator Operating Parameters 77
5.4	General Arrangement - Radiation Shield Refrigerator 78
5.5	Portable Thermal Control System Weight and Radiator Area 79
5.6	Portable Thermal Control System Operating Parameters 81
5.7	General Arrangement - Portable Thermal Control System 82
B.1	PTx Apparatus 95
B.2	Activity Coefficient Correlation - F22 + DME-TEG 98
B.3	Activity Coefficient Correlation - F21 + DME-TEG 100
B.4	Activity Coefficient Correlation - F21 + Chlorodecane 101
B.5	Viscosity of DME-TEG and TEG 102
C.1	Meteoroid Flux Distribution 107
C.2	Radiator Weights 109
	112
D.1	Separation Time - Linear E Device 119
D.2	Separation Time - Linear E ² Device 120
D.3	Analog Model of EHD Separator 121
D.4	Analog Separator Test Results 123
E.1	Semi-Passive System Weights (vs. Capacity) 125
E.2	Semi-Passive System Weights (vs. Radiator Temperature) 126
F.1	Vapor Compression System Weights (vs. Capacity) 128
F.2	Vapor Compression System Weights (vs. Radiator Temperature) 129
G.1	Wick Separator - Conceptual Design 132
G.2	Separator Model Schematic 133
G.3	Separator Model 134
G.4	Wick Assembly 135
G.5	Model Components 136

List of Illustrations (concluded)

<u>Figure</u>		<u>Page</u>
G.6	Experiment Flow Schematic	138
G.7	Experiment Apparatus (Front View)	139
G.8	Experiment Apparatus (Rear View)	140
G.9	Wick Separator Test Results	142
G.10	Failure Modes	144
G.11	Wick Separator Weight	148

LIST OF TABLES

<u>Table</u>		<u>Page</u>
1.1	Systems Weight Comparison	7
3.1	Component Types	30
5.1	Optimum Radiation Shield Refrigerator Design	75
5.2	Portable Thermal Control System Design	80
C.1	Component Selection	105

Section 1
INTRODUCTION AND SUMMARY

Every system, whether mechanical, electrical, or biological, operates best when it is maintained at a temperature within prescribed limits. In the environment of space the requirement for temperature control is complicated by the relative difficulty of rejecting heat.

Two methods are available for rejection of heat in space: (1) the evaporation or sublimation of a material to the vacuum of space; and (2) thermal radiation. When heat rejection requirements are small or mission durations short, evaporative systems requiring an expendable material or passive systems utilizing a low temperature radiator are adequate. As missions become more elaborate, however, active refrigeration techniques using higher temperature radiators are required.

A primary factor upon which competing systems for space missions are evaluated is the need to minimize system launch weight. The system weight here includes not only the weight of the refrigerator hardware and other directly related items, but also the weight of the power generation equipment and the fuel required to power the system. These additional weight considerations are called the "power weight penalty." In terms of power weight penalty, thermal power generally has the lowest relative weight penalty and rotating shaft power the highest weight penalty. In many missions the thermal power may result in no weight penalty; it may be waste heat from other, higher temperature systems.

The vapor absorption refrigeration system is driven primarily by thermal energy. The resulting savings in power weight penalty make such a refrigerator attractive for many space missions. The technology of vapor absorption refrigeration for land-based applications is highly developed. Vapor absorption systems are in common usage for applications ranging from home refrigerators to air conditioning plants for large buildings. The difficulty in adapting the present technology to the design of systems for space applications is that several of the system components, as presently designed, require the presence of a gravitational force for their proper operation. The primary purpose of this study, therefore, has

been to determine the feasibility of redesigning the vapor absorption refrigeration system to operate independent of gravity.

While this study has been directed primarily at the problems associated with zero or low-gravity applications of the vapor absorption refrigerator, the results of the study have a much wider significance. Many airborne and land-based refrigeration systems must meet equally stringent operating requirements of light-weight, low shaft power, and gravity independence. For example, helicopter and light-aircraft pilots may experience cabin temperatures up to 130°F and missions are aborted because of the heat. A lightweight refrigerator driven by waste heat from the engine would be immediately applicable. Another application is for a portable thermal control backpack unit which would provide cooling for a man wearing totally enclosed protective clothing.

The two examples given above are simply to indicate the immediate applicability of the information developed in this study to other unrelated problems. The number of such applications range from the cooling of army tanks, to combat refrigeration systems for food and medical supply storage, to refrigeration units for refrigerated trucks and railroad cars.

The tasks comprising this study have been:

a) Selection of compatible fluid pairs meeting the thermodynamic, thermo-physical, and safety requirements of the mission. The selection of fluid pairs having a non-volatile absorbent were considered necessary to permit elimination of the dephlegmator and rectifying column, which would be very difficult to design for zero gravity operation. A comprehensive literature and manufacturer search was followed by laboratory measurements of fluid properties not otherwise available. (See Section 2.6 and Appendix B.)

b) Analysis of the thermodynamic operating and performance parameters of vapor absorption systems using the selected fluid pairs. Computer calculation of the cycle parameters permitted evaluation of the relative effects of component inefficiencies and design compromises upon the performance and weight of the complete system. (See Section 2 and Appendix A.)

c) Conceptual design, analysis, and analog or functional testing of the most critical components, resulting in component weights characterized as a function of the operating parameters. (See Section 3 and Appendices C, D and G.)

d) Summation of the weights of representative vapor absorption refrigeration systems as a function of performance parameters and the comparison of these weights with the corresponding weights of competing thermal control methods such as semi-passive and vapor-compression systems. The comparison in this task is of a broad general nature with no specific mission restraints other than the cooling requirement and the operating environment (orbital or lunar). (See Section 4 and Appendices E and F.)

e) Preparation of optimized designs for two postulated reference missions. The two missions considered are: (1) A portable thermal control system for a spacesuit to be used by an astronaut during extra-vehicular activities; and (2) a system for refrigeration of thermal radiation shields protecting cryogenic storage tanks for long-duration space missions. (See Section 5.)

The results of the general system design and weight comparison are summarized in Figures 1.1 and 1.2 and in Table 1.1. In this comparison it is assumed that the heat required to drive the vapor generator is waste heat from other, high operating temperature systems on the mission vehicle. Therefore, no added weight penalty results from the generator heat requirement.*

As the figures indicate, the vapor absorption system is lighter than both the semi-passive and vapor compression systems. The weights of the semi-passive systems are large because of the relatively low radiator temperature. Better than 80% of the semi-passive system weight is attributable to the radiator for the system operating at its optimum radiator temperature.

For the vapor compression systems, the radiator weights are lower than

* The radiator normally used to reject the waste heat used by the generator could be reduced in size and this weight reduction credited to the absorption system. By not making this reduction, flexibility is introduced permitting shutdown of the refrigeration system without affecting the operation of the system providing the waste heat.

for the vapor absorption systems. However, the power for the vapor compression systems is required in the form of high-grade shaft power for which the power weight penalty is high. Over the operating region shown in the figures the power weight penalty for the vapor compression systems range from 35 to 90% of the total system weights.

A reference system design (worked example) for a low temperature radiation shield refrigerator, optimized on the basis of minimum system weight, resulted in a 242 lb system for 1 KW of cooling at -40°F evaporator temperature. The generated temperature is 250°F and the optimum condenser and absorber radiator temperatures are 56°F and 59°F , respectively.

A reference system design for a portable thermal conditioning unit for cooling of a spacesuit is a compromise design between minimization of system weight and minimization of radiator area. The resulting design is for an 89 lb system with a 2500 Btu/hr capacity at 40°F evaporator temperature. The total radiator area is 27 ft^2 (both sides) when operated at 110°F .

The analysis, design study, and laboratory tests of critical component elements have indicated the feasibility of operating a vapor absorption refrigeration system totally independent of gravity. A program to demonstrate the practical operation of a complete refrigeration system, including the study of such factors as control, off-design performance, load transients, and failure modes, should be pursued. Such a program should first demonstrate the operation of a bread-board refrigeration system capable of functioning in any orientation with respect to gravity. Such a demonstration would verify the predicted independence of gravity and would provide high confidence that the system will operate successfully in space.

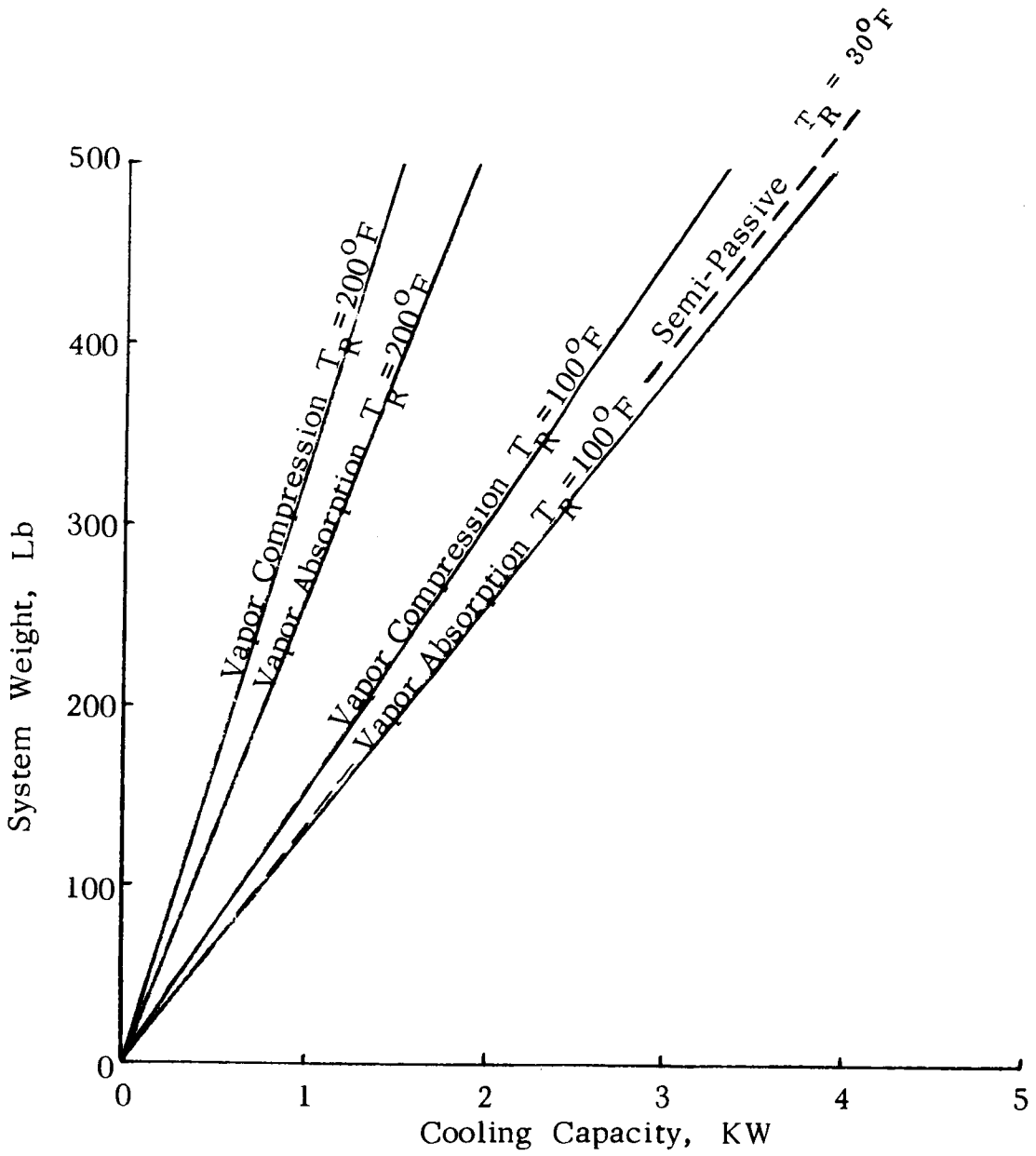


Figure 1.1 Thermal Control Systems Weight Comparison on the Basis of Cooling Capacity

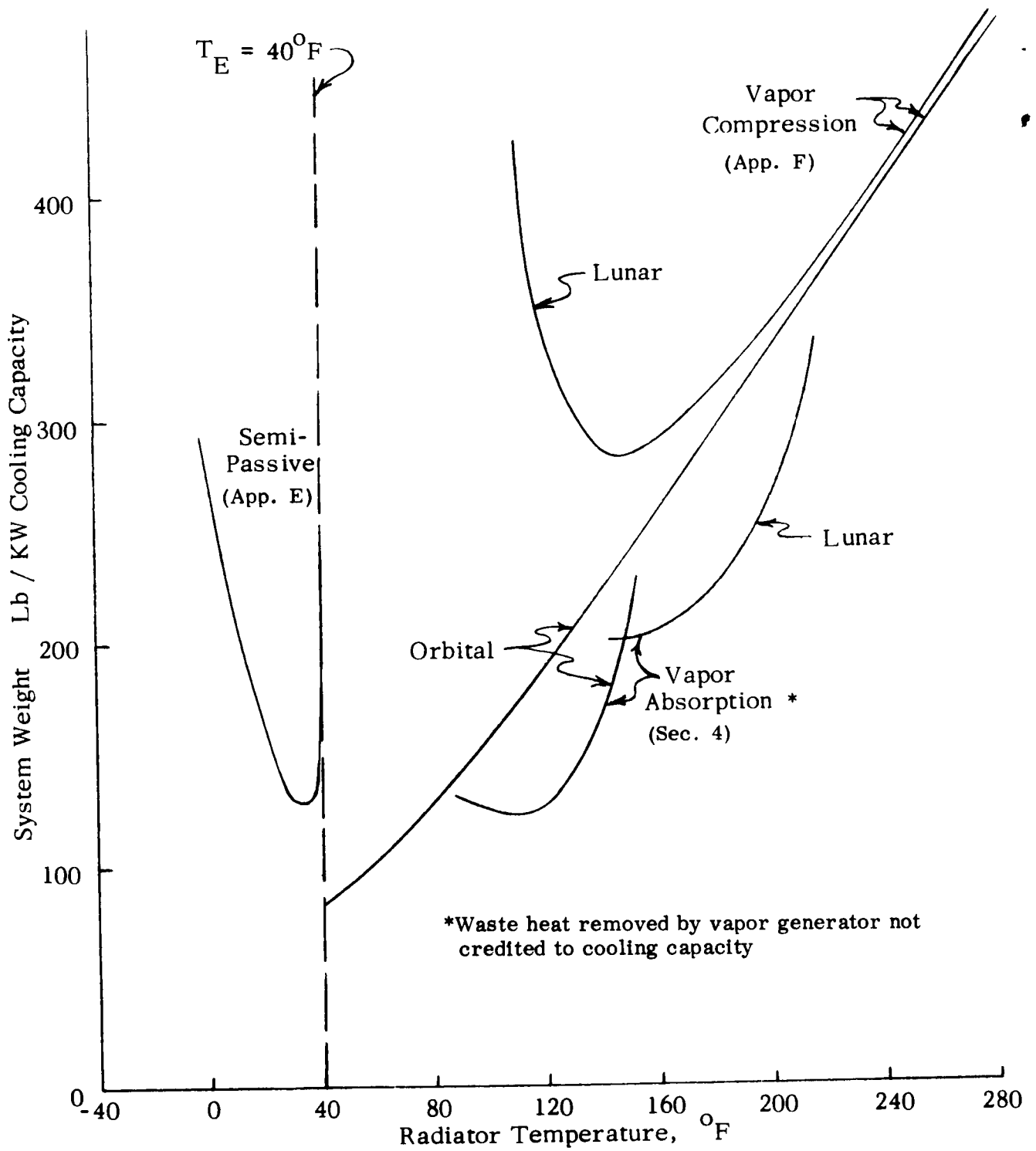


Figure 1.2 Thermal Control Systems Weight Comparison on the Basis of Radiator Temperature

Table 1.1

SYSTEMS WEIGHT COMPARISON*

System	Radiator Temperature	Radiator Weight	Power Penalty	System Weight
Semi-Passive	30° F	113 lb	13 lb	130 lb
Compression	100	44	105	160
Compression	200	25	280	325
Absorption**	100	82	8	125
Absorption**	200	130	28	270

*All systems compared on basis of a 40°F evaporator or load heat exchanger temperature.

**Vapor generator temperature of vapor absorption systems is 350°F

Section 2
CYCLE ANALYSIS AND FLUID SELECTION

2.1 Introduction

A refrigerator is a machine that transfers heat from a low temperature and rejects it at a higher temperature. In order to perform such an operation, work must be put into the system, usually in the form of shaft work (in the case of the vapor compression system). The relation between the minimum work requirement of the machine and the heat removed from the low-temperature body (the evaporator) is defined by the second law of thermodynamics. Ideally, in a reversible system, if a quantity of heat Q_1 is to be removed from a body at a temperature T_1 and rejected to a sink at a higher temperature T_2 , the condenser in Fig. 2.1, the second law of thermodynamics states that the minimum work required is given by:

$$W = Q_1 \left(\frac{T_2 - T_1}{T_1} \right) \quad 2.1$$

For ideal cycles, which are conceptually useful in analyzing the limits of a system's capability, the work necessary to remove a given quantity of heat from a fixed temperature T_1 and reject it at a higher temperature T_2 is always the same and is independent of the type of cycle used. Ideally, therefore, the type of cycle or working material (refrigerant) used in the system does not affect the work requirements of a refrigerator, provided that it is operated between the same temperature levels. In real systems, however, a number of effects raise the mechanical work requirement of the machine above the ideal minimum value as calculated by the second law of thermodynamics.

Just as work must be put into a system in order to transfer heat from a lower to a higher temperature, work may be recovered from the system by reversing the cycle and taking in heat at the higher temperature and rejecting it at the lower temperature. This is readily seen by reversing the arrows in Fig. 2.1.

A system which makes use of the availability of heat at a high temperature is the absorption refrigeration system (see Fig. 2.2). In this system, the refrigerator

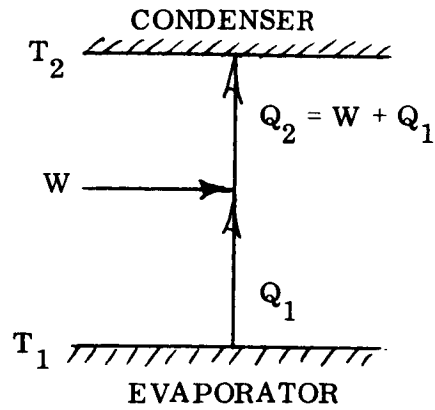


Fig. 2.1 Schematic--Ideal Refrigerator

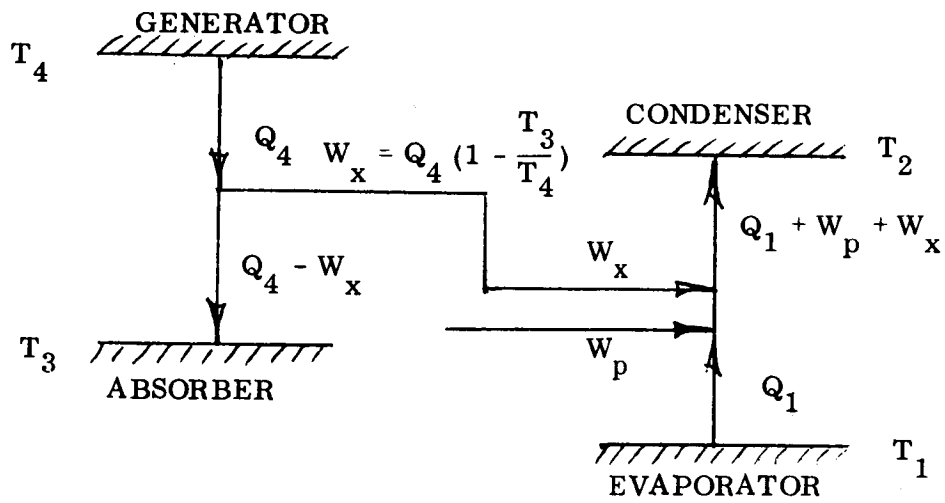


Fig. 2.2 Schematic--Vapor Absorption Refrigerator

transfers heat from a temperature T_1 and rejects it at T_2 . The evaporator-condenser section of the vapor absorption system is identical in performance to that of the refrigerator of Fig. 2.1. The total work requirement of the absorption refrigerator is therefore the same as that of the system shown in Fig. 2.1; that is,

$$W_x + W_p = W = Q_1 \left(\frac{T_2 - T_1}{T_1} \right). \quad 2.2$$

The generator-absorber section of the refrigerator, accepting heat at temperature T_4 and rejecting it at T_3 , contributes towards the total work required by the refrigerator an amount equal to:

$$W_x = Q_4 \left(\frac{T_4 - T_3}{T_4} \right). \quad 2.3$$

The independent shaft work ideally required by the absorption-refrigeration system is then equal to:

$$\begin{aligned} W_p &= W - W_x \\ &= Q_1 \left(\frac{T_2 - T_1}{T_1} \right) - Q_4 \left(\frac{T_4 - T_3}{T_4} \right). \end{aligned} \quad 2.4$$

It is interesting to point out that if the system were operated ideally, under certain conditions, one could operate this type of refrigerator while simultaneously obtaining work from the system. This would be true when the value of W_p given in Eq. 2.4 is negative. In the vapor absorption system, the work W_x is not actually converted into shaft power. This is avoided by using the same working fluid, the refrigerant, in both the condenser-evaporator and the generator-absorber sections of the system. The arrangement of the system is shown schematically in Fig. 2.3.

As indicated in Fig. 2.3, the pressures in the condenser and the generator are essentially equal as are the pressures in the evaporator and the absorber. A solvent is used in the absorber-generator section to enable the absorber to reject heat at a temperature which is higher than the evaporator temperature. The heat is released as the refrigerant vapor is absorbed.

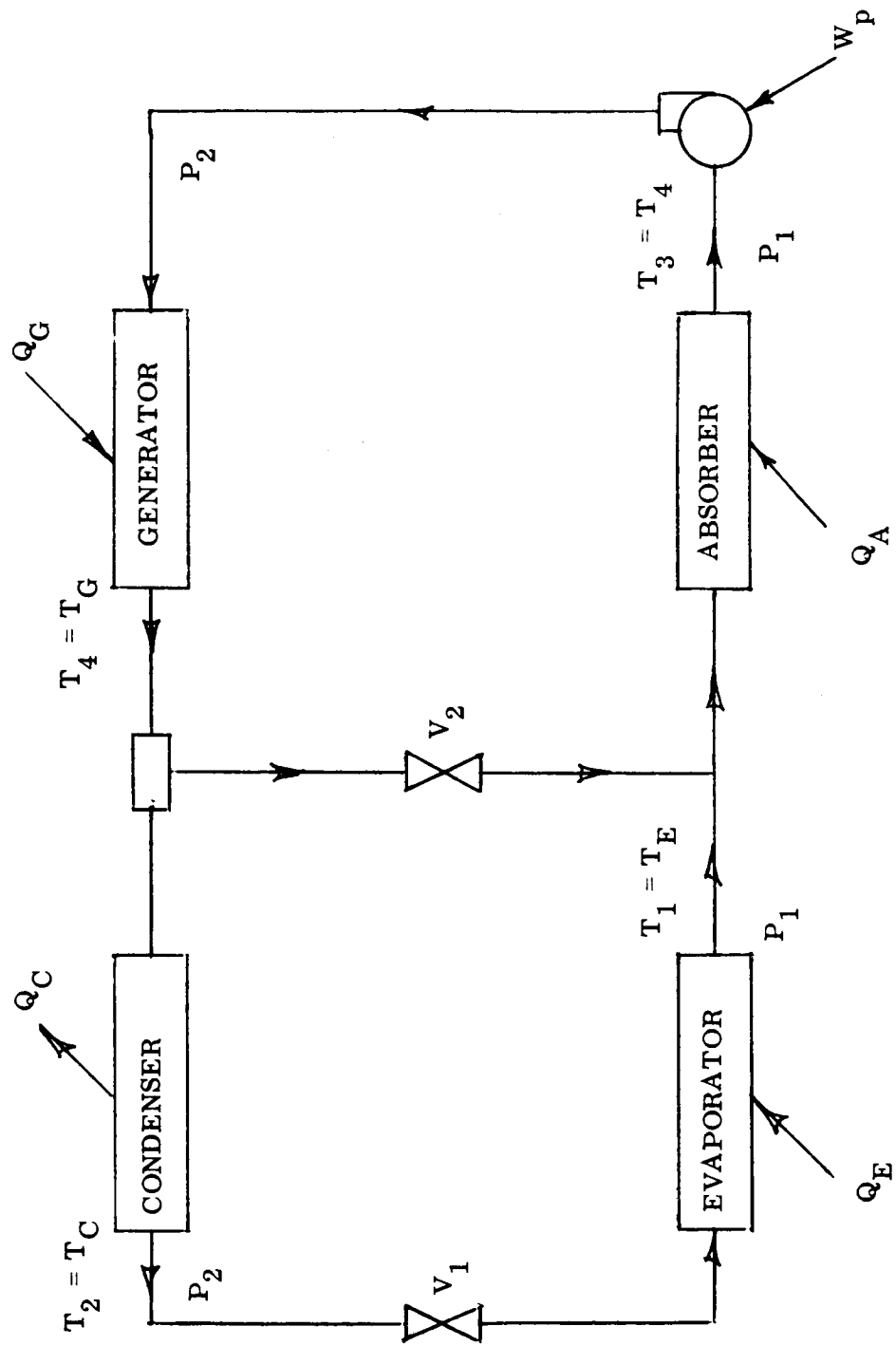


Fig. 2.3 Flow Diagram--Simple Vapor Absorption Cycle

2.2 Sources of Inefficiency in the Absorption Refrigerator

In the system shown in Fig. 2.3 , the use of the two throttle valves V_1 and V_2 are a source of inefficiency in the process since they degrade the energy with no useful work being recovered. As a result, the power consumption W_p of this system is considerably greater than the theoretical requirement W_p calculated from Eq. 2.4. In this case, the choice of the refrigerant will affect the actual power requirement, since different refrigerants have different vapor pressure-temperature relationships and hence have different values of pressure drops across the throttle valves.

The choice of the solvent in this case shall also affect the power requirement since the relative quantities of flow through the throttle valves shall depend on the solubility properties of the refrigerant in the solvent. If a large quantity of recycle has to be used, i. e. , a large flow through valve V_2 , then the work requirements shall be high. The solubility properties then affect directly the loss in available energy caused by the flow through the throttle valves.

Pressure drops due to the flow of the fluids through the pipes of the system also cause an increase in the power requirements of the system. The higher the fluid flow rates and the greater the fluid viscosities, the greater is the work necessary to overcome the friction.

In addition to the above hydrodynamic inefficiencies, there are thermal inefficiencies resulting from finite heat transfer coefficients which necessitate the use of finite temperature differences wherever heat has to be transferred.

The final net effect of all the inefficiencies in the system is to increase the power requirements above the theoretical value. The choice of the fluids to reduce these inefficiencies to their optimum values is discussed later for the case of an absorption-refrigeration system to be used in space or in lunar missions.

2.3 Operational Limits of an Absorption Refrigeration Cycle

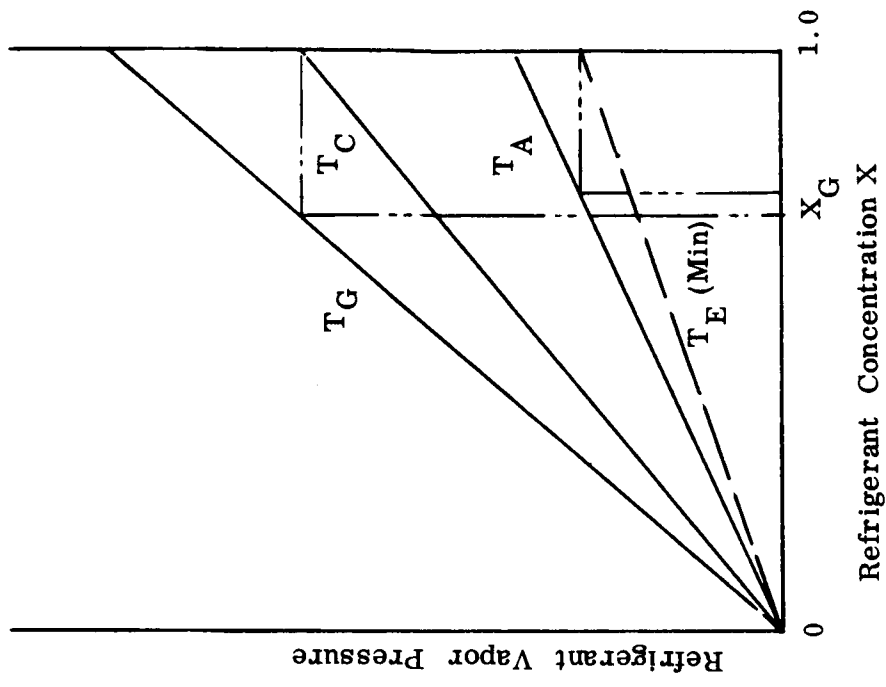
A thermodynamic limitation on the operating temperatures is set by circulating the same fluid pair through the evaporator-condenser and the

absorber-generator subsystems. This limitation defines a minimum (or maximum) operational temperature on one component whenever the other three component temperatures have been chosen. This is made clear on the P-T-x diagrams in Fig. 2.4.

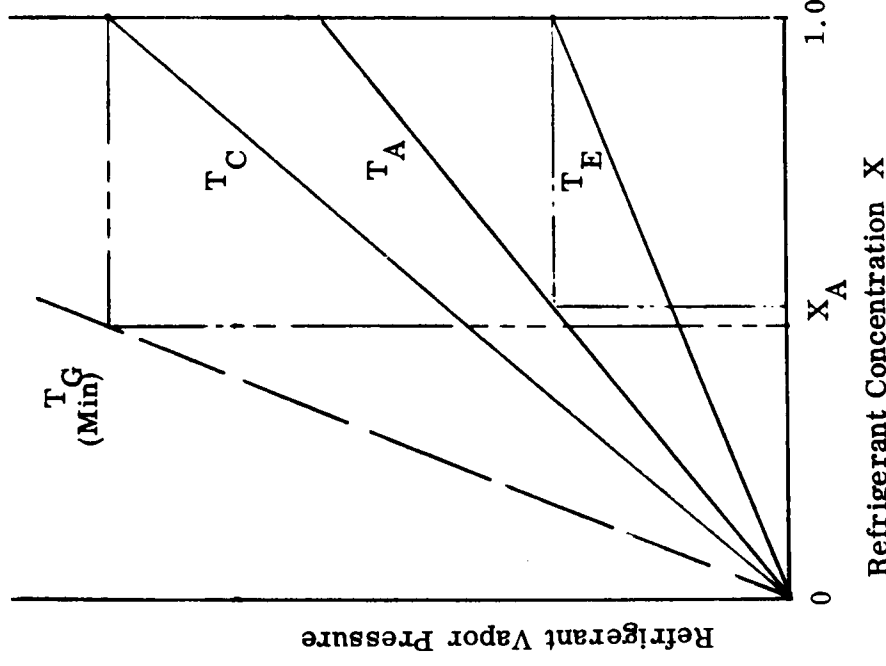
In Figs. 2.4a and 2.4b, the abscissa is the refrigerant concentration in the liquid, the ordinate is the equilibrium vapor pressure of refrigerant in equilibrium with the liquid at the component temperature. Take the case when the three temperatures (T_E , T_A and T_C have been fixed) (Fig. 2.4a). The pressure in the evaporator is therefore the vapor pressure of pure refrigerant at T_E . Since the pressure in the absorber is essentially that of the evaporator, the absorber pressure is therefore fixed. Now, since the absorber pressure and its temperature have been fixed, the concentration of the refrigerant in the liquid leaving the absorber is essentially fixed by the P-T-x relationship. When the condenser temperature T_C has been chosen, the pressure in the condenser, and in the generator is therefore set. In order for the system to operate, the refrigerant concentration in the liquid leaving the generator must be lower than that of the liquid leaving the absorber. In this case, then, there exists a minimum generator temperature below which the system cannot be operated as a refrigerator.

Taking the case when T_A , T_C and T_G have been chosen, a similar argument shows that a minimum evaporator temperature exists below which the system cannot be made to operate. When T_C and T_G are fixed, the concentration in the liquid leaving the generator is fixed. Since the concentration of refrigerant in the liquid leaving the absorber must be higher than that of the liquid leaving the generator, then, at the set absorber temperature, there exists a minimum pressure in the absorber below which the system cannot operate as a refrigerator. Since the absorber pressure is essentially that of the evaporator, there exists therefore a minimum evaporator temperature below which the system cannot be made to operate.

Similar reasoning sets a maximum limit on T_C when T_E , T_A and T_G are fixed and on T_A when T_E , T_C and T_G are fixed.



(a)



(b)

Fig. 2.4 Cycle Operating Limits

The limitation mentioned above makes it necessary in some cases to utilize staged absorption-refrigeration systems. In a lunar mission, for example, where radiator temperatures have to be high, it may not be possible to attain relatively low evaporator temperatures if the absorber and the condenser are designed to be radiators. In such a case for single-stage operation, very high generator temperatures are required. Generator temperatures are, however, limited by the chemical stability of the fluids and it may not be possible to operate a refrigerator under these conditions. A two-stage system, in which the absorber and condenser temperatures are maintained low by cooling them by means of a secondary absorption-refrigeration unit, avoids the necessity of having high generator temperatures. Generator temperatures considerably lower than a single stage may then be used in both stages. For example, to maintain an evaporator temperature of 40°F while using radiator temperatures of 200°F , a generator temperature of about $500 - 600^{\circ}\text{F}$ is required in a single stage. In two stages, a generator temperature of only, say 250°F may be used in the high temperature stage.

2.4 Cycle Analysis

A cycle analysis was based on mass and enthalpy balances on the system components. (See Appendix A.)

The enthalpy of the fluids at every point in the system is defined by the temperature and pressure at that point. (The temperature alone is sufficient to define thermodynamically a two-phase single-component system such as the evaporator and condenser fluids). Once the temperatures of the components have been chosen within the operational limits of the cycle, it is a simple matter to perform a simple cycle analysis. The temperatures of the evaporator and condenser set the lower and upper pressures of the system. These are also essentially the pressures in the absorber and the generator respectively. The compositions (and enthalpies) of the fluids in these two components can therefore be determined. The fluid flow rates and heat loads of the various components can then be calculated for any given refrigeration capacity.

A computer program (Appendix A) was developed to calculate the heat fluxes of a system such as that shown in Fig. 2.5 under different operating conditions. Implicit in the program are a number of thermodynamic assumptions which are explained below:

1. Frictional pressure drops are negligible compared to the pressure difference between the condenser and the evaporator.
2. Mass transfer resistances in the absorber and in the generator were taken into account by means of an efficiency assigned to the performance of each of these components. These efficiencies are a function of the design of the component.
3. The effect of pressure on the enthalpy of the absorber-refrigerant solution is negligible.
4. Heats of solution of refrigerant vapor in absorbent are equal to the latent heat of vaporization. This was found to be true within about 10 per cent for the systems of interest.
5. No solvent is carried into the condenser. Vaporization or entrainment of solvent causes a degradation in the cycle performance (Appendix A).

2.5 Heat Fluxes in an Absorption Refrigeration System

Heat fluxes (per KW cooling capacity) were calculated for various component temperatures. As an example to show the expected trends, two evaporator temperatures were used: one ($T_E = 40^{\circ}\text{F}$) represents the requirement for thermal control of a spacesuit for extravehicular missions; the other ($T_E = -40^{\circ}\text{F}$) represents a cooling system for cryogenic tank thermal radiation shields.

The calculations were made based on the flow diagram shown in Fig. 2.5 . The fluid properties used in the calculations were those of F-22 as refrigerant and DME-TEG as solvent. (See section on Fluids Selection.)

In this system, the heat from the liquid leaving the generator is recuperated before introducing it into the absorber. This was accomplished by flowing this liquid in a heat exchanger (the recuperator) against the cooler liquid leaving the absorber. In the particular examples taken here, the temperature of the weak

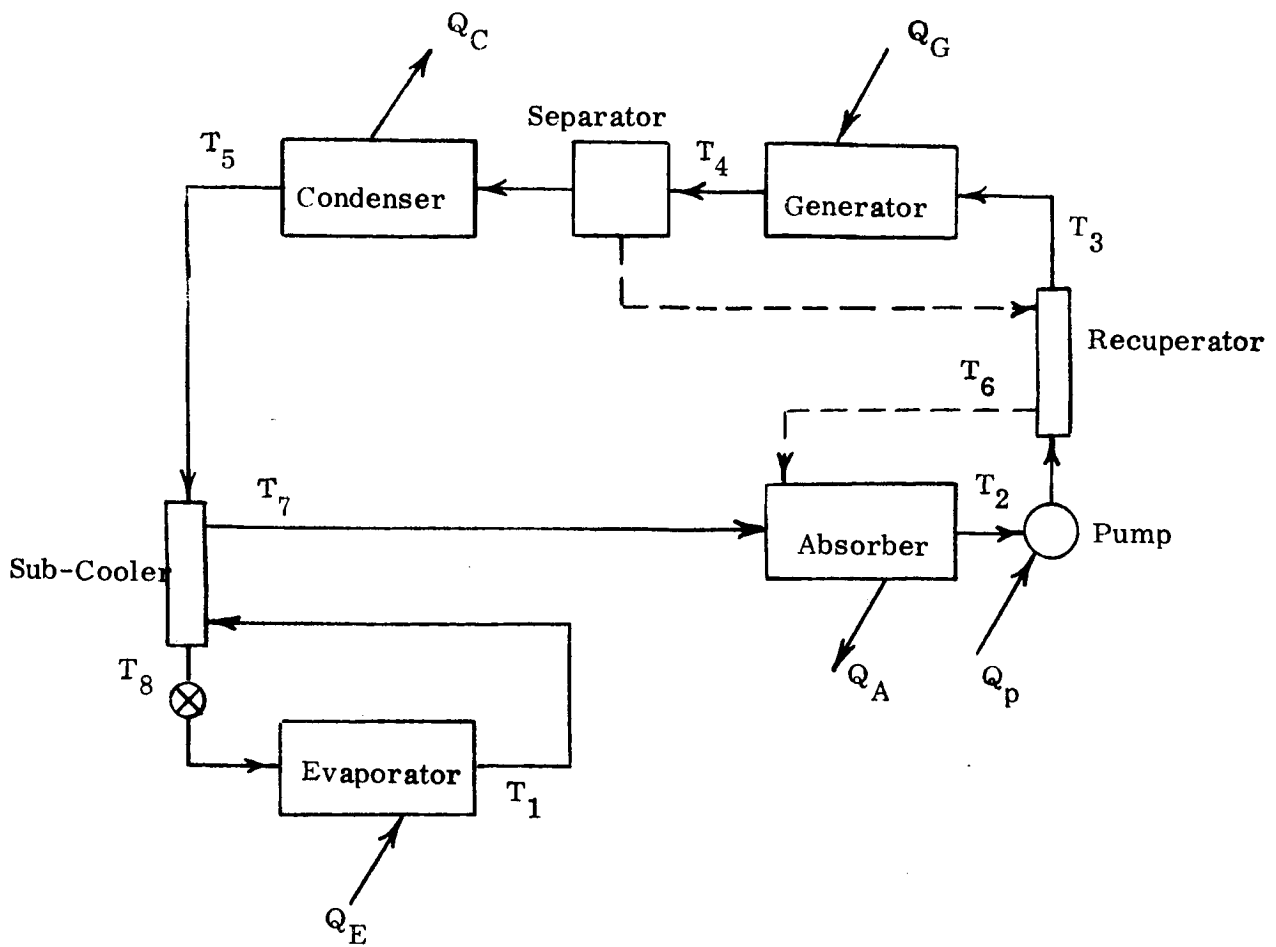


Fig. 2.5 Flow Diagram--Improved Vapor Absorption Cycle

solution leaving the recuperator was assumed to be 5°F higher than the temperature of the strong solution leaving the absorber.

Based on later calculations which showed that the refrigerator weight was lowest under these conditions, the condenser and absorber temperatures (radiator temperatures), were taken to be equal. The calculated results plotted in Figs. 2.6 through 2.9 are therefore for the cases when $T_A = T_C$.

These results show that at fixed evaporator and generator temperatures, the heat fluxes through the absorber, generator and recuperator are greater at the higher radiator temperatures. This increase is a result of the higher fluid flow rates through these components (Figs. 2.8 and 2.9). This, in turn, is caused by the rapid decrease in refrigerant concentration of the weak solution, which necessitates large rates of fluid recirculation between the absorber and generator.

Fluxes through the recuperator are considerably larger at the higher generator temperatures (Fig. 2.6). The recuperator therefore performs the important function of reducing the amount of heat rejected through the absorber. It thus allows a considerable saving in system weight since the absorber is one of the heaviest components in the system.

The flux through the condenser is reduced slightly as the condenser temperature is raised. This is due to the smaller change in enthalpy of the refrigerant as the condenser and generator temperatures approach one another.

Finally, note that the pump power requirements for the vapor absorption system are very low within a wide range of operating temperatures, in spite of the fact that a relatively high vapor-pressure refrigerant (F-22) was used in the calculation of the performance.

2.6 Fluids Selection

The criterion for designing a piece of equipment for use in space is to minimize the system launch weight. A refrigerator to be used in space or for

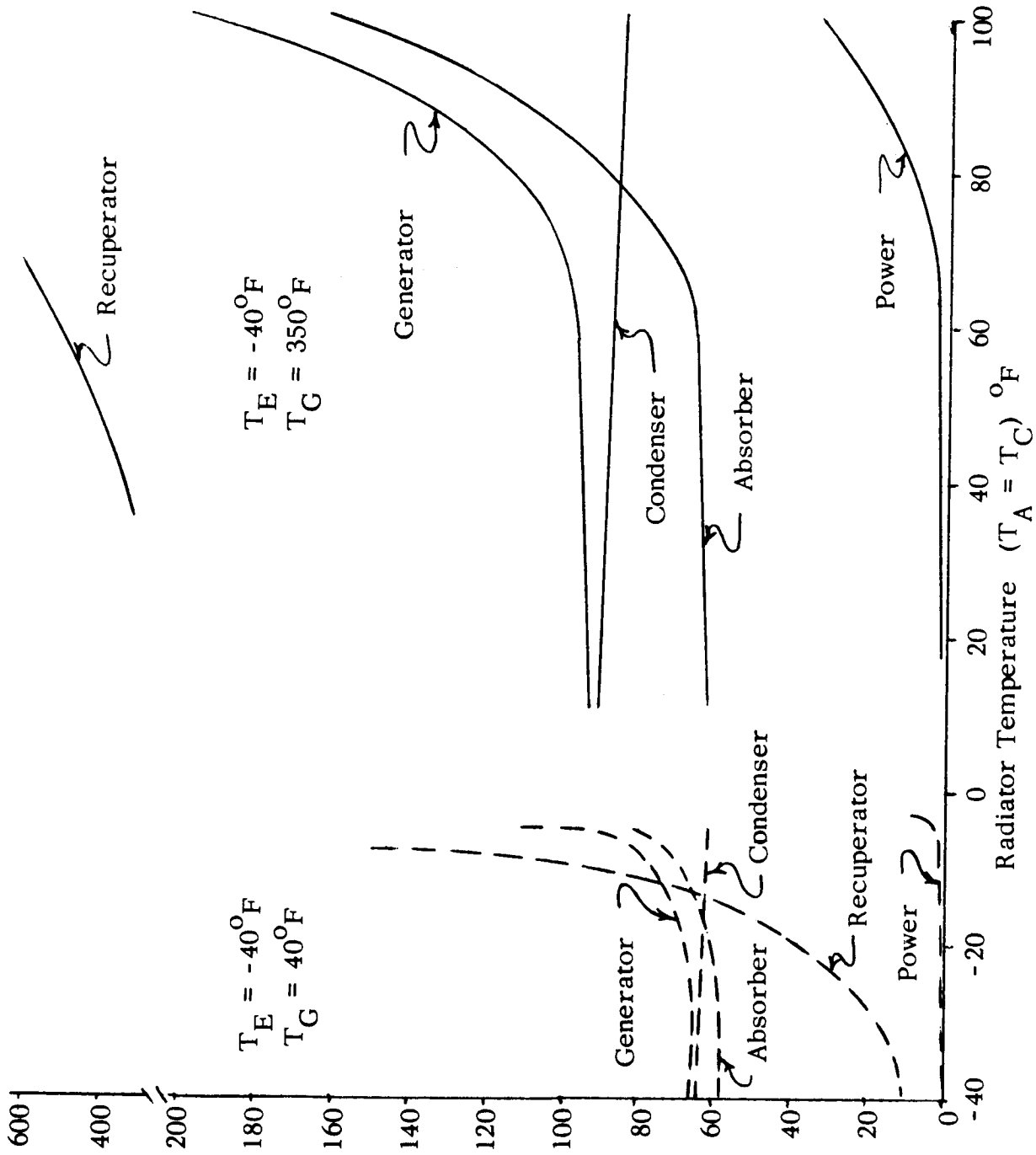


Figure 2.6 Component Heat Fluxes ($T_E = -40^\circ\text{F}$)

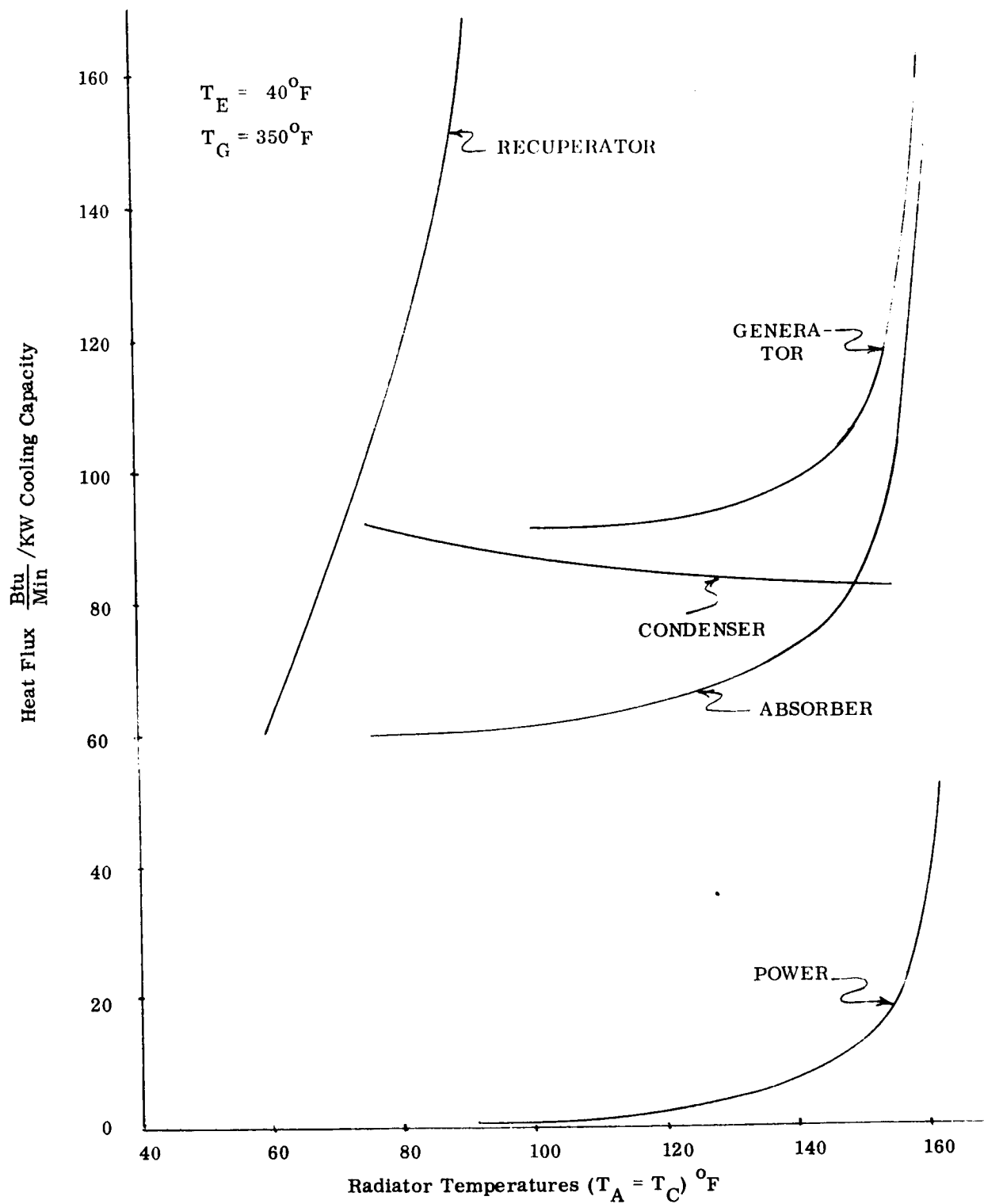


Fig. 2.7 Component Heat Fluxes ($T_E = 40^\circ\text{F}$)

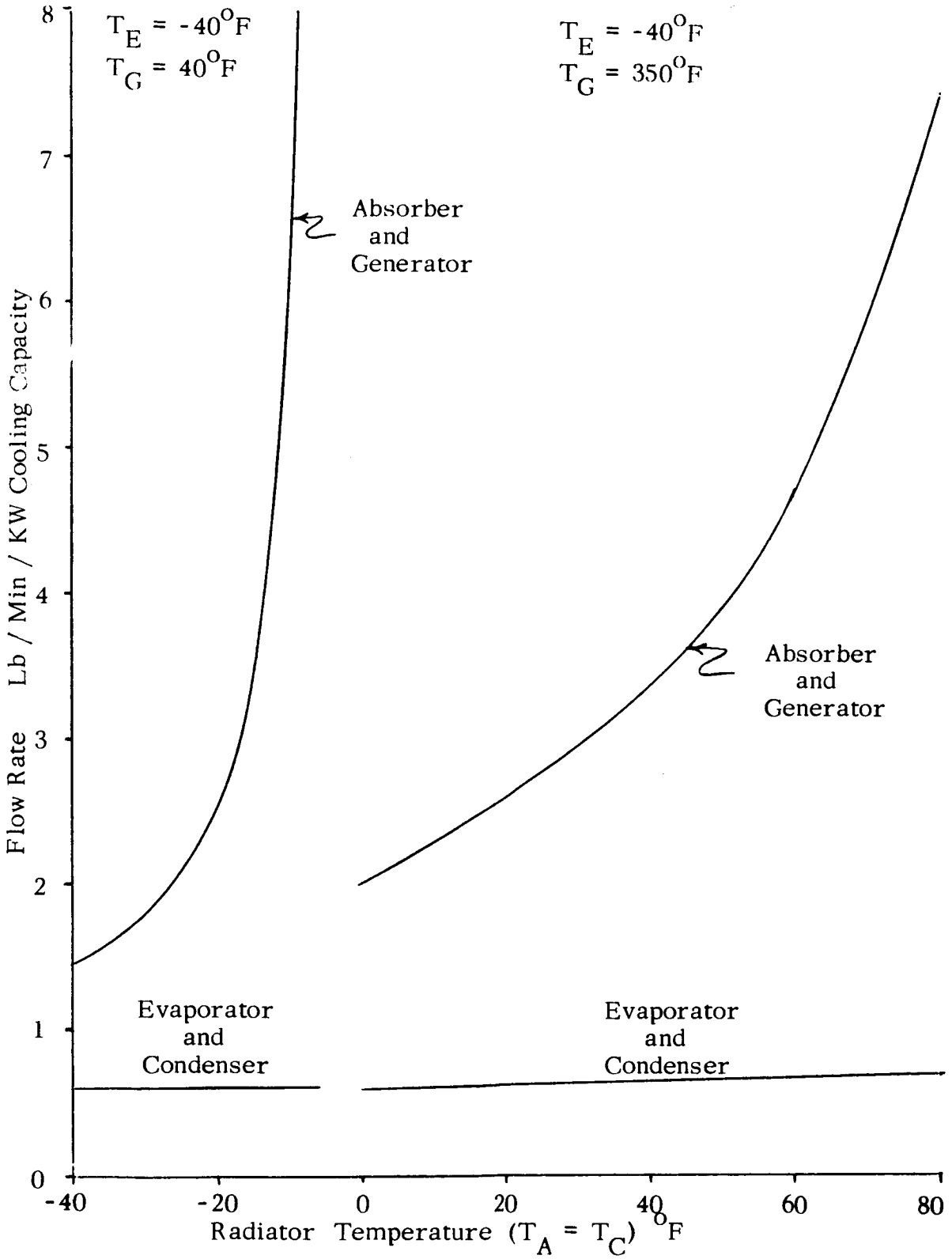


Figure 2.8 Flow Rates ($T_E = -40^\circ\text{F}$)

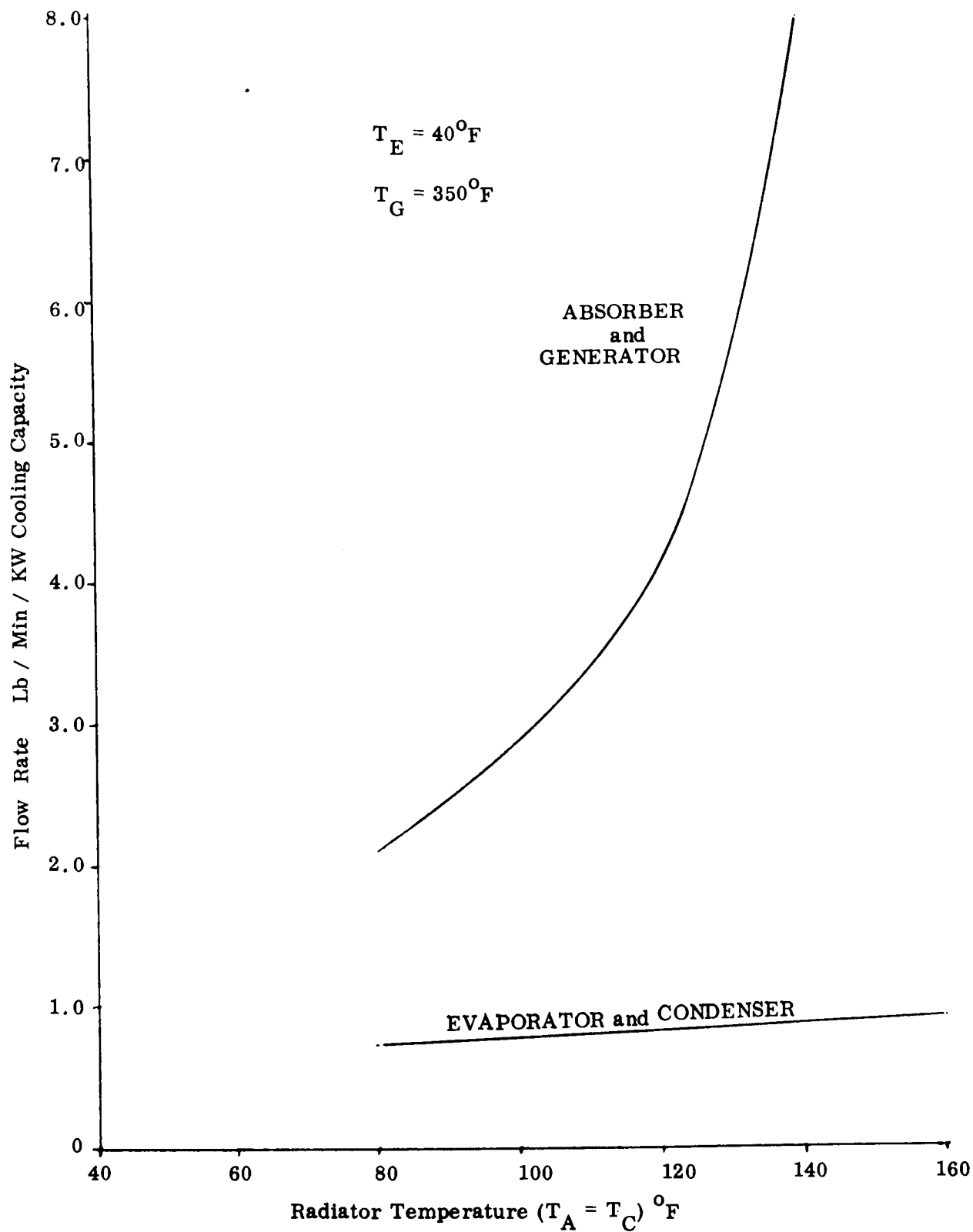


Fig. 2.9 Flow Rates ($T_E = 40^\circ\text{F}$)

lunar missions, therefore, has to be designed such that its total weight, including the weight penalties associated with the energy requirements is minimized. Since weight penalties for power requirements are high--and generally increase with the length of the mission--and since waste heat at a relatively high temperature is normally available from other systems on the mission vehicle, the absorption refrigeration system, which can make use of this waste heat, is an attractive system for temperature control in space missions.

An accurate estimate of the minimum weight of a system can be made only after completing an extensive cycle analysis and a detailed weight analysis of the components. By repeating the cycle and weight analyses for a number of refrigerant-absorbent pairs, the best pair can be selected; that is, the pair yielding the lowest total system weight without sacrificing safety and reliability of operation.

A number of requirements for a refrigerant-absorbent pair limit the fluid search considerably. In addition to having suitable thermodynamic properties that would yield a low refrigerator weight, a number of operational and safety requirements must be fulfilled.

1. The fluids must have a low toxicity and present no explosion hazard with air or oxygen.
2. They must be reasonably stable from the chemical standpoint so that decomposition would not occur during the lifetime of the equipment.
3. The fluids and their decomposition products, if any, must be non-corrosive towards the materials of construction in the system.
4. The fluids should be selected to permit augmentation of the component operations independent of gravity. (For example, for electrohydrodynamic (EHD) augmented operation, fluids having a high dielectric constant, a high resistivity, and a high dielectric strength are required.)
5. The absorbent should have a low viscosity to minimize frictional losses.
6. The absorbent should have a low vapor pressure at the generator temperature to permit effective component separation in the evaporator without the need of an elaborate rectifying system.

It is clear that some compromise between the fulfillment of all the above requirements is necessary for the proper optimum choice of a refrigerant-solvent pair. The limits and safety factors set for each of the above requirements are therefore a reflection of the importance attached to it.

The requirement for low toxicity and lack of explosion hazard rule out the lower alcohols, ethers, ketones, amines and hydrocarbons as refrigerants. In addition, the conductivities of the first four classes are relatively high and it would, therefore, be undesirable to use them in EHD systems.

The halogenated hydrocarbons offer a wide range of properties and appeared to be the most promising group of compounds for use as refrigerants. They are non-flammable, many are chemically stable with low toxicity and all have low electrical conductivities.

In addition to being a good solvent of the refrigerant, the absorbent must have a low vapor pressure to allow easy separation of the refrigerant. Tetraethylene glycol (TEG), the dimethyl ether of tetraethylene glycol (DME-TEG), and heavy (low vapor pressure) hydrocarbons have the required characteristics. The electrical conductivity of the oils are lower than that of TEG or of DME-TEG, and in an EHD system, may be preferable.

The final choice of a refrigerant-solvent pair from among those satisfying the criteria mentioned above depends on the weight of the resulting refrigeration system. The objective of this part of the study was to determine which pair yields the lowest weight for a given set of conditions.

At this point, it should be made clear that the pair which yields the lowest weight for a given set of operating conditions (component temperatures) is not necessarily the one that would yield the lowest weight for all possible sets of conditions, and one should be wary of any such extrapolation.

In general, under a given set of operating conditions (component temperatures), the weights of all components are directly proportional to the energy transferred in them. For a given refrigeration load, the weights of the pump (and pump power penalty), the absorber, generator, recuperator, and condenser are therefore

dependent on the fluid flow rates through them. Frictional pressure drops are also dependent on fluid flow rates, and it is therefore advantageous to use a fluid pair that tends to minimize the flow rates through the various parts of the system. This can best be achieved by choosing fluids with the following properties:

1. A refrigerant with a high latent heat of vaporization at the evaporator temperature.
2. A refrigerant-solvent system which exhibits negative non-ideality from Raoult's Law. This allows a larger concentration difference between the generator and absorber solutions than would exist with an ideal solution. Solvent recirculation is therefore reduced.
3. A solvent with a low vapor pressure. This allows a clean separation between refrigerant vapor and generator solution.
4. A solvent with a relatively low molecular weight. Mass flow rates of solvent are thus reduced.

Note that pump power requirements were found to be generally very low under a wide range of operating conditions (Figs. 2.6 and 2.7). Pump weight and power penalty are therefore only a small fraction of the total system weight. The selection of a fluid pair therefore primarily depends on the safety and reliability of the fluid system. The fluids selected should, naturally, also be amenable to the vapor-liquid separation scheme to be used.

A number of possible fluids meeting the requirements of the absorption-refrigeration system were investigated. As mentioned earlier, the ultimate choice of fluids depends on the required operating conditions; and a number of promising refrigerants and solvents are briefly discussed below.

Refrigerants^(1, 2)

1. F-22

Advantages

- i) high latent heat of vaporization (= 100.45 Btu/lb at normal boiling point)
- ii) low toxicity (Group 5a in U.L. Classification)
- iii) good chemical stability (maximum temperature for continuous exposure in the presence of oil, steel and copper = 275 - 300°F for continuous periods of operation of about one year).

- iv) very low hydrolysis rate (0.1 gm/liter of water/year in the presence of steel at 86°F and 1 atm.)
- v) good electrical properties
- vi) has relatively high solubility in DME - TEG

Disadvantages

- i) has a relatively high vapor pressure (83 psia at 40°F)

2. F-21

Advantages

- i) high latent heat of vaporization (= 104.15 Btu/lb at normal boiling point)
- ii) good electrical properties
- iii) low vapor pressure (12.2 psia at 40°F)
- iv) is highly soluble in the solvent DME - TEG

Disadvantages

- i) relatively high rate of decomposition (Ref. 1)
- ii) somewhat more toxic than Group 5 of the U. L. Classification, but much less toxic than Group 4

3. F-40

Advantages

- i) high latent heat of vaporization (175 Btu/lb approx. at 32°F)
- ii) electrical properties good
- iii) vapor pressure relatively low

Disadvantages

- i) high toxicity (Group 4 of the U. L. Classification)
- ii) F-40 in DME-TEG exhibits a relatively low negative deviation from Raoult's Law (Appendix B)

4. F-113

Advantages

- i) low vapor pressure (2.6 psia at 40°F)
- ii) good electrical properties

Disadvantages

- i) relatively low latent heat of vaporization
- ii) non-ideality is not exhibited in solution with DME-TEG
- iii) somewhat more toxic than Group 5 of the U. L. Classification, but much less toxic than Group 4

5. Ammonia

Advantages

- i) high latent heat of vaporization
- ii) highly soluble in TEG⁽³⁾

Disadvantages

- i) high toxicity
- ii) highly flammable
- iii) high vapor pressure
- iv) high electrical conductivity

6. Water

Advantages

- i) high latent heat of vaporization
- ii) exhibits large negative deviations from Raoult's Law with many solvents
- iii) non-toxic and non-hazardous
- iv) chemically stable
- v) low viscosity
- vi) low vapor pressure

Disadvantages

- i) relatively high triple point (32.0^oF) (possibility of freezing in condenser under standby operation)
- ii) high electrical conductivity

Solvents

1. DME-TEG⁽¹⁾

Advantages

- i) good solvent for most Freons
- ii) low viscosity

- iii) low vapor pressure; high boiling point
- iv) relatively low molecular weight
- v) high dielectric constant

Disadvantages

- i) relatively high electrical conductivity

2. TEG

Advantages

- i) good solvent for most Freons and ammonia
- ii) low vapor pressure; high boiling point
- iii) low molecular weight
- iv) high dielectric constant

Disadvantages

- i) relatively high viscosity (Appendix B)
- ii) relatively high electrical conductivity

3. Paraffinic Petroleum Oils and Chloroparaffins

Advantages

- i) the higher homologues of the series have low vapor pressure
- ii) high dielectric constant; low electrical conductivity

Disadvantages

- i) the higher homologues have high molecular weight
- ii) the higher homologues have a high viscosity

The fluid pair F-22 and DME-TEG was judged to be the most suitable system to use whenever power penalties are relatively low or whenever the range of operating conditions is such that power consumption is small. Under all the practical conditions investigated with the F-22 and DME-TEG system, power consumption and power penalties (using a solar cell) were very small. No justification then exists for using a lower vapor-pressure refrigerant.

Section 3

CRITICAL COMPONENT DESIGNS

The critical components of a vapor absorption refrigerator for low-gravity applications are the condenser, evaporator, absorber, vapor generator, and liquid vapor separator (see Fig. 2.5). Two-phase flow occurs in each of these components. It is difficult to predict the behavior of two-phase flow under normal circumstances. Even less is known about two-phase flow in zero g. In order to design components that will perform reliably in two-phase flow under zero gravity conditions, it is necessary to be able to control the flow.

Three mechanisms for controlling the two-phase flow that are of particular interest are inertial forces, electrical forces, and surface tension forces. For each of the critical components mentioned, devices can be envisioned which could use any one or combinations of these flow control mechanisms. The selection of the best design for each component ultimately is based upon minimizing the weight and maximizing the reliability and ease of operation of the total refrigeration system.

Table 3.1 summarizes the types of devices which could result by using each of the three flow-control mechanisms in each of the critical components.

In all of these components except the liquid vapor separator, in addition to the fluid flow requirements, there are also heat transfer requirements. In the condenser and the absorber heat is rejected, and in the evaporator and vapor generator heat is added. There must therefore be a radiator associated with both the condenser and the absorber and a heat source associated with both the evaporator and vapor generator. In each case there is the problem of transferring the heat between the component and its respective radiator or heat source.

Normally this heat transfer is accomplished by circulating a heat transfer fluid between the component and the radiator or heat source. There is an obvious advantage and a significant savings in weight when these components are integrated directly with their respective radiator or heat source. In the descriptions of the component designs given in the following sections, it is assumed that this integration is made whenever possible.

Table 3.1
COMPONENT TYPES

Component	Augmentation Mechanism			
	Inertia	Surface Tension	Electric	
Condenser	Spiral Condenser	Tapered or Capillary Tube	Concentric Cylindrical Electrodes	(AC mode)
Evaporator	Twisted Tape	Wick-Lined Tube	Concentric Cylindrical Electrodes	(AC mode)
Absorber	Ejector	Not Practical	Concentric Cylindrical Electrodes	(DC mode)
Vapor Generator	Annular Flow Twisted Tape	Wick-Lined Tube	Concentric Cylindrical Electrodes	(AC mode)
Liquid-Vapor Separator	Twisted Tape in Wick-Lined Tube		Nested Cones	(AC mode)
	Wick "sock"			

3.1 Condenser

Studies have been reported by Feldmanis⁴, Ginwala⁵, Honea⁶, and others on the design of condensers for operation in weightless environments. The tapered-tube design from Feldmanis is simple, reliable, and lends itself to direct integration with the condenser radiator (see Fig. 3.1).

The tapering of the condenser tubes from the vapor inlet to the liquid outlet has two effects on the fluid flow. First, the reduction in cross-sectional area tends to maintain a relatively higher average fluid velocity as the vapor condenses (reducing the total volume flow rate) and this improves the average heat transfer coefficient between the fluid and the tube wall. Second, the surface tension of the liquid tends to draw the liquid toward the smaller, outlet end of the tube. This effectively separates the condensate from the remaining vapor.

In low-capacity vapor absorption refrigerators (1 to 5 KW of cooling) the refrigerant flow rates are low (approximately 0.8 lb/min of refrigerant per KW of cooling, depending upon the refrigerant used), and the normal condenser tube size would be relatively small. A simple test was conducted in which Freon vapor entered a vertical, 0.080 inch diameter condenser tube at the bottom and the condensate withdrawn at the top. Stable operation was easily obtained even with the force of gravity working in the adverse direction. The results of this test indicate that the difficulty of providing small diameter tapered tubes can be avoided for this application. In the capillary tube condenser design the liquid is forced to the outlet by a pressure force while the surface tension maintains a stable liquid-vapor interface.

The size and weight of the capillary tube condenser-radiator is dictated by the thermal radiation and meteoroid protection requirements (see Appendix C). Figure 3.2 shows the specific weight of the radiator as a function of temperature for lunar and orbital missions.

A condenser design that uses inertial forces to permit zero gravity operation is the spiral counterflow arrangement by Ginwala⁵. This design does not readily lend itself to integration with the radiator and would therefore weigh considerably more than the capillary tube condenser-radiator.

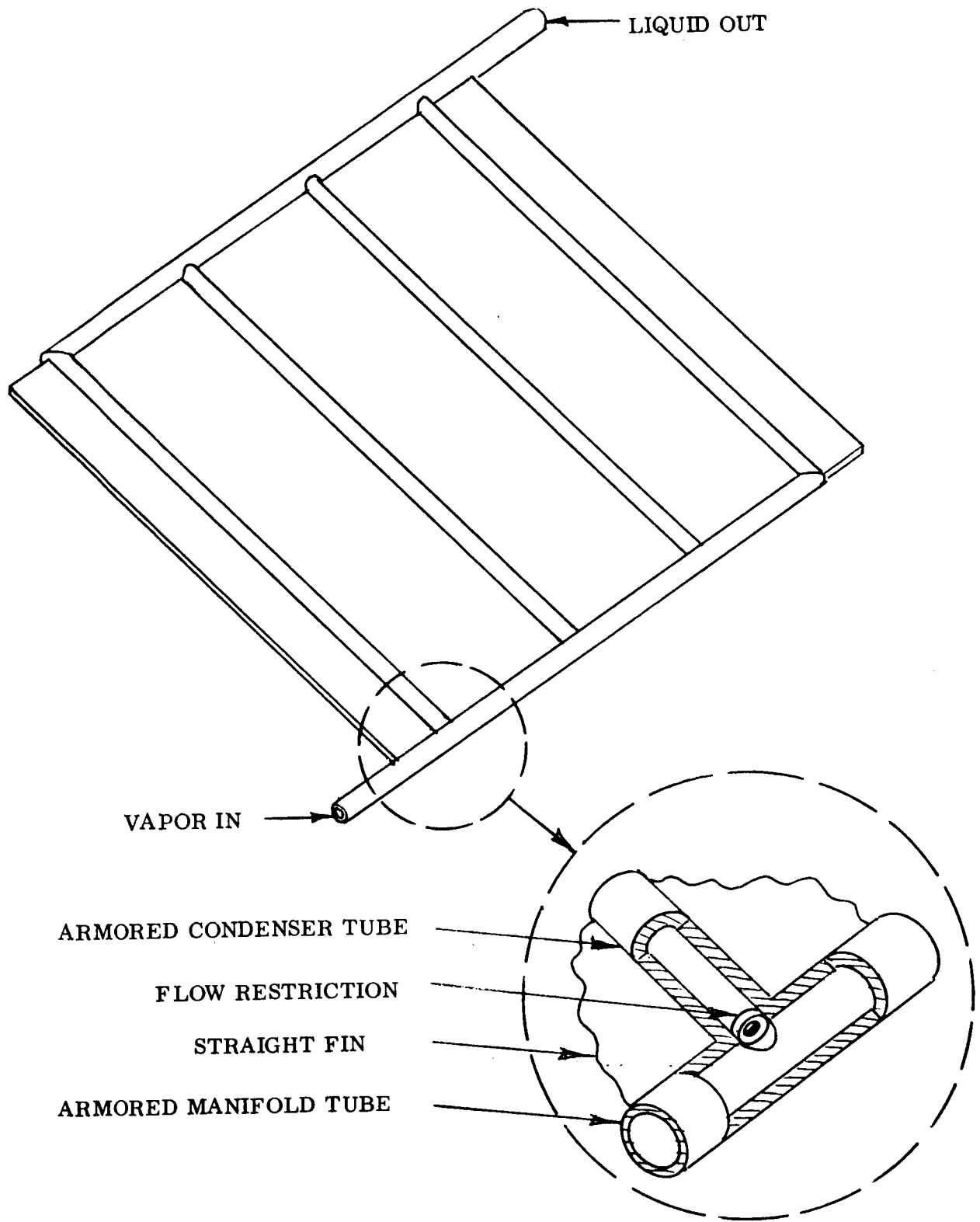


Fig. 3.1 Condenser-Radiator

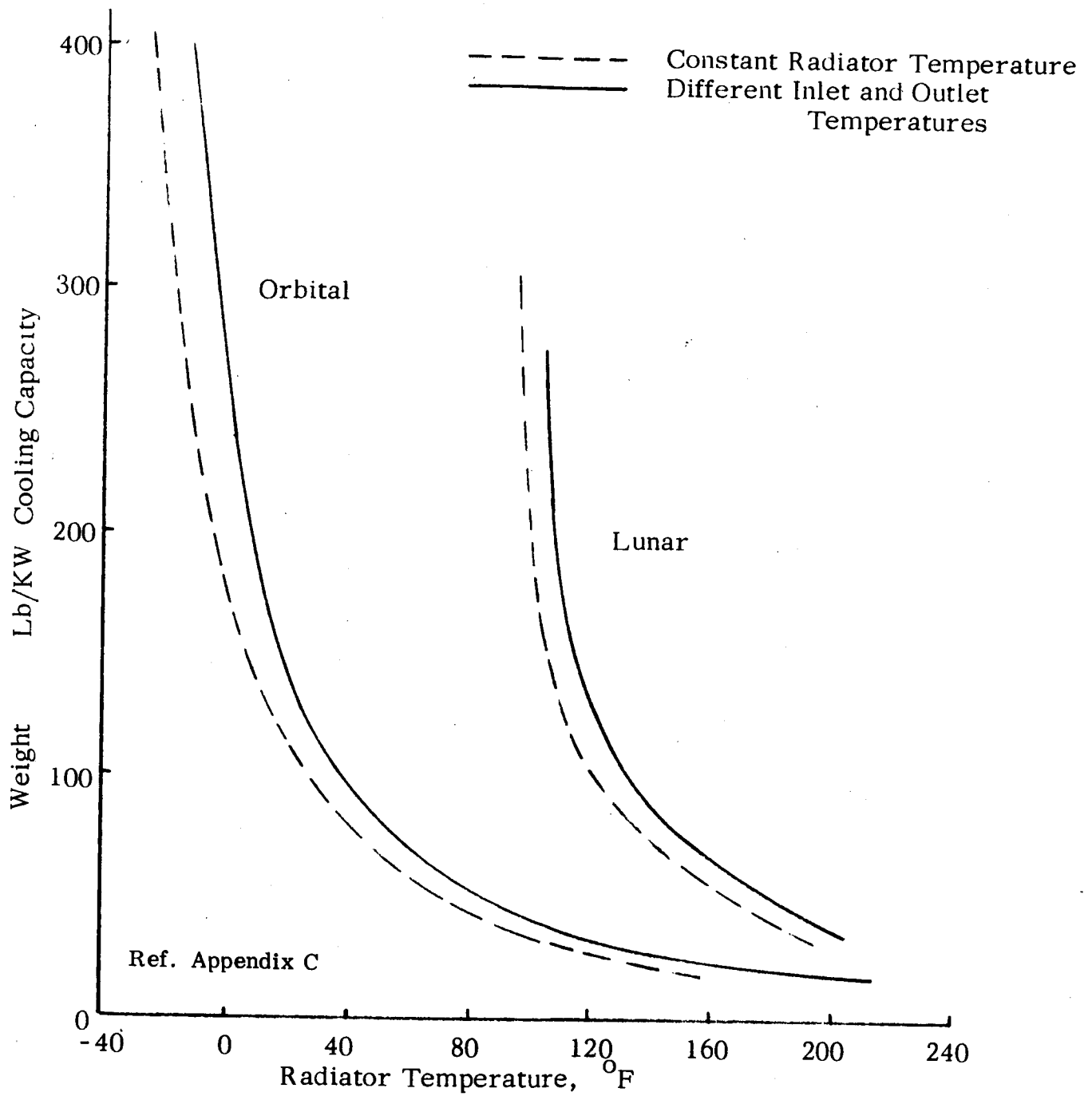


Figure 3.2 Radiator Weights

The surface tension effects in Feldmanis¹ tapered tube design could be enhanced by using electric fields to collect the condensate to a center, cylindrical electrode and to help draw the condensate toward the liquid outlet. The rate of heat transfer by radiation is what determines the size and weight of the condenser-radiator, however, so no weight reduction would be expected from the addition of the electric flow control. The added complexity, decreased reliability, and added weight of the EHD condenser all make it less desirable than the capillary tube condenser-radiator.

The capillary tube design will be used in the systems evaluations presented in Section 4.

3.2 Evaporator

A typical evaporator for normal refrigerator applications would be a simple finned-tube heat exchanger as shown in Fig. 3.3a. Other evaporator configurations for cooling of liquid flows or for cooling of radiation shields are shown in Figs. 3.3b and 3.3c. The rate of heat transfer is a function of the heat transfer coefficient on both sides of the heat exchanger. Any standard text on heat transfer^{7, 8, 9} will show that the highest heat transfer coefficients result from the boiling of liquids and the lowest from flowing gases. Therefore, in the evaporator, the liquid should be in contact with the heated tube wall for best evaporator performance.

By simply installing a twisted ribbon inside the tube of the evaporator (inset on Fig. 3.3), the centrifugal forces induced hold the liquid phase in contact with the tube wall.* The size and weight of the evaporator heat exchangers (Figs. 3.3a and 3.3b) are determined by the overall heat transfer coefficient and the total temperature between the heat source and the refrigerant liquid. The weight

* To make the twisted tape evaporator totally independent of gravity, all that is required is to maintain a high enough fluid velocity (accepting the required additional pressure drop—3 to 5 psi for a 1 KW evaporator) such that the liquid phase cannot stagnate under an adverse acceleration of 1 g. Note that if the system operates in 1 g in any orientation, it will be totally inertia-dominated. Low g operation will therefore have no special problems.

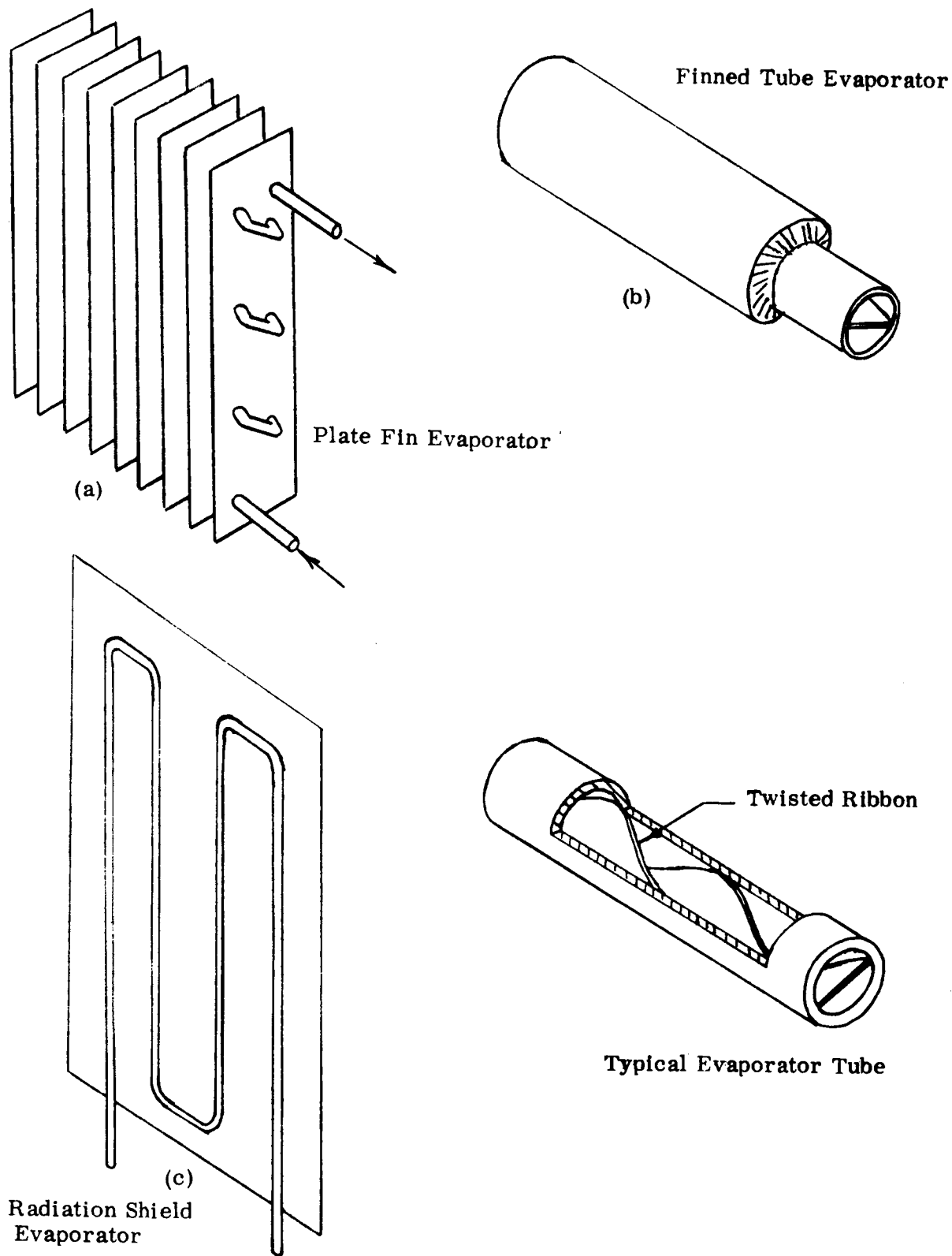


Fig. 3.3 Twisted Tape Evaporator

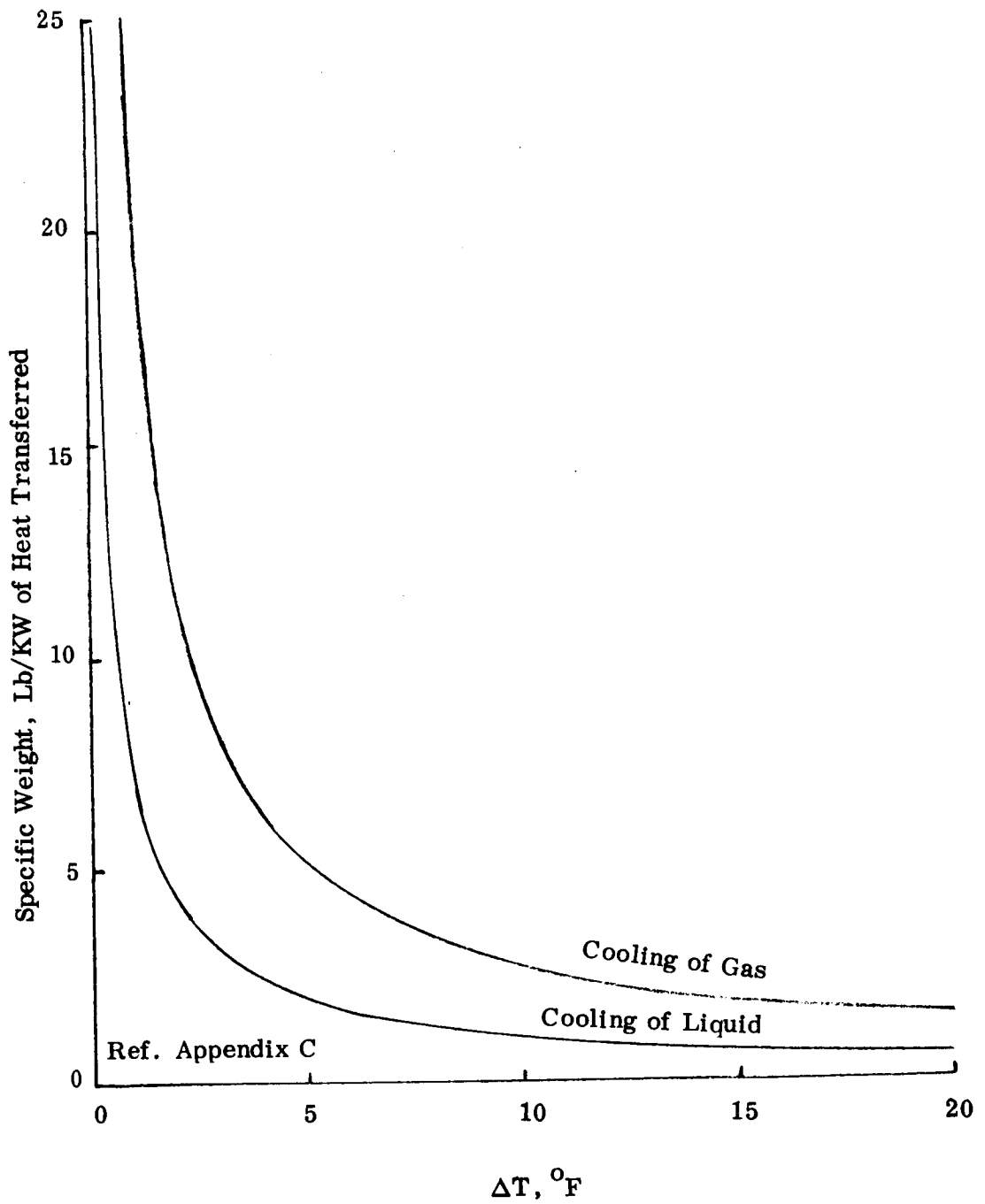


Fig. 3.4 Evaporator Weight

of the cold shield evaporator depends upon the boiling heat transfer coefficient and the temperature difference from the shield to the fluid but is primarily fixed by the shield area requirement. Figure 3.4 shows these weight relationships.

Surface tension could be used to hold the refrigerant liquid to the evaporator tube wall by lining the wall with a porous wicking material. A major drawback of the wicking arrangement is that the heat transfer coefficient for the boiling liquid is significantly reduced by vapor hold-up in the wick restricting the flow of liquid to the tube surface^{10,11}. The reduced heat transfer coefficient necessitates an increase in surface area and consequently an increase in evaporator weight.

As was the case with the condenser, the use of electric forces to control the flow in the evaporator could do no better than to equal the heat transfer rates of the twisted tape device. The added complexity and reduced reliability make such a system much less desirable than the twisted tape device.

The twisted tape evaporator is used in all the systems evaluations presented in Section 4.

3.3 Absorber

The performance of an absorber for use in a vapor absorption refrigerator is a function of two separate rate processes: a) the rate of solution of the refrigerant vapor into the refrigerant-weak solution and b) the heat rejection rate (for removal of the heat of solution). Generally speaking, each of these rate processes is maximized by high relative velocities; between the liquid and the vapor for the solution rate and between the fluids and the cooling surface for the heat rejection rate.

In a normal gravity environment the motion of the vapor bubbles through the liquid due to buoyancy can be sufficient. In the absence of gravity the motion must be generated by other means. Both inertial forces and electric forces are capable of generating the required motion. (Surface tension forces tend more toward stabilizing the fluids and, therefore, are not applicable to the gravity independent absorber problem.)

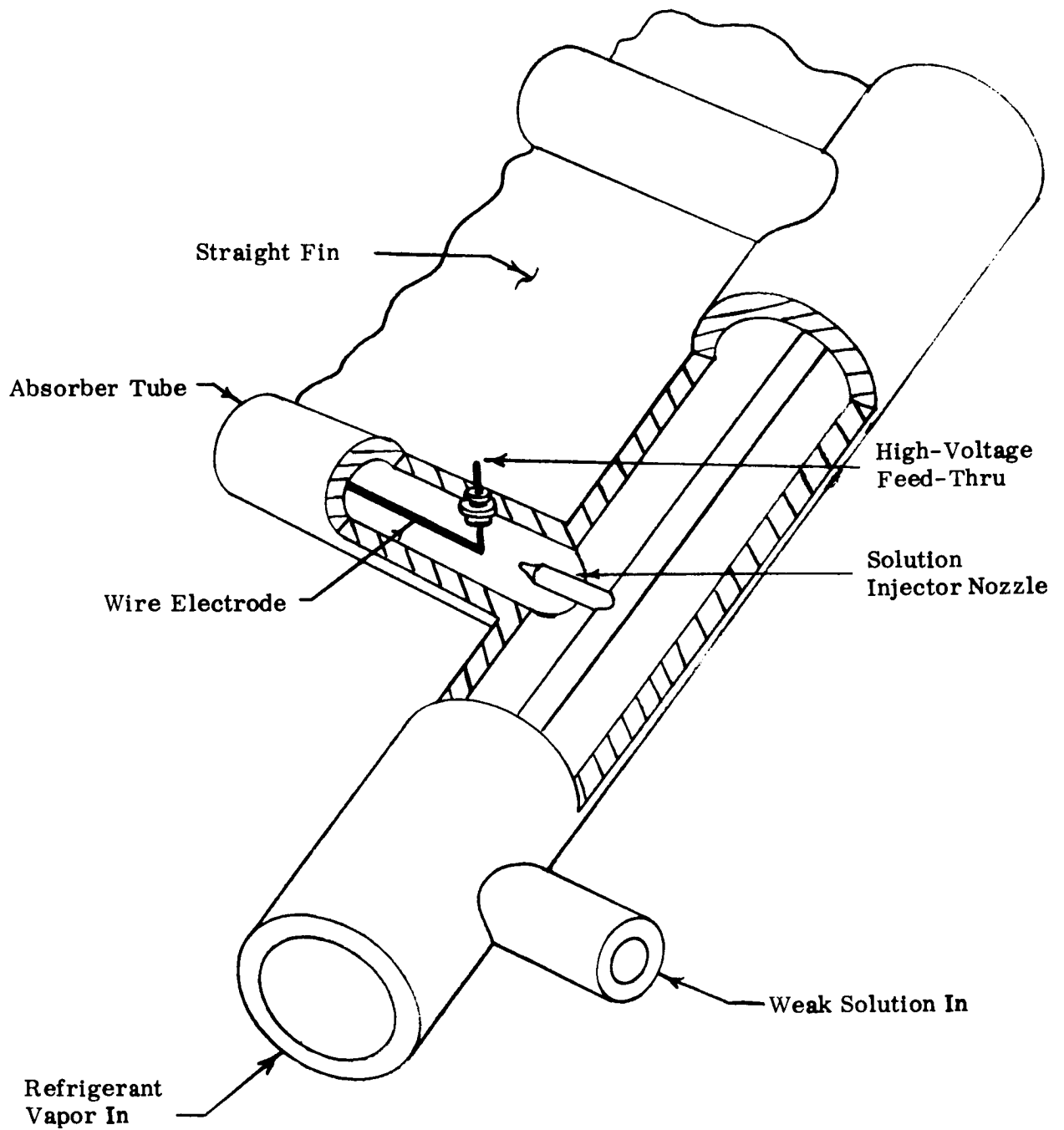


Fig. 3.5 EHD Absorber-Radiator

3.3.1 EHD Absorber-Radiator

Figure 3.5 shows one absorber-radiator configuration that used the instability resulting from a strong DC electric field between the center high voltage electrode and the grounded tube wall to cause violent mixing of the refrigerant vapor and the solution. The instability is the result of the coulombic force between the electric field and the charges that collect on the liquid/vapor interfaces due to the finite conductivity of the dielectric fluids used. (See Refs. 12, 13, and 14 for a more complete treatment of electrohydrodynamic instabilities and electroconvection.)

The detailed design and weight analysis of the EHD absorber-radiator or Fig. 3.5 must consider both of the rate processes to determine which one is limiting. If the heat rejection rate is the limiting factor, the absorber-radiator weight will depend upon the radiating area required as presented in Appendix C, Subsection C.1. If the solution rate is limiting, the weight will depend also on the volume hold-up required to give the vapor bubbles time to dissolve completely.

Assuming the worst case of no relative velocity between the liquid and the vapor, the mass transfer coefficient of a dissolving bubble or droplet is given by the equation:

$$\text{Sherwood Number} = \frac{2Rh_D}{D} = 2\gamma \quad 3.1$$

where R is the bubble radius,
 h_D is the mass transfer coefficient,
 D is the diffusion coefficient, and
 γ is a "shrinking factor" that accounts for time variation of concentration and temperature.

For the case considered here (solution rate-limiting) the rate of decrease of bubble size can be expressed as:

$$-\frac{dR}{d\theta} = \frac{D\gamma}{\rho R} (C_s - C_o) \quad 3.2$$

where θ is time,
 ρ is the density of the bubble,
 C_s is the saturation concentration, and
 C_o is the concentration in the bulk.

If γ is averaged over the period of interest and therefore assumed independent of bubble size, Eq. 3.2 can be integrated to give the solution time for the bubble having the initial radius R_o .

$$\theta_o = \left(\frac{\rho}{2D}\right) \frac{R_o^2}{\gamma(C_s - C_o)} \quad 3.3$$

It is expected that the values of γ would be very complex and therefore best determined experimentally.

The strong dependence of solution time on bubble size suggests breakup of the bubbles as an effective means of increasing the solution rate. To determine the effect of EHD mixing on the bubble size analog tests were conducted using equal density immiscible liquids to simulate the liquid/vapor mixture in zero g.* (Corn oil simulated the liquid phase and silicone oil the vapor.) The results of these tests showed that total homogenization of the mixture is possible and that bubble breakup to an estimated 10 to 100 micron size is easily attainable.

As a result of these tests it was concluded that the EHD absorber-radiator would be heat rejection rate limited and the radiator weight, therefore, will be as shown in Fig. 3.2 .

A DC power supply is required for the operation of the EHD absorber. An estimate of the power required can be made by assuming typical values for the radiator design dimensions, the fluid properties, and the voltage. The load will be purely resistive for direct current and the power will be given approximately by:

$$P = \sigma E^2 V \quad 3.4$$

* Color, 16 mm films of the EHD absorber liquid analog tests were submitted previously and constitute a part of this report.

where

- P is the power dissipated in watts per square foot of radiator surface,
- σ is the conductivity of the mixture (10^{-9} mho/cm for DME-TEG),
- E is the electric field strength (assumed to be 1000 volts/cm), and
- V is the volume of the mixture per square foot of radiator surface (assumed $10 \text{ cm}^3/\text{ft}^2$)

The power requirement is, therefore, equal to $P = 0.01 \text{ watts}/\text{ft}^2$. The power supply weight is given approximately as 100 lbs/kw at power ratings less than 50 watts.

3.3.2 Ejector Absorber-Radiator

The condensing ejector is a form of jet pump in which two-phase rather than just single-phase fluids are present. The performance of the condensing ejector is much improved over that of the jet pump because of favorable thermodynamic conditions at the ejector inlet. Momentum transfer occurs with simultaneous pumping and condensing action. (For a complete analysis of the condensing ejector see Ref. 15).

In the absorber of a vapor absorption refrigerator, refrigerant vapor is mixed with a liquid absorbent. This solution is then pressurized and heated to boil off refrigerant vapor at the higher pressure. The remaining weak solution is returned to the absorber to collect more low pressure refrigerant. The conditions coming into the absorber, therefore, are the weak (refrigerant-poor) solution at high pressure and the refrigerant vapor at low pressure, an ideal situation for applying the condensing ejector principle.

The condensing ejector analysis is not, of course, directly applicable to the absorber situation. In the common condensing ejector the change of state of the vapor to liquid is promoted by removing heat from the vapor (either by heating up sub-cooled pumping liquid or by removing heat through the ejector wall). In the vapor absorber system, in addition to removing heat from the vapor (by conduction through the ejector wall), it is also required that a difference exist between the equilibrium concentration at the absorber conditions and the actual concentration in the absorber.

This latter requirement is what makes the absorber analysis different than in the conventional system. The minimum static pressure in the absorber is limited (by the minimum equilibrium concentration required) and additional mixing is required to insure that fresh, low concentration solution is always in contact with the vapor.

The ejector could be a single length of space radiator tube as shown in Fig. 3.6 . The high-pressure weak solution would serve as the driving or pumping force to aspirate the refrigerant vapor. This mixture would give up its heat of solution to the tube walls and emerge as a rich liquid at a relatively high pressure.

Heat transfer equations show that a high velocity mixture stream is preferable. The momentum equation also indicates that a high velocity mixture would be preferable since the mean and outlet static pressure of the stream would be increased. The increase in pressure along the length of tube increases the equilibrium saturation concentration and effectively makes the system more efficient. However, these high velocity advantages are offset by tube friction pressure drop and decreased solubility time in given length tubes. Also, to obtain these high velocities, the static pressure at the tube entrance must be dropped to values approaching the equilibrium conditions of the entering weak solution, thus reducing the solution rate in the inlet region where a high solution rate would be desirable. This problem can be offset in part by atomizing the weak solution, decreasing the droplet diameter, and thereby increasing the solution rate as discussed in Section 3.3.1 .

The ejector absorber-radiator design can be applied to a wide range of refrigerator capacity requirements. In addition, other systems modifications can be made to better take advantage of the benefits of the ejector.

For example, an ejector absorber-radiator for a 1 KW cooling capacity refrigerator would require a 10 ft. long, 0.050 in. diameter ejector tube followed by the conventional liquid pump to boost the pressure to the level of the generator. In this case, the friction pressure drop along the very small tube strongly affects the momentum balance pressure rise, thus necessitating a pump between the absorber and the generator. The small diameter tube is necessary to achieve

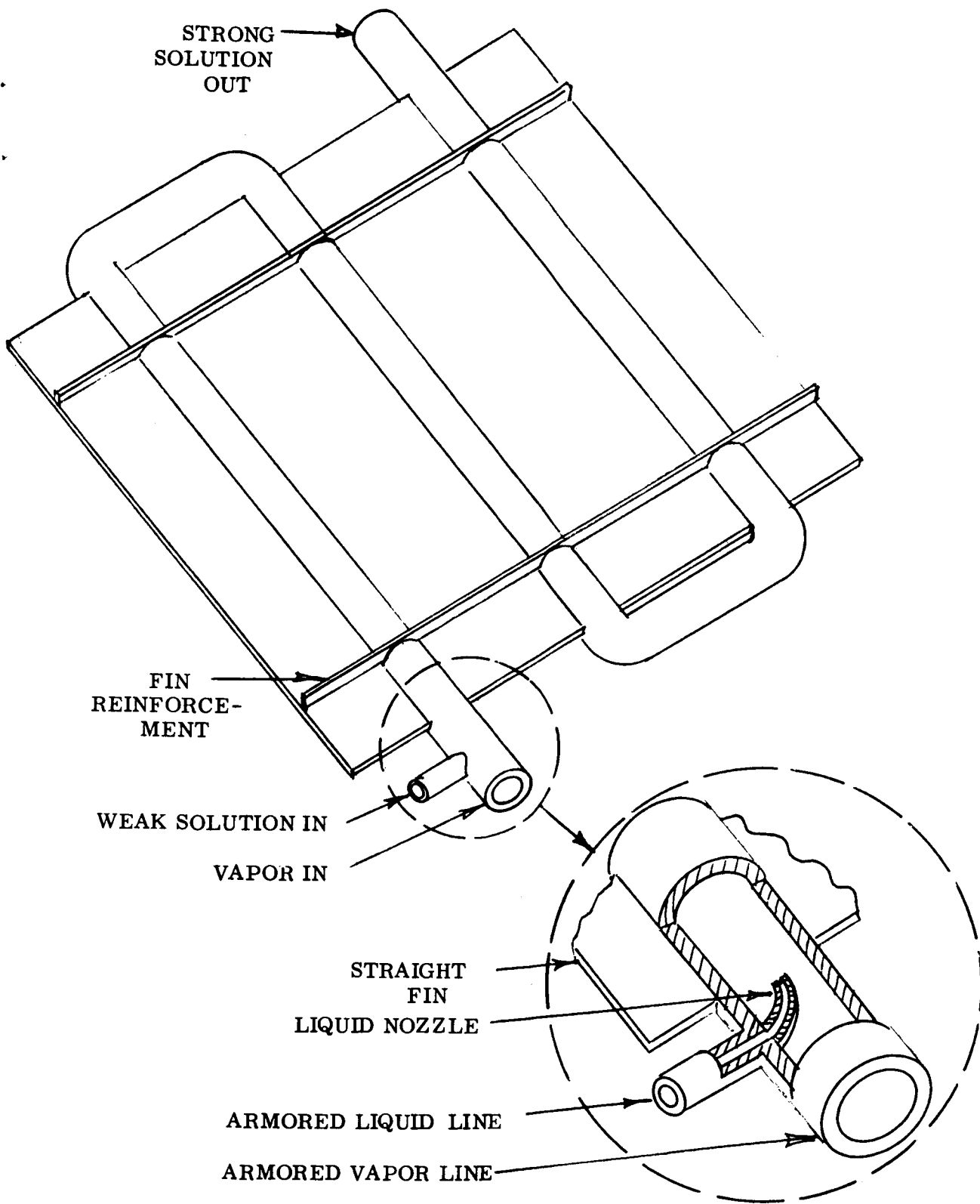


Fig. 3.6 Ejector Absorber-Radiator

the absorber requirements of heat transfer and mixing. For larger capacity systems, the diameter increases with the square root of the capacity increase and the length increases very slightly. For a system approaching 16 KW capacity, a 0.20in. diameter ejector tube, again 10 ft. long, would be used. Instead of locating the pump between the absorber and the generator, however, the pump could be located in the weak solution line immediately before it enters the absorber. Here the friction pressure drop has a small effect upon the total outlet pressure of the absorber the average pressure level in the absorber is increased and a higher outlet concentration is attainable.

As with the EHD absorber-radiator design (Section 3.3.1) the ejector absorber-radiator operation can be limited by either the solution rate or the heat rejection rate. Based upon the above results it would appear that the radiation heat transfer is the limiting factor. Consequently the ejector absorber-radiator weights will be as shown in Fig. 3.2 .

3.3.3 Conclusions

Both of the preceding absorber designs lend themselves well to the gravity independent refrigerator application. However, on the basis of the greater simplicity and the higher outlet concentration theoretically possible with the ejector design, it would be the more desirable of the two. The system designs of Section 4 will be based on the ejector absorber-radiator design.

3.4 Vapor Generator

Other than the difference in mass quality of the vapor at the outlet, the vapor generator is identical to the evaporator in operation. The mass quality of the vapor leaving the evaporator is close to 100%, while that leaving the vapor generator can vary over a wide range depending upon the cycle and the fluids used.

As far as improving the heat transfer coefficient is concerned, the twisted tape and surface tension devices again appear most applicable. The surface tension device may be particularly attractive, permitting the integration of both the vapor generator on the liquid-vapor separator into one device. However, as for the evaporator the heat transfer coefficient for the surface tension device is less than that for the twisted tape device.

The actual configuration of the vapor generator depends to a great extent upon the source and form of heat supply to the generator. If the heat is derived from the waste heat of a power system, the device would be a relatively simple heat exchanger. If solar heat is used, the device would form the receiver of a solar collector.

The specific weight of the vapor generator tube (consisting only of the tube itself and the integral twisted tape) is given in Fig. 3.7. The generator tube requirements are based solely on the heat transfer requirements.

For the system designs of Section 4 the twisted tape vapor generator design will be assumed.

3.5 Liquid-Vapor Separator

The liquid-vapor separator is the most critical component in the vapor absorption refrigerator system as far as low or zero gravity operation is concerned. While a small amount of liquid carry-over into the condenser or of vapor in the weak solution is to be expected, excessive amounts will rapidly degrade the systems performance as is shown in Appendix A.

The three basic methods of performing the separation under zero-g conditions (electric forces, surface tension, and inertial forces) were examined.

3.5.1 Electrohydrodynamic Separator

If two dielectric fluids are introduced into an electrostatic field, the fluid having the higher dielectric constant will be collected and held in the region having the highest field strength. This is the basic principle of the electrohydrodynamic (EHD) separator.

Figure 3.8 is a conceptual design of a liquid-vapor separator based on the EHD separator principle. The liquid in the two-phase flow is drawn toward the base of the nested cones where it is collected and withdrawn. The vapor exhausts at the apex of the cones.

An analysis of the EHD separator was performed and is reported in Appendix D. The results of the analysis are presented as the time required to separate liquid droplets of various diameters from the two-phase flow for different voltages and levels of adverse acceleration.

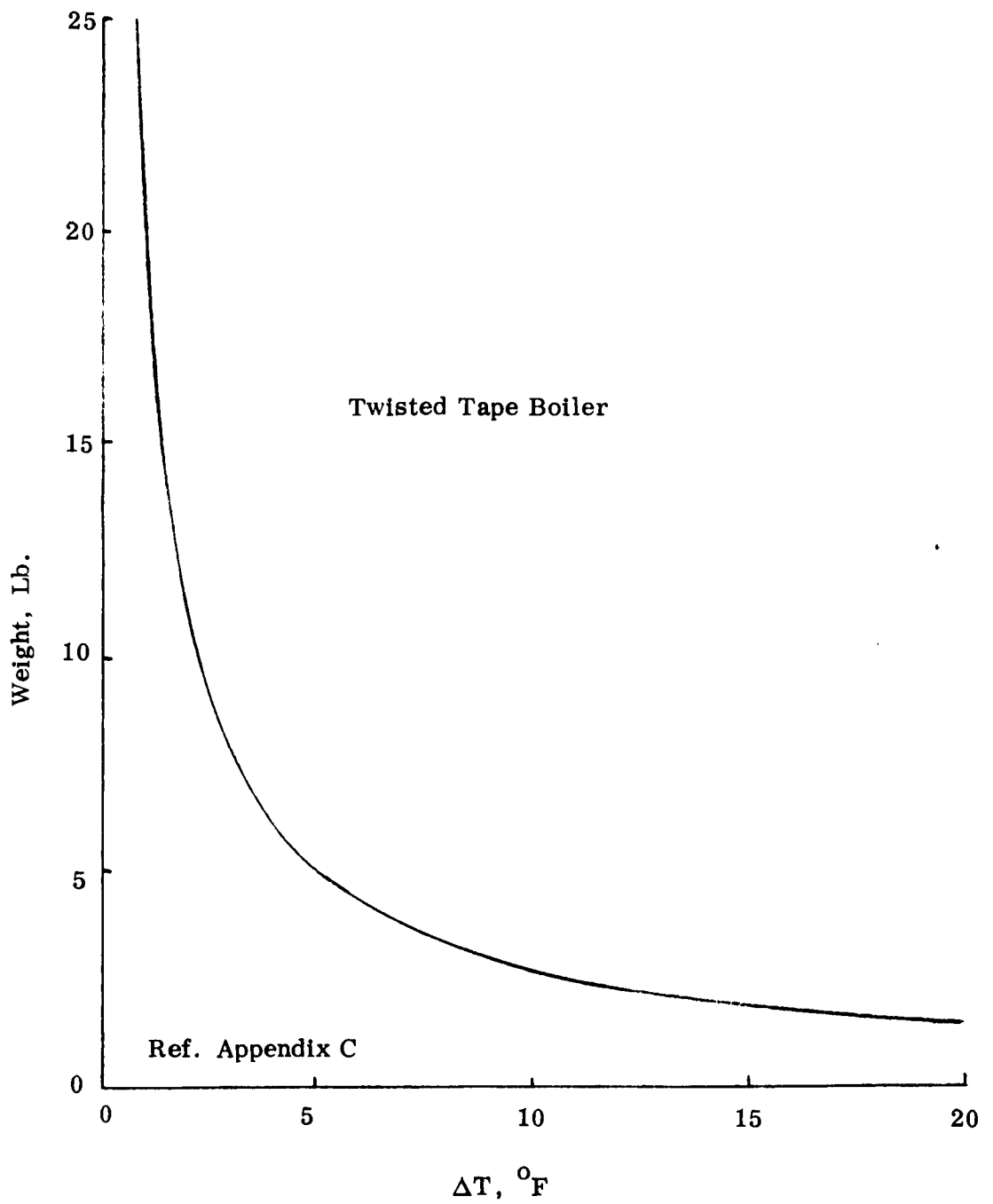


Fig. 3.7 Vapor Generator Weight

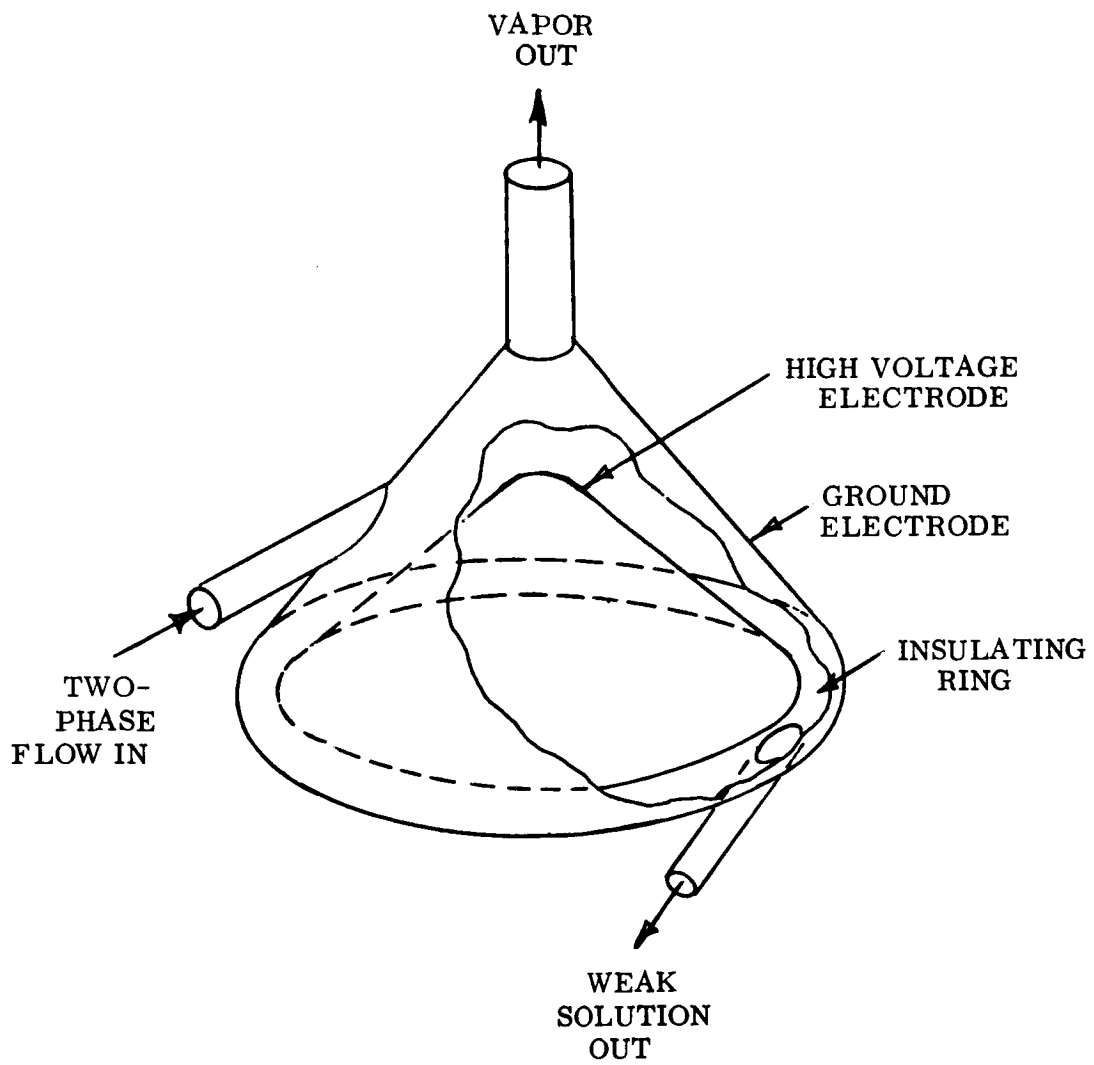


Fig. 3.8 EHD Separator

The diameter of the droplet, which determines the relative drag on the droplet, has a strong effect on the separation time (smaller droplets requiring a longer separation time). The amount of entrained liquid carryover with the vapor will depend on the droplet size distribution and the separator length. (One feature of the nested cone configuration is that, as long as the force on the droplet is great enough to overcome the drag of the vapor rising to the vapor outlet, the effective length of the separator is infinite.)

A major drawback of the EHD separator is that it is not gravity independent. For each level of adverse acceleration there is a minimum threshold voltage below which the separator will not operate. Above the threshold voltage the separation time is relatively independent of the voltage. The EHD forces (obtainable at electric field strengths below the breakdown field strength of the fluids) are orders of magnitude less than the gravitational force of the earth. The EHD separator would be applicable only to orbital or interplanetary missions.

Liquid-liquid analog tests demonstrated the hydrodynamics of the EHD separator and verified the accuracy of the separator analysis (see Appendix D).

3.5.2 Surface Tension Separation

A "sock" de-mistor is one relatively common form of surface tension dependent liquid-vapor separator. A modification of the sock de-mister for use in the gravity independent vapor absorption refrigerator is shown in Fig. 3.9. In this device all of the inlet flow is directed through the wicking "sock." The liquid droplets are caught by the wick and the vapor allowed to pass through. The liquid is then sucked out of the wick in a region where it is free of vapor.

An extensive series of tests were run to demonstrate the operation of a representative separator model using Freon 113 and dimethyl ether of tetraethylene glycol. A detailed account of the apparatus and the test results are presented in Appendix G. The wick plugging problems reported by Ginwala⁵ were not encountered. The results of careful degassing of the system were in agreement with the experiments reported by Langston.

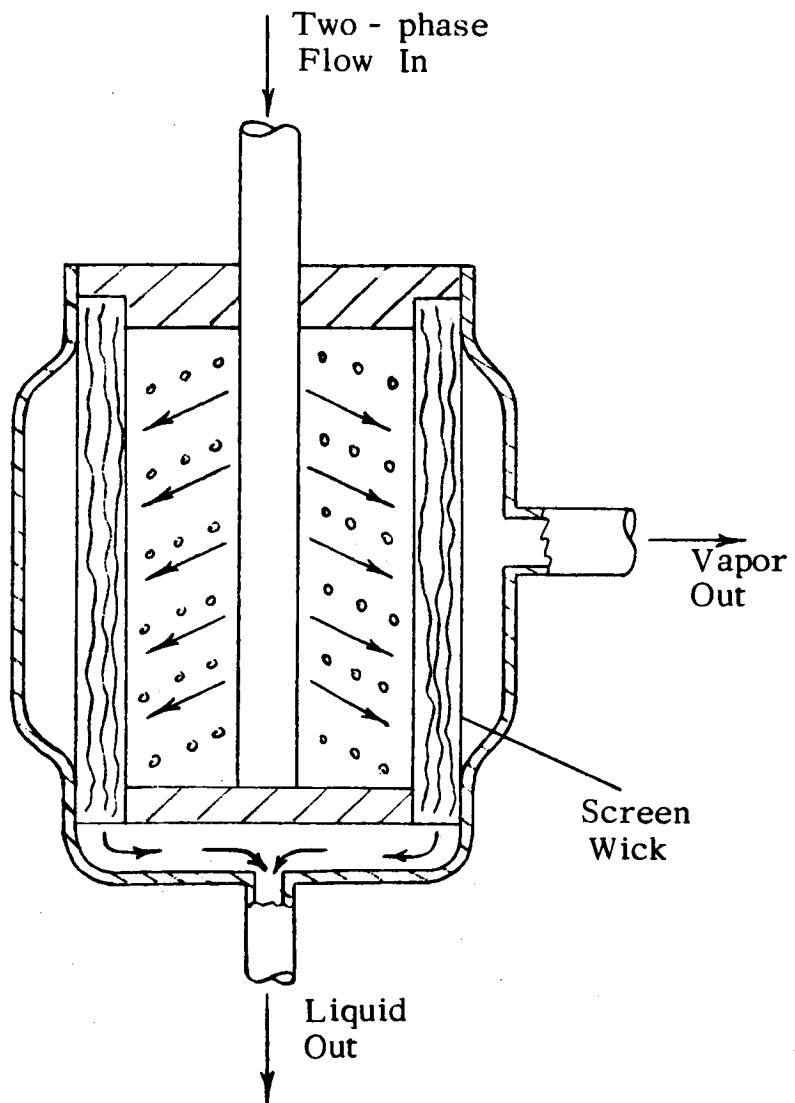


Figure 3.9 Wick Separator

An accurate design analysis of the wick separator requires the experimental determination of the physical properties of the wick used (such as is being done by Langston¹¹). An estimate of the weight of the wick separator has been made in Appendix G, however. The results are shown in Fig. 3.10.

3.5.3 Vortex Separator

Figure 3.11 shows one configuration for a vortex liquid/vapor separator. The two-phase flow enters the separator where the twisted tape induces centrifugal forces which tend to throw the liquid droplets radially outward. The droplets are absorbed into the capillary pores of the wicking. Pure liquid is withdrawn from the wicking as in the surface tension separator.

The droplet size is important in the vortex separator as it was in the EHD separator. The smaller droplets have a higher drag and therefore require a longer time (longer separator length) to be separated from the vapor stream. Knowing the configuration of the two-phase flow entering the separator, the length of the separator can be adjusted to give any desired degree of separation. Here again the emphasis is placed on describing the configuration of the two-phase flow.

3.5.4 Wick "Generator/Separator" Concept

The performance of wick-lined boiler tube has been investigated in detail by Costello and Redeker¹⁰. They found that, while the overall heat transfer rate decreased for a given temperature difference, the burn-out heat flux actually increased. They also determined that the vapor generated at the heated surface does move through the wicking to the surface. The capillary action of the wicking then draws more fresh liquid to the heated surface.

Figure 3.12 shows conceptually the design of the "wick boiler" device. The primary advantage of the "wick boiler" is that the liquid is always held in control and an independent separator is not required. Also, it has the possible capability of performing the liquid/vapor separation in either zero or 1 g in any orientation.

The primary disadvantage of this concept is that a higher temperature heat source is required to drive the boiler because of the lower heat transfer coefficient.

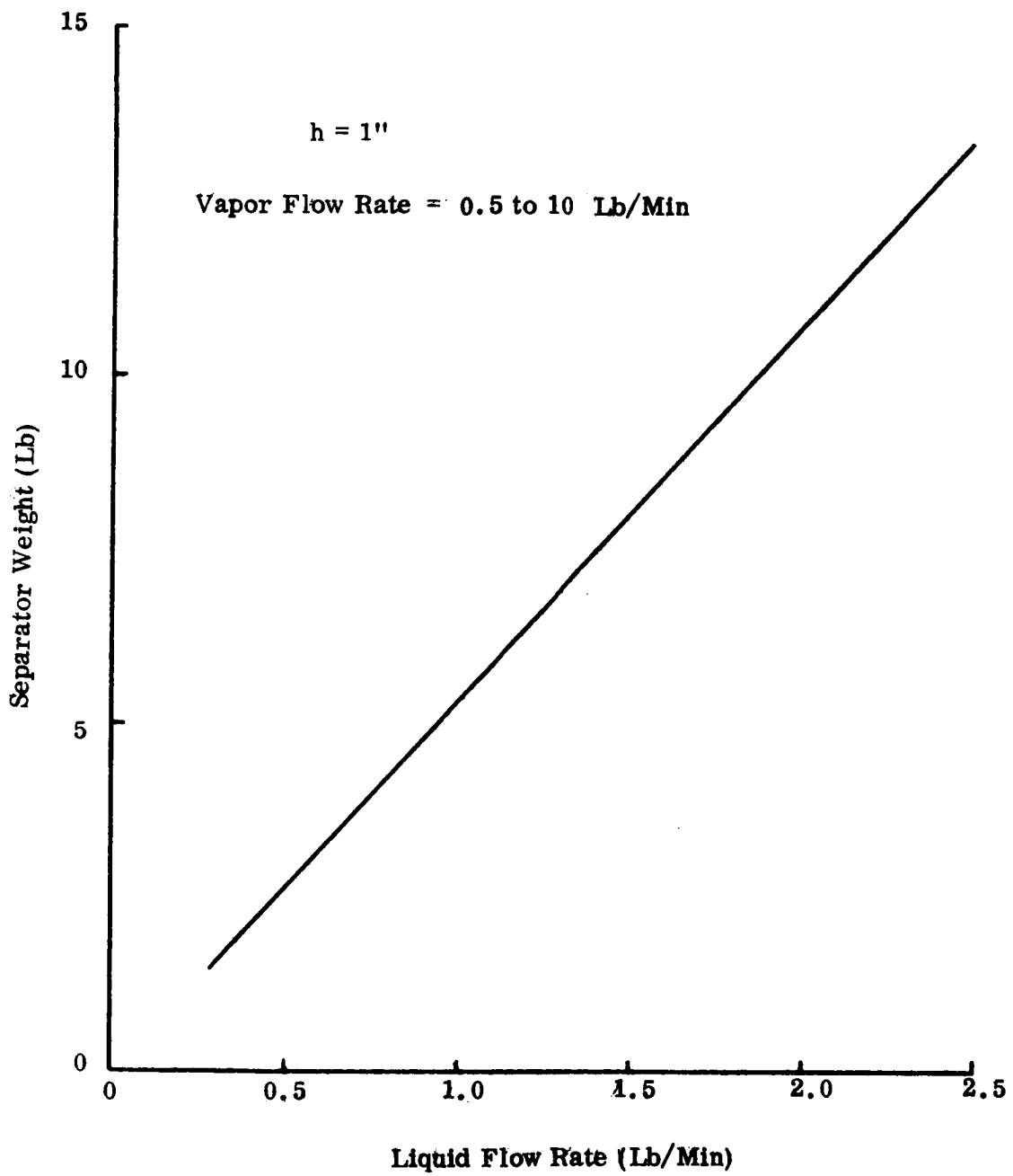


Fig. 3.10 Wick Separator Weight

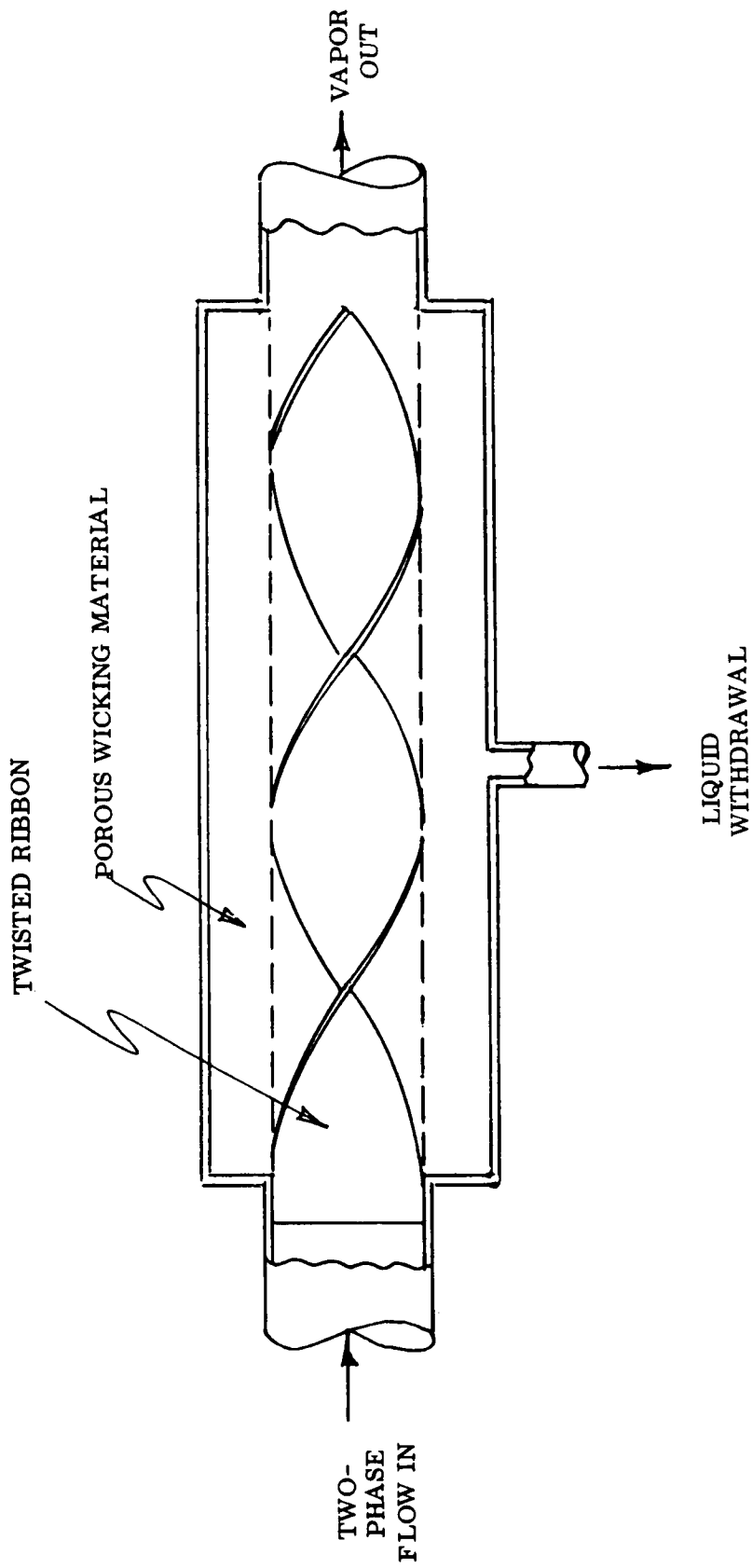


Fig. 3.11 Vortex Separator

3.5.5 Conclusions

On the basis of the above discussion and the requirements for gravity independence, reliability, and flexibility to meet a variety of system applications, the wick separator of sub-section 3.5.2 was selected as the best design. The system weight analyses of Section 4 are based on the wick separator design.

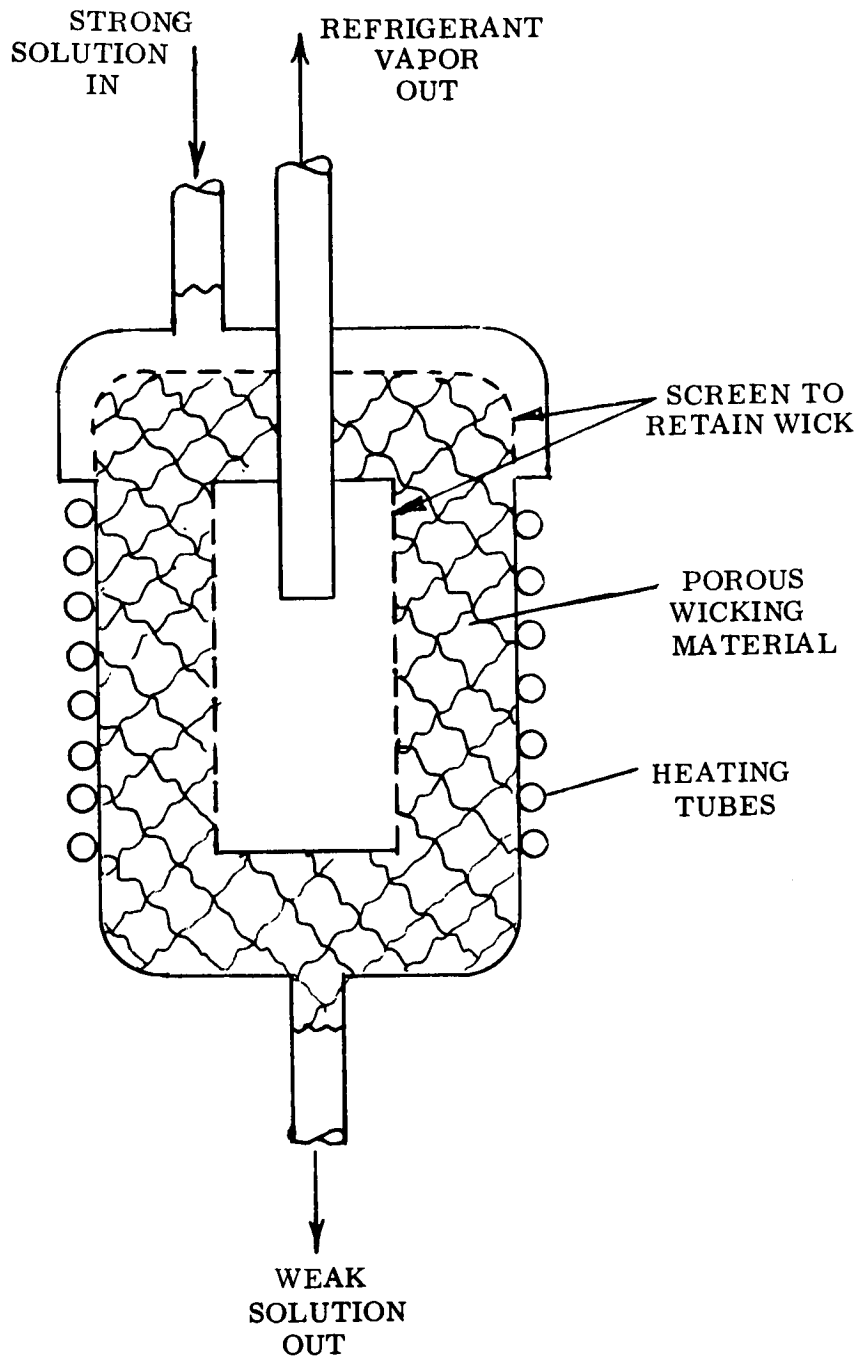


Fig. 3.12 Wick Generator/Separator

Section 4

SYSTEMS COMPARISON

There are two general classes of systems for controlling of temperature-- passive (including semi-passive) and active. In the passive and semi-passive systems the heat transfer is the result of the natural desire of heat to pass from a higher temperature source to a lower temperature sink. In an active system a heat pump is used to take heat from a lower temperature source and reject it at a higher temperature sink.

Because of their simplicity and reliability, the passive and semi-passive systems have been preferred over active systems for the thermal control of the equipment and environment on most space missions to date. However, in space, where thermal radiation is the primary mechanism for the rejection of heat, the low temperature radiators of the passive and semi-passive systems become very large as the heat rejection requirements increase. The incentive to go to active cooling systems to conserve weight by raising the radiator temperature then outweighs the disadvantage of added complexity.

The most common active refrigeration system is the vapor compression refrigerator. With the vapor compression system the radiator temperatures can be raised significantly at a great reduction in weight. The primary disadvantage of the vapor compression system for space applications, however, is that the power required to drive the compressor must be available as high-grade shaft power which is available only by accepting a high-power weight penalty.

An active refrigeration system that requires only small quantities of shaft power is the vapor absorption system. As was explained in detail in Section 2, the vapor absorption system runs primarily on heat. In many instances this heat is available as waste heat from other systems on the space mission vehicle at no weight penalty.

In the following sections, systems will be described to fulfill two general classes of thermal control requirements: orbital applications where there is a relatively free choice of radiator temperature and lunar applications where the radiator

temperature must be maintained above some limiting temperature because of the high environmental heat influx to the radiators resulting from re-radiation from the lunar surface.

4.1 Semi-Passive Thermal Control Systems

The general arrangement of a semi-passive thermal control system in which a heat transfer fluid is circulated between the source of heat and the radiator is shown in Fig.4.1 . A typical heat transfer fluid is a 60% ethylene glycol and water solution. In Appendix E a detailed design analysis of the semi-passive system is presented.

Figure 4.2 shows the weight of the semi-passive system as a function of the cooling rate for various load temperatures for both orbital and lunar applications. It is significant to note that due to the high radiator temperatures required, semi-passive systems are not applicable to environmental temperature control on lunar missions.

4.2 Vapor Compression Refrigeration Systems

The vapor compression refrigerator is the simplest and most common active refrigeration system. Figure 4.3 indicates how the refrigerant is vaporized at low pressure by adding heat to the evaporator. The vapor is then compressed resulting in a high-pressure, high-temperature vapor. The vapor is condensed by the rejection of heat in the condenser and returned through an expansion valve to the evaporator. In Appendix F is presented a detailed analysis of vapor compression refrigeration systems for orbital and lunar applications.

Figure 4.4 shows the weight of the vapor compression system as a function of the cooling load and the load temperature for orbital and lunar applications.

4.3 Vapor Absorption Refrigeration Systems

The basic vapor absorption refrigerator is the single stage system shown in Fig.2.5 . The operational limits of the system, as described in Section 2. are a function of the fluids used. With Freon 22 as the refrigerant, 350^oF is the

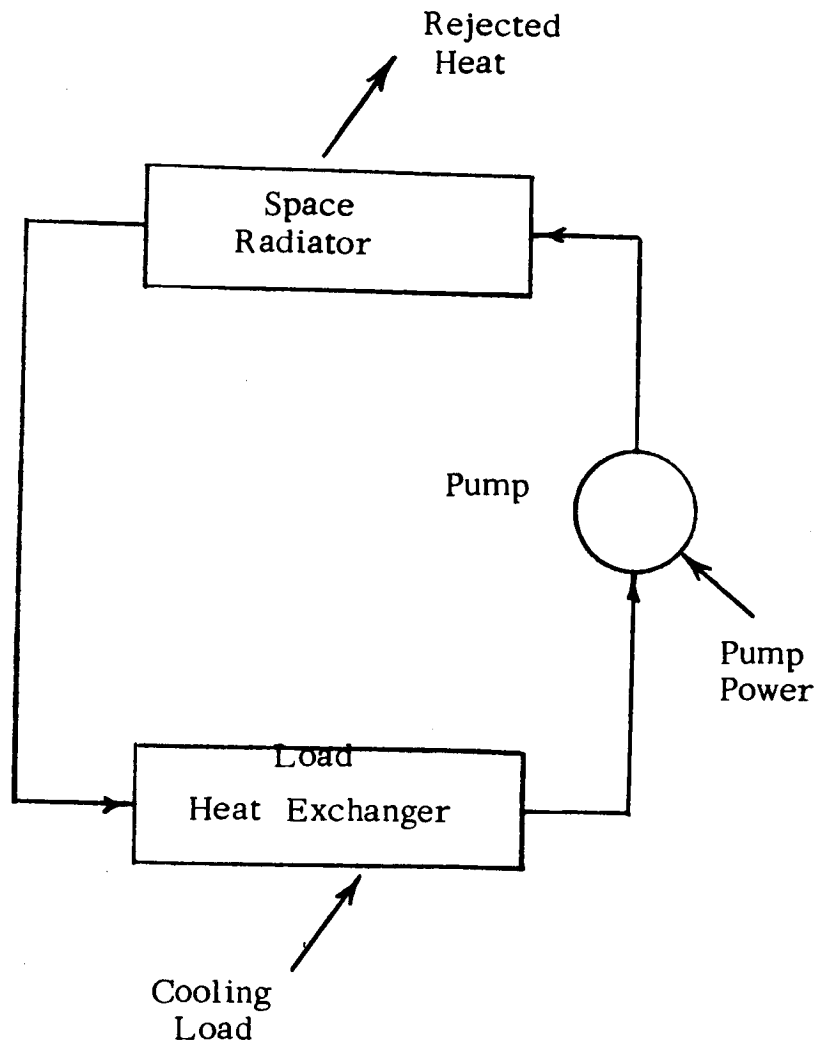


Figure 4.1 Flow Diagram--Semi-Passive System

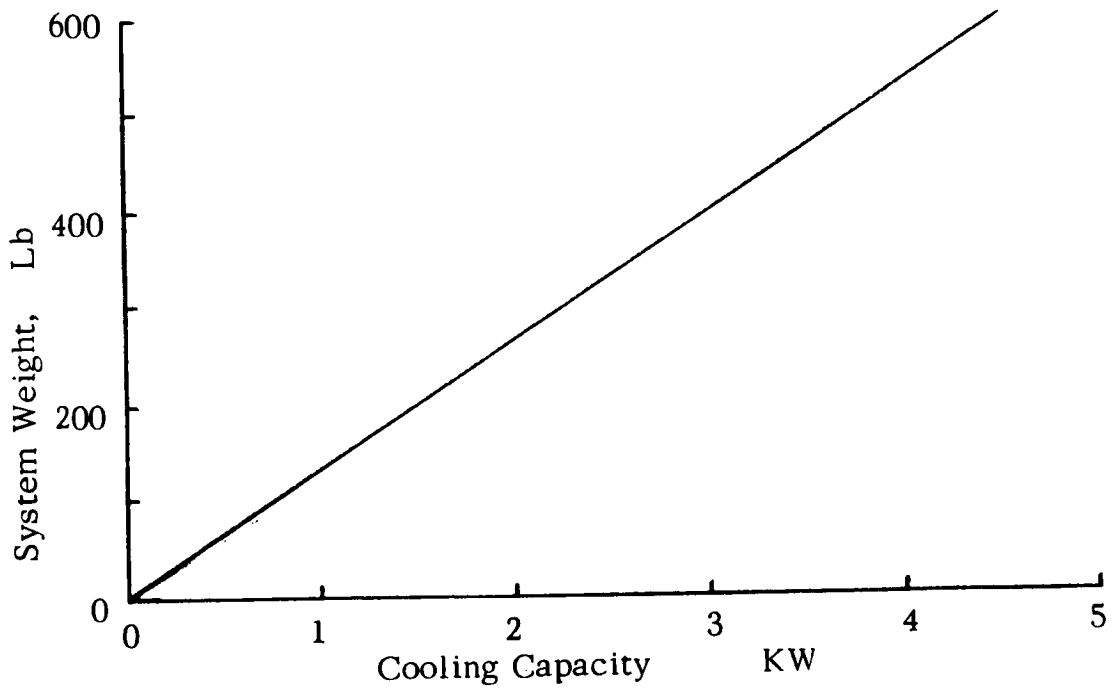
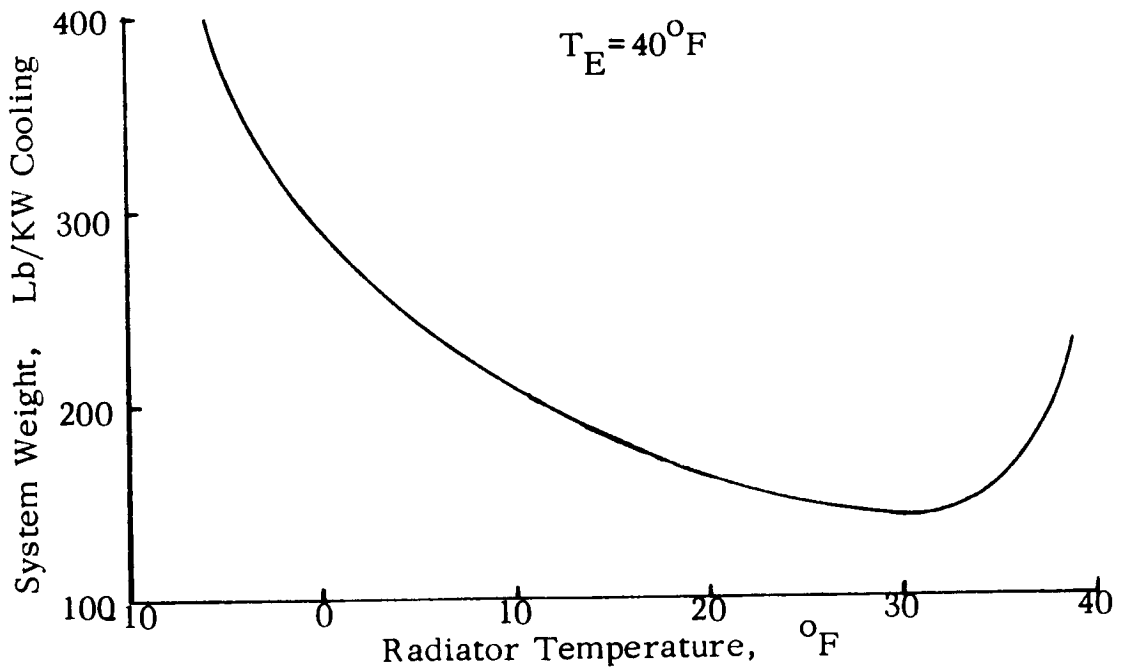


Figure 4.2 Semi-Passive System Weights

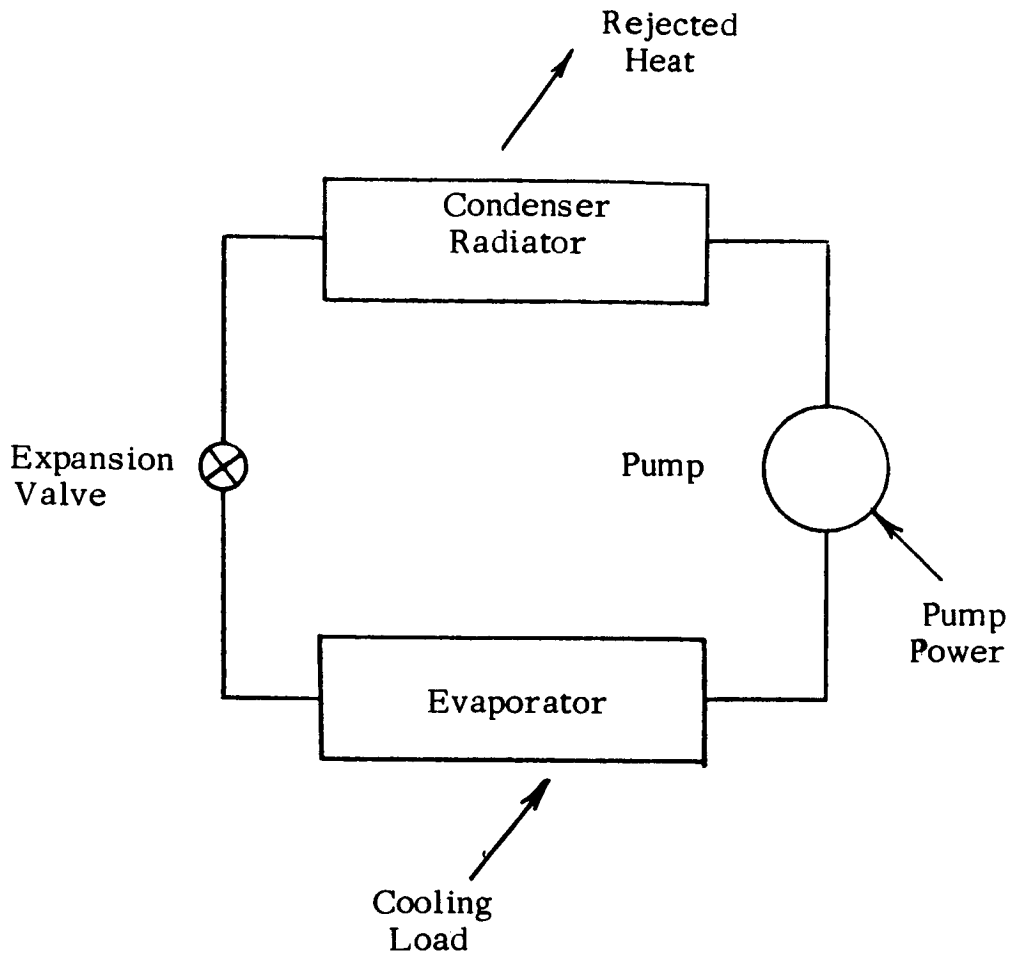


Figure 4.3 Flow Diagram--Vapor Compression Refrigerator

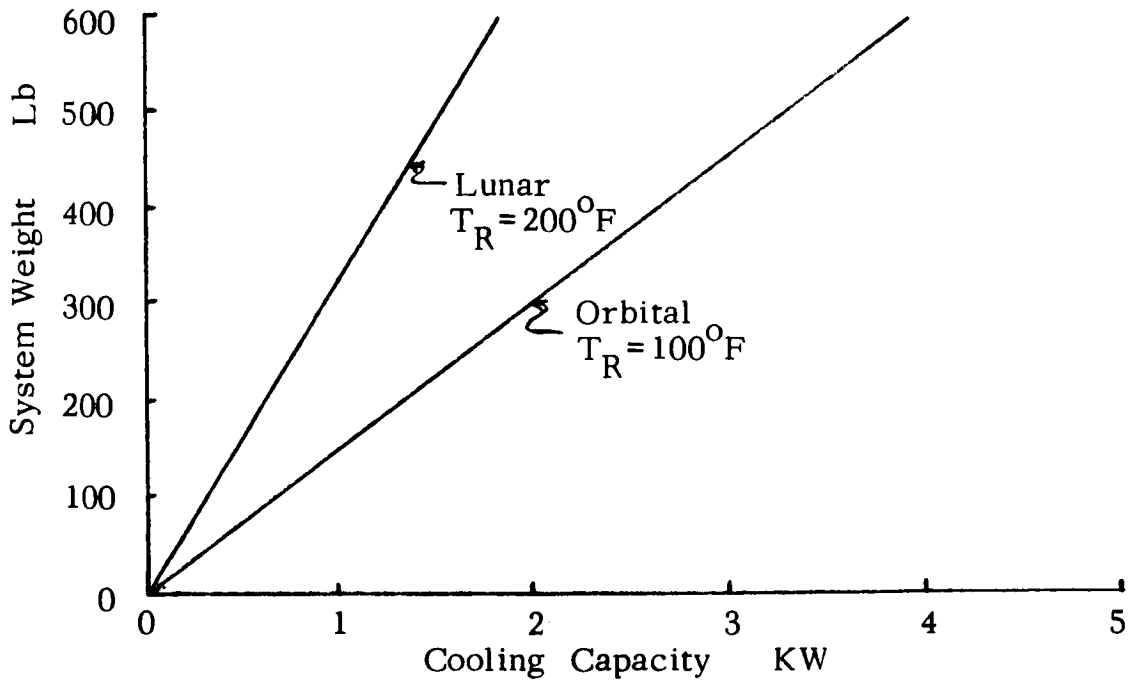
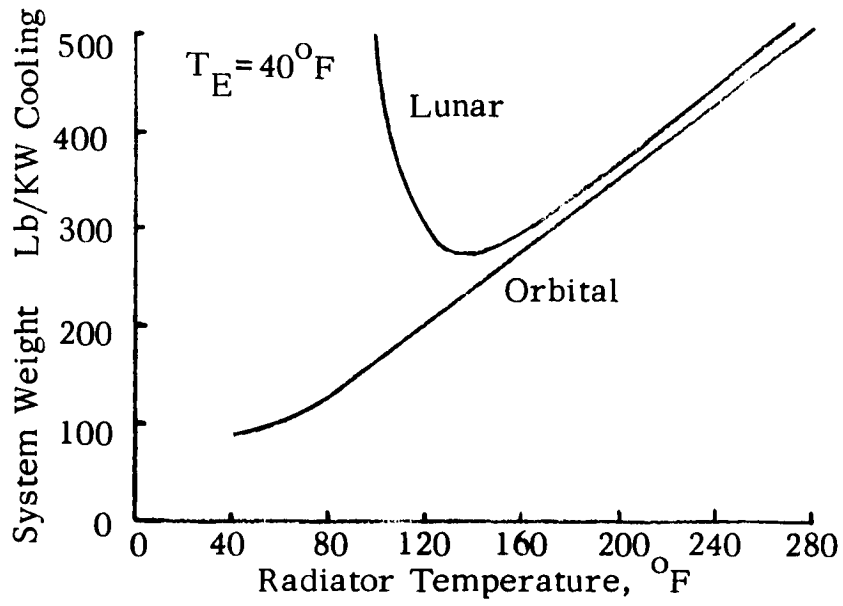


Figure 4.4 Vapor Compression System Weights

maximum generator temperature for continuous operation without significant Freon decomposition. At this generator temperature and a 40^oF evaporator temperature required for environmental temperature and humidity control, the maximum practical radiator temperature is about 120^oF. Such a system would not be applicable to lunar missions.

To achieve higher radiator temperatures a two-stage refrigeration system is required (Fig.4.5) where the condenser and absorber of the lower stage are cooled by the evaporator of the upper stage at some intermediate temperature. Without raising the generator temperature above the 350^oF maximum or changing the 40^oF evaporator temperature, radiator temperatures as high as 230^oF can be attained.

By combining the results of the cycle analysis (Section 2) and the component design and weight analysis (Section 3 and Appendix C) the system weights for a wide range of operating conditions can be derived. Figures 4.6 and 4.7 show the weights of vapor absorption refrigerators as a function of the cooling load and as a function of radiator temperature (for a particular cooling load).

4.4 Comparison and Conclusions

By super-position of Figs.4.2a,4.4a, and 4.6 and of Figs.4.2b ,4.4b, and 4.7, the relative weights of semi-passive, vapor compression, and vapor absorption systems can be compared (see Figs. 1.1 and 1.2) for a wide variety of operating requirements and conditions. The weight advantage of the vapor absorption system is readily apparent.

Looking deeper into the differences between the vapor absorption systems and the other competing systems, one fact stands out. In the case of the vapor absorption systems the weights associated with the major components and the power weight penalty are of the same relative magnitude. With the semi-passive and vapor compression systems, however, one particular item dominates the weight of the system. For the semi-passive system it is the radiator which accounts for as much as 80 % of the total system weight. For the vapor compression systems it is the power weight penalty which accounts for up to

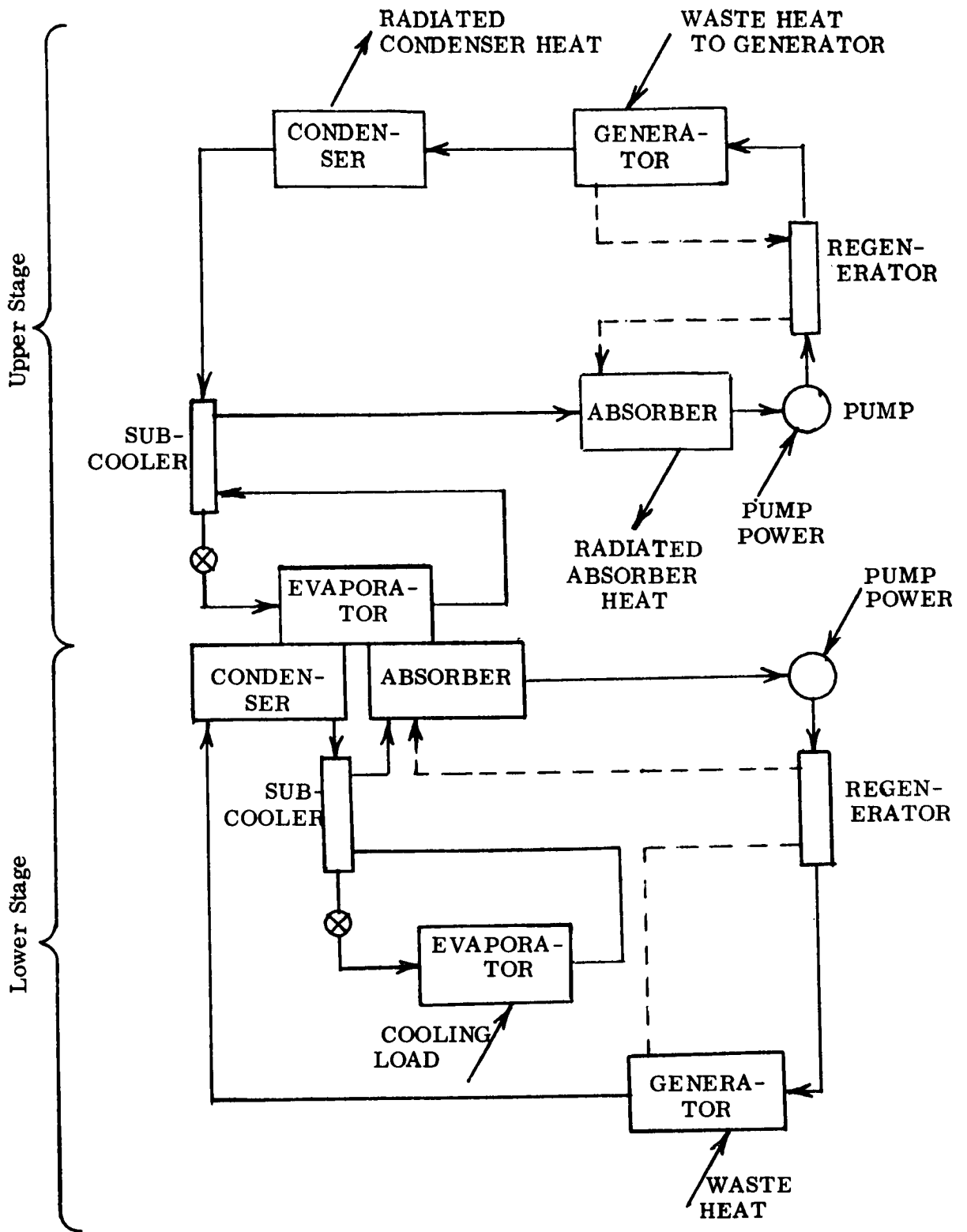


Fig. 4.5 Two Stage Vapor Absorption Cycle

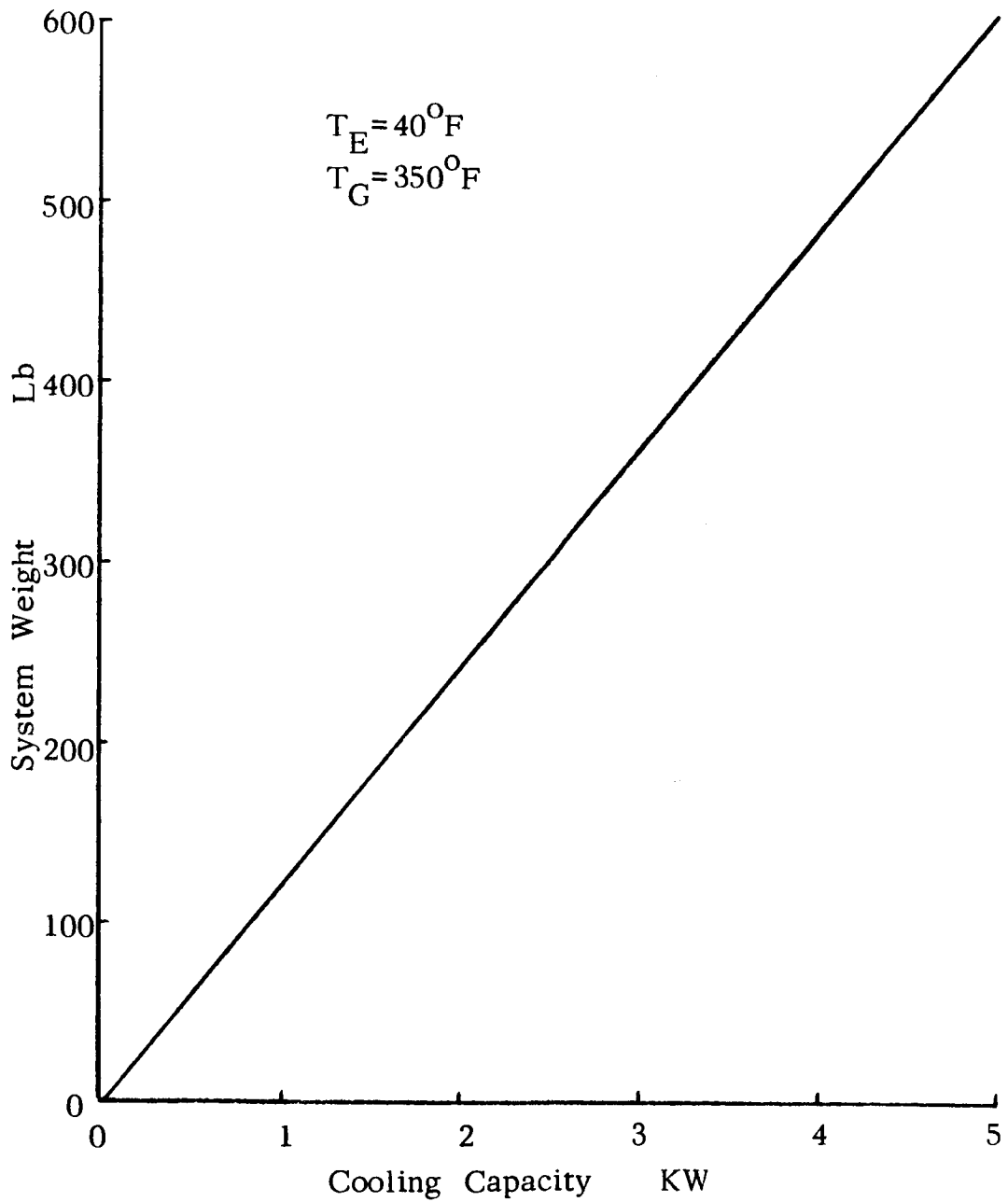


Figure 4.6 Vapor Absorption Refrigerator Weights (vs. Cooling Capacity)

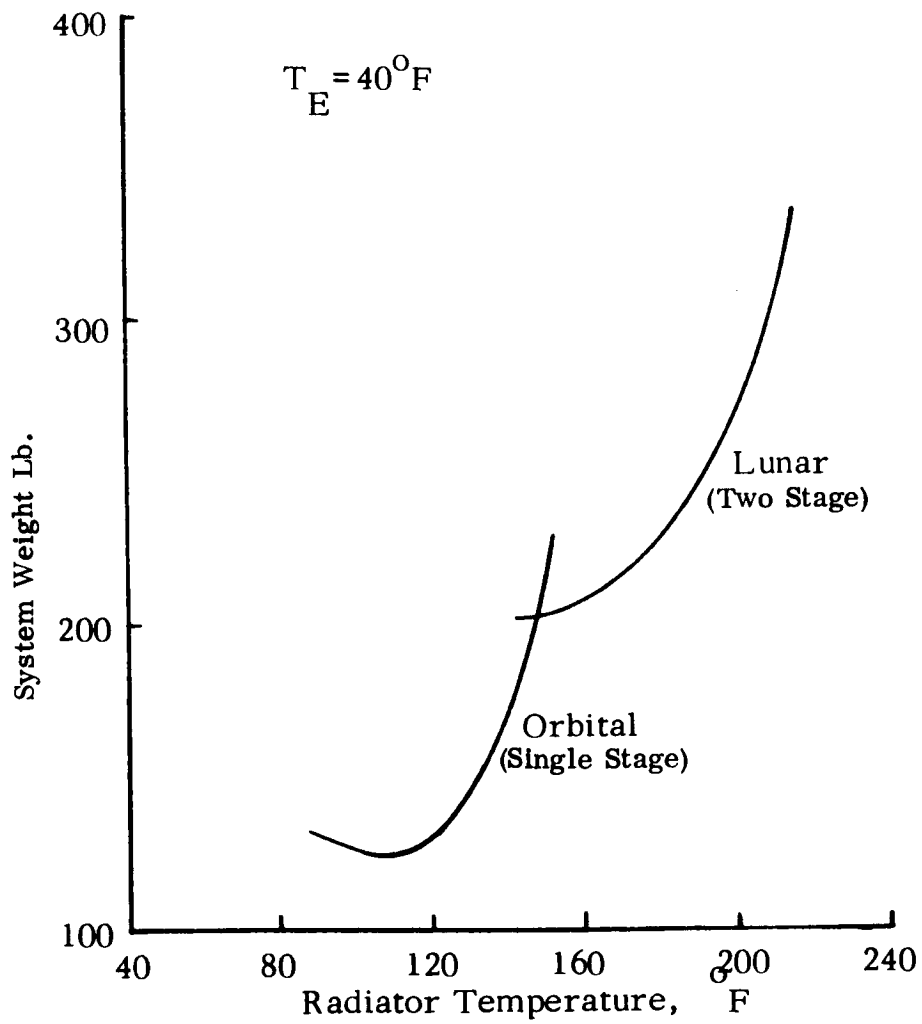


Figure 4.7 Vapor Absorption Refrigerator Weights (vs. Radiator Temperature)

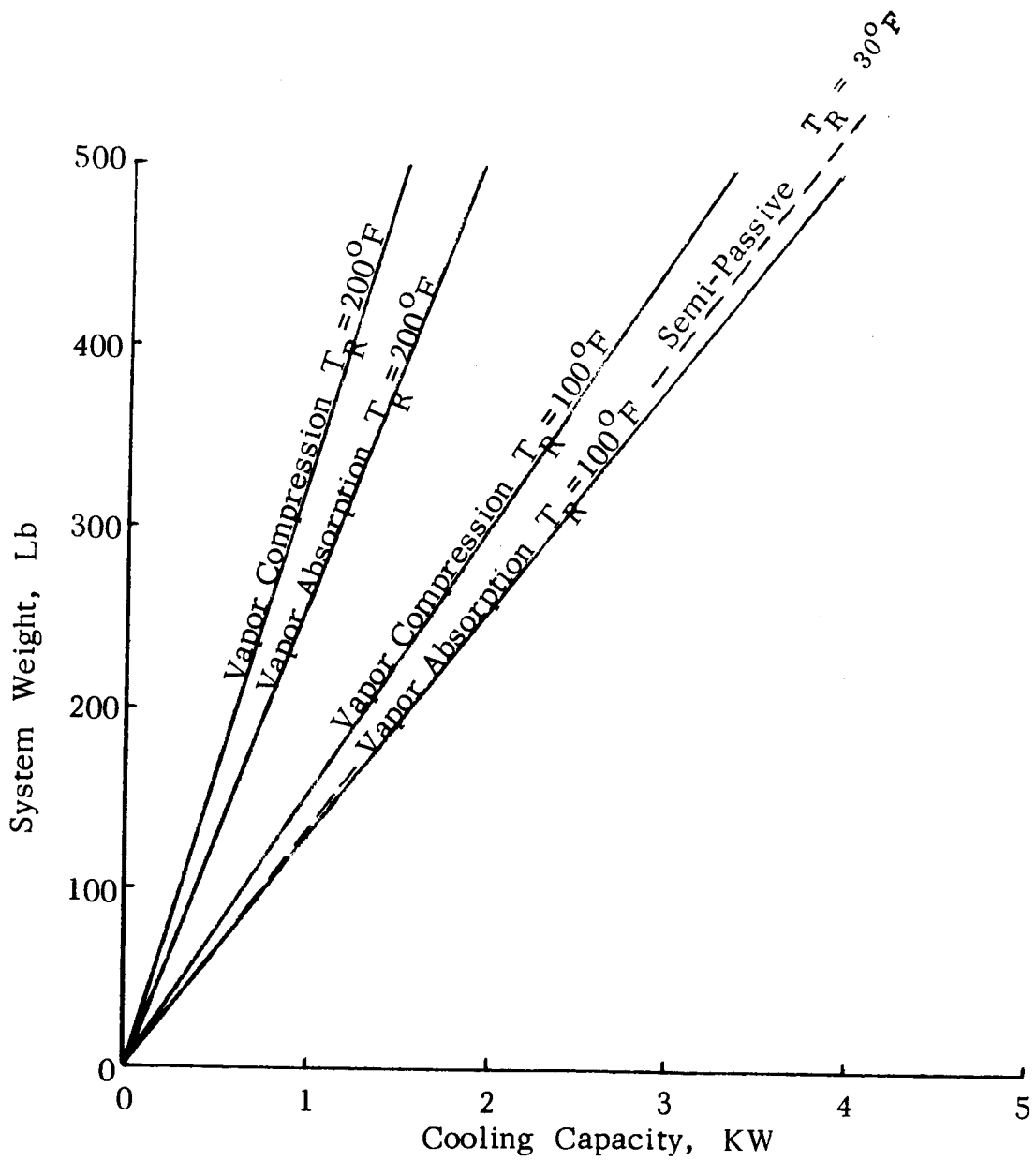


Figure 1.1 Thermal Control Systems Weight Comparison on the Basis of Cooling Capacity

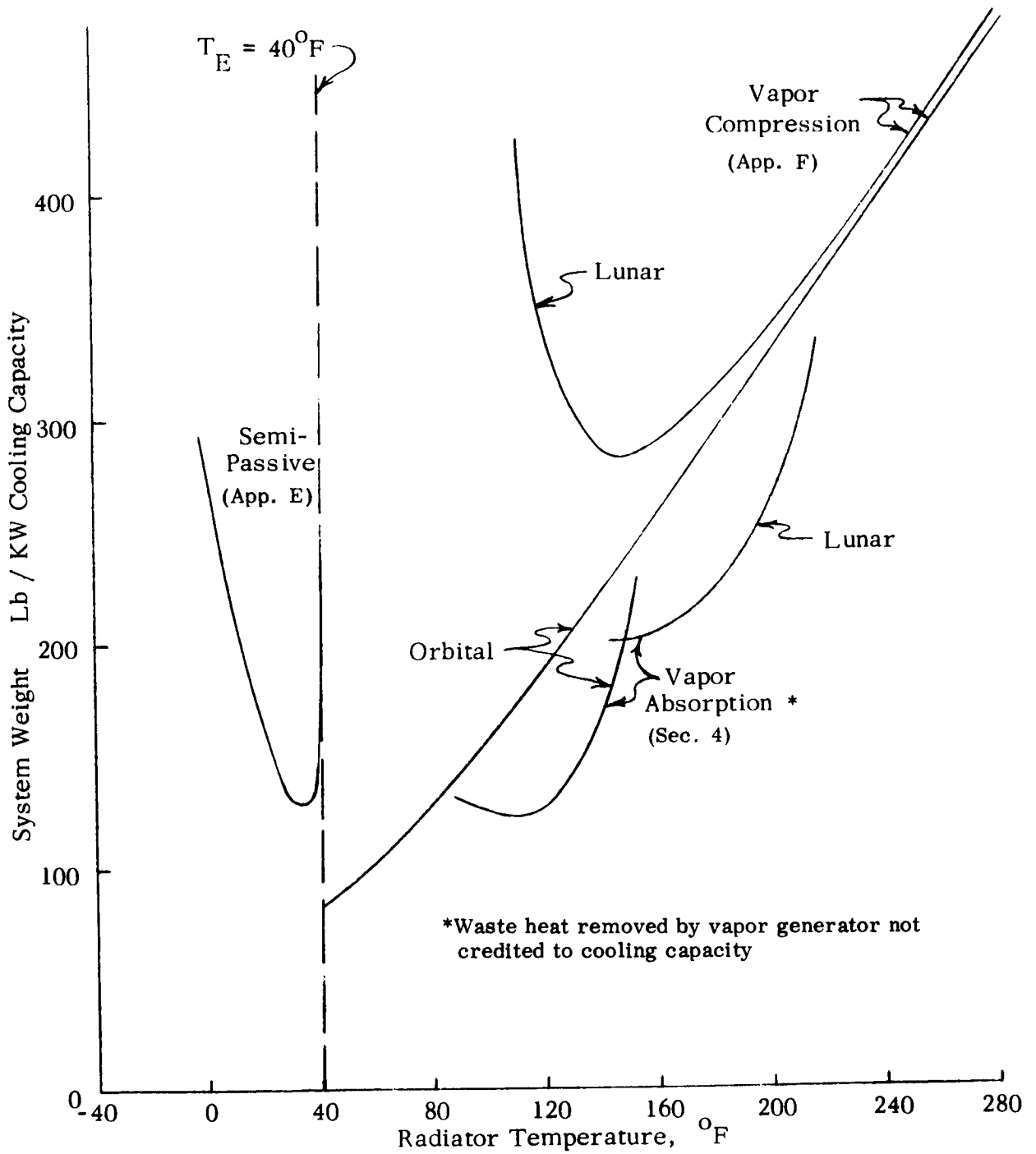


Figure 1.2 Thermal Control Systems Weight Comparison on the Basis of Radiator Temperature

90 % of the system weight. As a general matter an optimum will occur when no one factor dominates. Such is the case with the vapor absorption system.

Section 5
REFERENCE SYSTEMS DESIGNS

A wide variety of refrigerator applications could potentially benefit from the use of a vapor absorption refrigerator as described in the preceding sections. In Section 4 a general design approach was followed to determine typical vapor absorption system weights as a function of the operating variables. The weights of a comparable semi-passive and vapor compression systems were also determined (Appendices E and F) and compared to the vapor absorption system weights. The designs of Section 4 were not completely optimized.

To develop a deeper understanding of the intricate weight and performance trade-offs possible with the vapor absorption systems, two reference missions were postulated for detailed system designs. The first reference design (Subsection 5.1) was optimized on the basis of weight. The second reference design (Subsection 5.2) was a compromise of design between minimum weight and minimum radiator area.

The two reference missions for which detailed worked example designs were prepared are:

1. Radiation Shield Refrigerator

Cryogenic liquids (such as liquid oxygen and liquid hydrogen) are of interest for long duration interplanetary missions as a source of breathing oxygen and as fuel for fuel cells, propulsion, etc. Present state-of-the-art cryogenic tanks generally use some form of multi-layer insulation to minimize radiation losses into the tank. The total weight penalty of insulated tanks (insulation weight plus weight of liquid boil-off) can be very large for long duration missions. An active refrigeration system that reduces the boil-off rate by providing a low temperature radiation shield could potentially result in a lower total weight penalty than the insulated system.

The mission and system constraints postulated for the design study are:

- a) Mission duration -- 400 days
- b) Radiation shield temperature -- -40°F

- c) Refrigeration load -- 1 KW
- d) Electrical power -- Solar cells
 $O_2 - H_2$ Fuel cells
- e) Thermal power -- 40°F environmental heat
 140°F fuel cell exhaust
 Nuclear element
- f) Fluids -- Freon 22
 Dimethyl ether of tetraethylene glycol

2. Portable Thermal Control System

A portable thermal control system is required to cool and dehumidify the spacesuits used during extra-vehicular activities (EVA). Such a system would best be arranged as a backpack unit. Cooling during EVA excursions is presently being provided by the evaporation of water to the vacuum of space. As missions become longer the amount of water required for EVA thermal control increases proportionately. For longer missions an active refrigeration system not requiring the use of an expendable material could potentially result in a lower launch weight penalty.

The mission and system constraints postulated for the design study and optimization are:

- a) Mission duration -- 90 days
- b) EVA duration -- 4 hours daily
- c) Evaporator temperature -- 40°F
- d) Refrigeration load -- 2500 Btu/hr maximum
- e) Electrical power -- Rechargeable batteries
- f) Thermal power -- Nuclear element
- g) Fluids -- Freon 22

Dimethyl ether of tetraethylene glycol

For each of these designs the performance of the refrigeration cycle was calculated using the computer program listed in Appendix A and explained in Section 2. The weights of the different components were calculated using the expressions developed in Section 3 and Appendix C which relate the component weights to their required performance.

The fluid pair selected for both designs is Freon 22 and dimethyl ether of tetraethylene glycol. A maximum generator temperature of 350°F has been selected as the highest practical operating temperature for continuous operation without the serious possibility of decomposition of the Freon.

5.1 Radiation Shield Refrigerator

The first task of the design optimization was to determine the optimum generator temperature (T_G). Computer calculations were made to determine the system weights for various generator and radiator temperatures. The absorber and condenser temperatures were assumed to be equal for this set of calculations. (Previous experience has shown that at optimum conditions the radiator temperatures, absorber and condenser, will be very nearly equal.) The results of these calculations are shown in Fig. 5.1(a).

The points of minimum system weight for each T_G on Fig. 5.1(a) are replotted in Fig. 5.1(b) as a function of T_G . The vertical limit line at 350°F represents the maximum temperature that the Freon 22 refrigerant can be run without resulting in serious decomposition.

It is apparent that no definite optimum generator temperature exists within the region of interest. However, above 250°F , there is virtually no weight reduction with increase of T_G . Since the rate of decomposition of Freon is higher at higher temperatures, 250°F was selected as the most desirable operating temperature.

In the above calculations the absorber and condenser temperatures were assumed to be equal. It is unlikely that this condition would actually be the true optimum. The second task of the design optimization is, therefore, to determine the proper optimum absorber and condenser temperatures.

In Fig. 5.2(a) are plotted the total system weights as a function of absorber temperature (T_A) for four values of condenser temperature (T_C), all for a generator temperature of 250°F as specified above. The points of minimum system weight for each T_C are then replotted in Fig. 5.2(b) as a function of T_C . Also

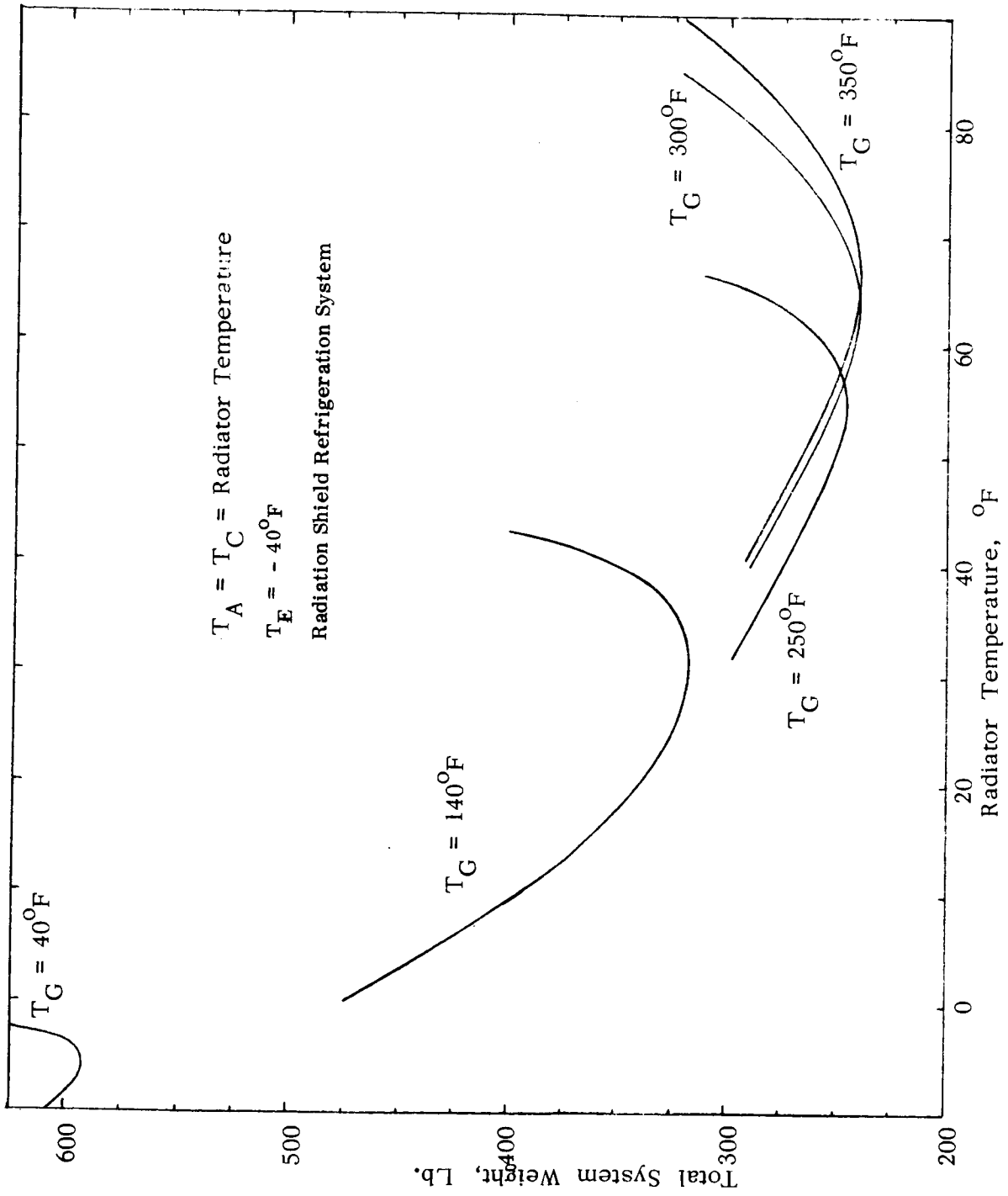


Figure 5.1 (a) Generator Temperature Optimization

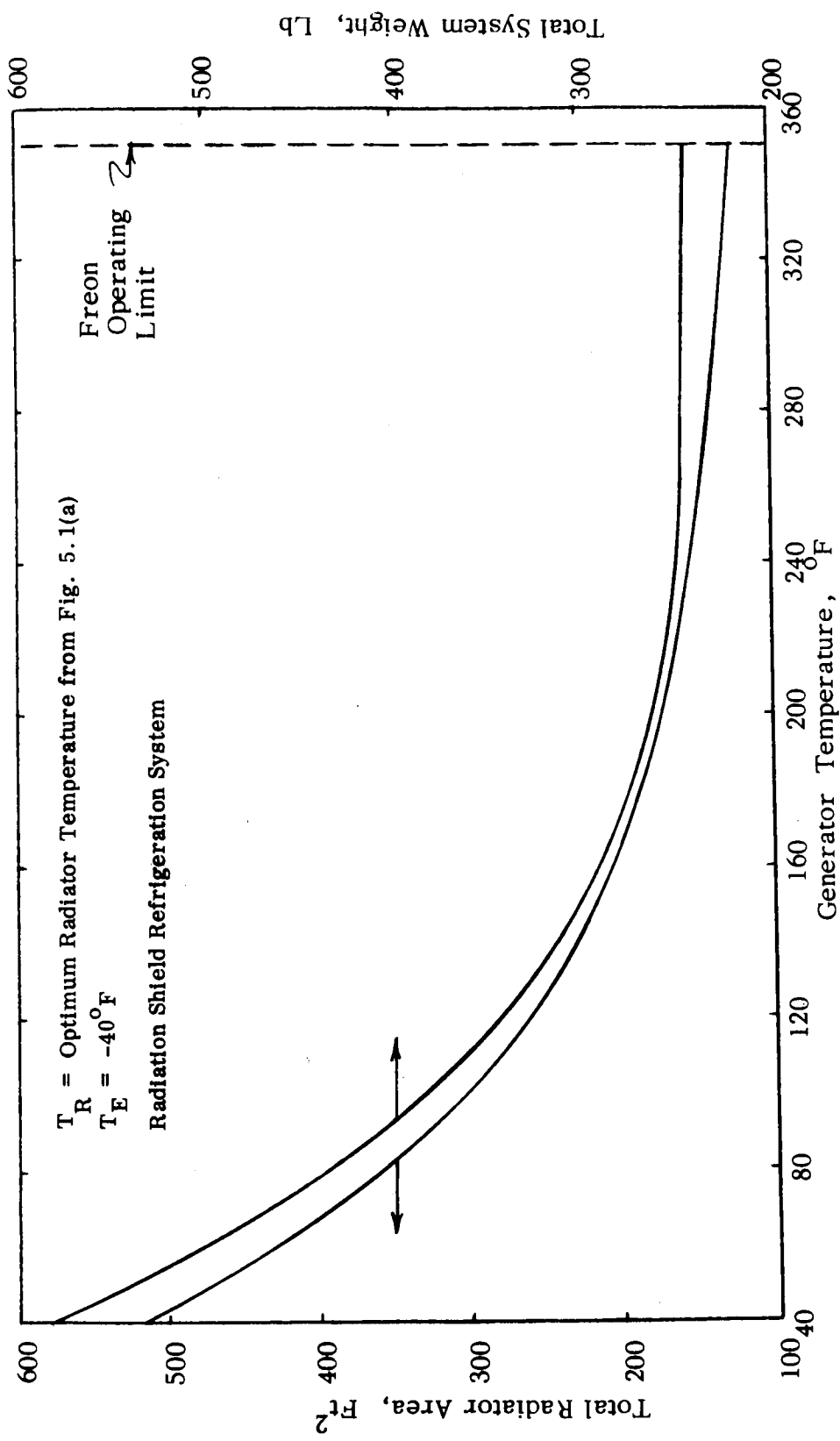
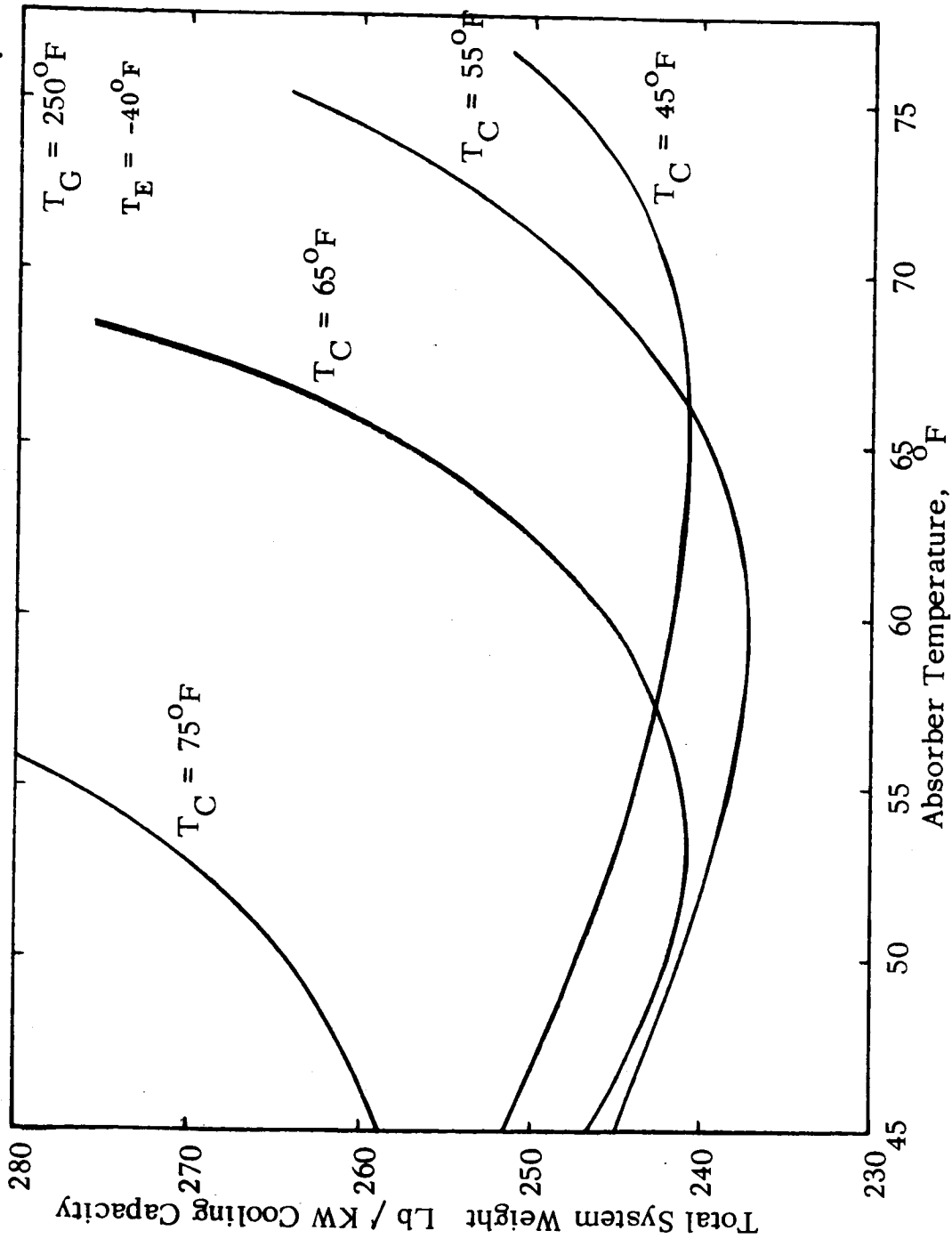


Figure 5.1 (b) Generator Temperature Optimization



Radiation Shield Refrigerator System

Figure 5.2 (a) Radiator Temperature Optimization

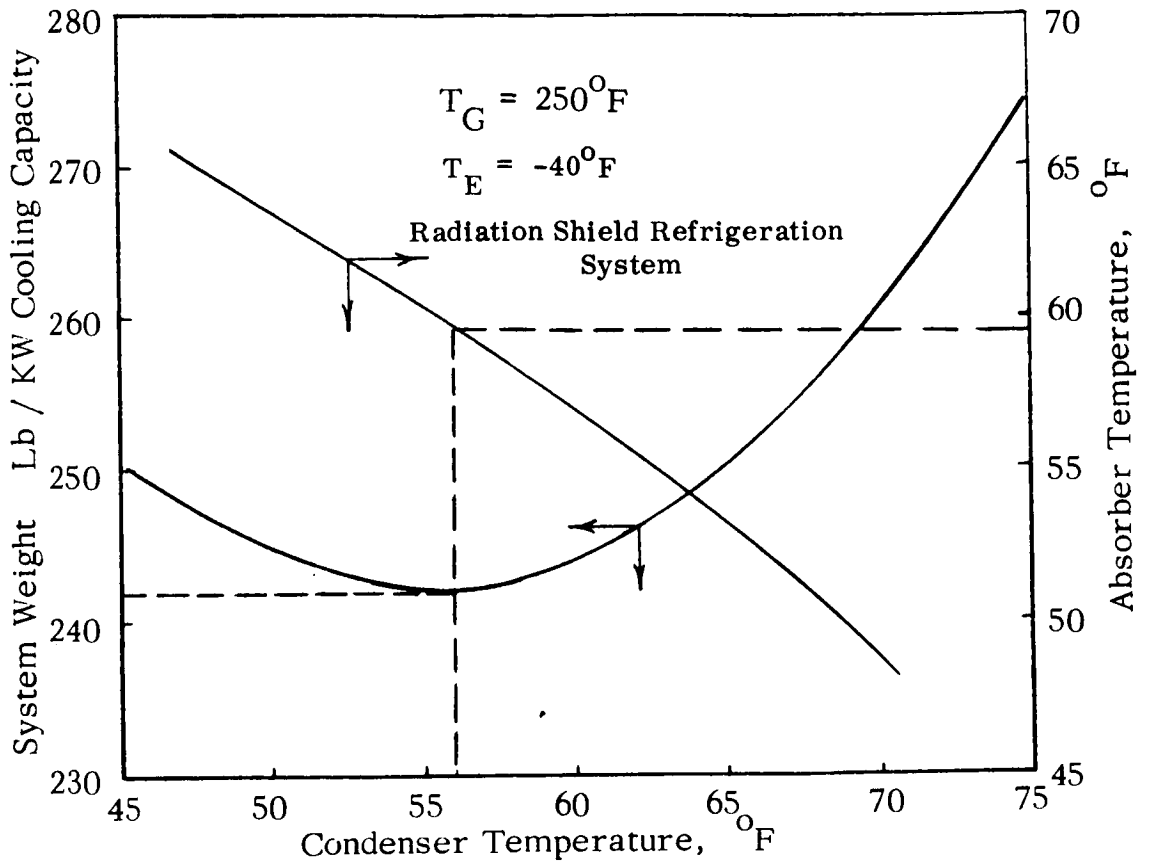


Figure 5.2 (b) Radiator Temperature Optimization

on Fig. 5.2(b) are plotted the absorber temperatures at which the minimum weights occur. The optimum system design is seen from Fig. 5.2(b) to occur at $T_C = 56^\circ\text{F}$ and $T_A = 59^\circ\text{F}$. The system weight at this optimum is at a minimum of 242 pounds.

The cycle parameters and component weights for the optimum system design are summarized in Table 5.1 and Fig. 5.3. A conceptual general arrangement of the cryogenic storage tank and radiation shield refrigerator system is shown in Fig. 5.4.

Table 5.1
OPTIMUM RADIATION SHIELD REFRIGERATOR DESIGN

<u>Component</u>	<u>Temperature</u>	<u>Weight</u>
Generator	250 ^o F	7.8 lbs.
Condenser	56 ^o F	78.3 lbs.
Absorber	59 ^o F	67.0 lbs.
Evaporator	-40 ^o F	1.6 lbs.
Recuperator	--	5.0 lbs.
Sub-Cooler	--	1.1 lbs.
Pump	--	1.0 lbs.
Heat Source	--	49.6 lbs.
Power Weight Penalty	--	11.0 lbs.
Miscellaneous	--	<u>19.6 lbs.</u>
System Total	--	242.0 lbs.

5.2 Portable Thermal Control System

The radiation shield refrigerator of the previous section was optimized on the basis of minimum weight. The portable thermal control system, although the weight is still a very important consideration, must pay greater attention to the radiator area. A overly large extended area would be cumbersome to maneuver.

There is an advantage in having the two radiators (condenser and absorber) combined into one piece of hardware for the backpack system. As the optimum radiator temperatures for the previous design were so nearly equal, any penalty associated with forcing the radiators here to be at the same temperature should be negligible.

Calculations were made for the system weights and radiator areas as a function of radiator temperature for two values of generator temperature. These results are shown in Fig. 5.5.

To optimize on the basis of minimum radiator area the highest generator temperature (350°F) should be used. At the optimum radiator temperature for minimum radiator area, however, the system weight is more than doubled its minimum value. The rate of increase of radiator area as the radiator temperature is reduced from its optimum is very small initially while the weight reductions are considerable. A compromise design is most desirable. By operating at a radiator temperature of 110°F the radiator area is only about 5 ft² above its minimum value and the weight is at its minimum value for the generator temperature used.

The component weights and operating conditions for the portable thermal control system design are summarized in Table 5.2 and Fig. 5.6. A conceptual general arrangement of the portable thermal control system is shown in Fig. 5.7.

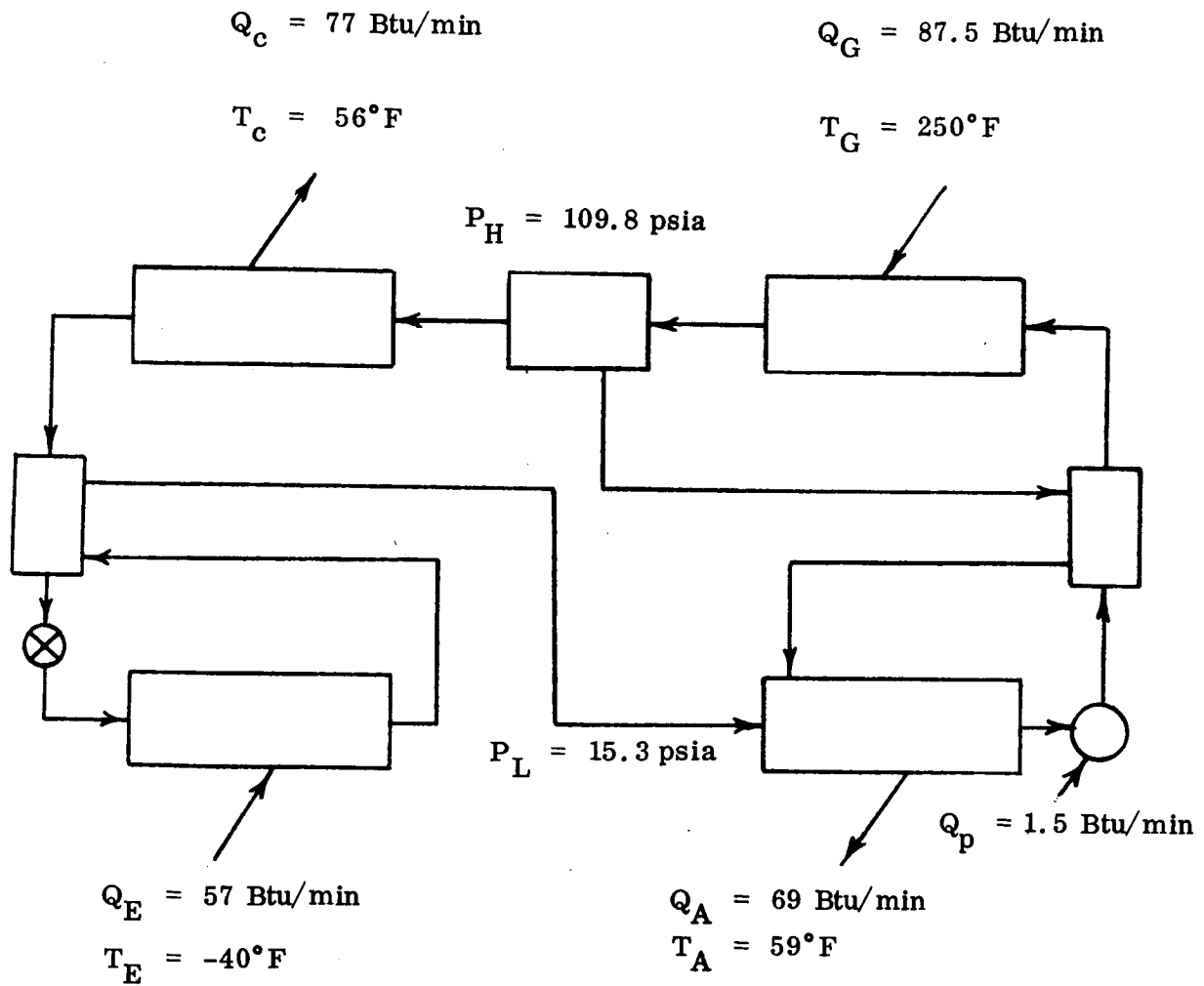


Figure 5.3 Radiation Shield Refrigerator Operating Parameters

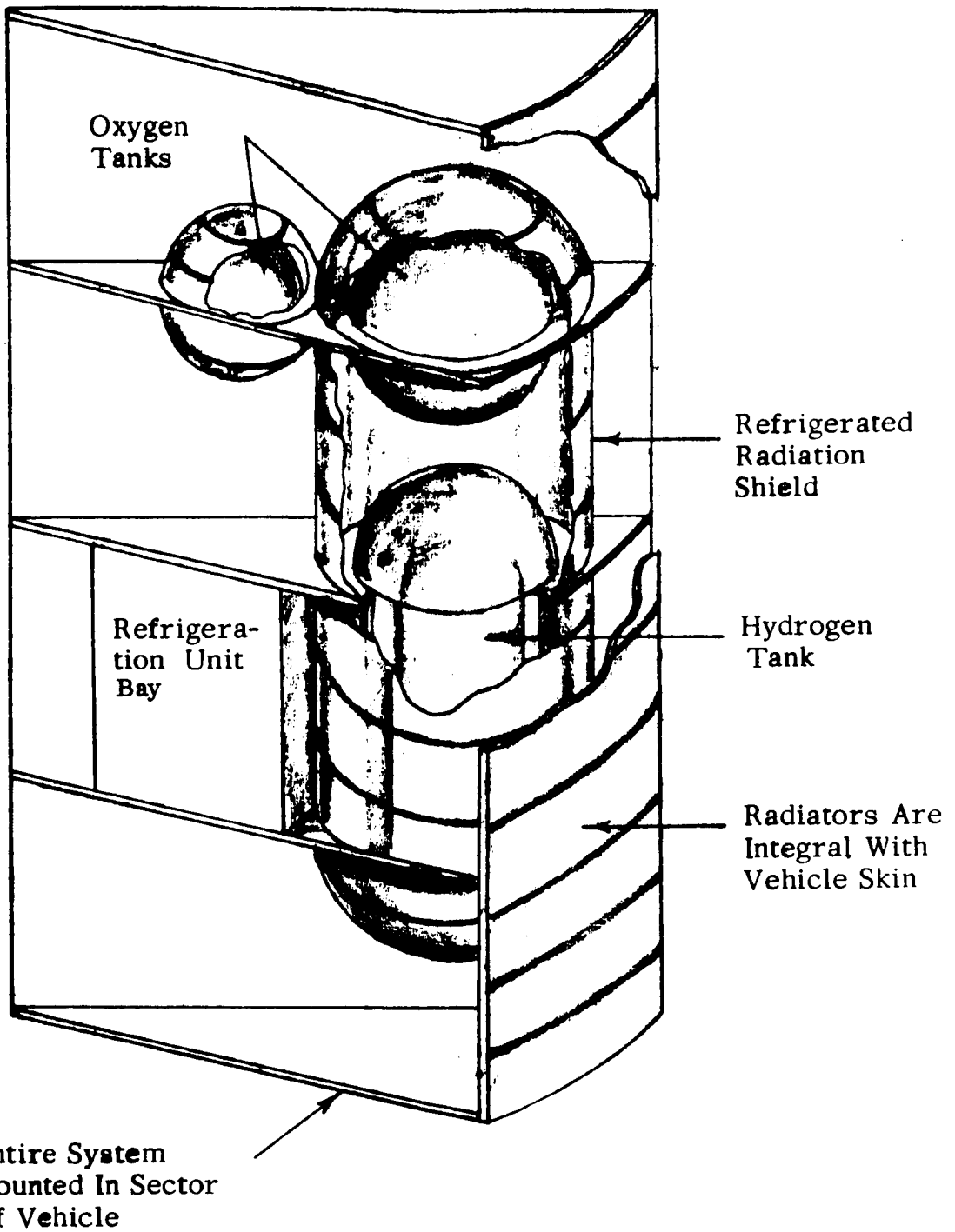


Figure 5.4 General Arrangement -- Radiation Shield Refrigerator

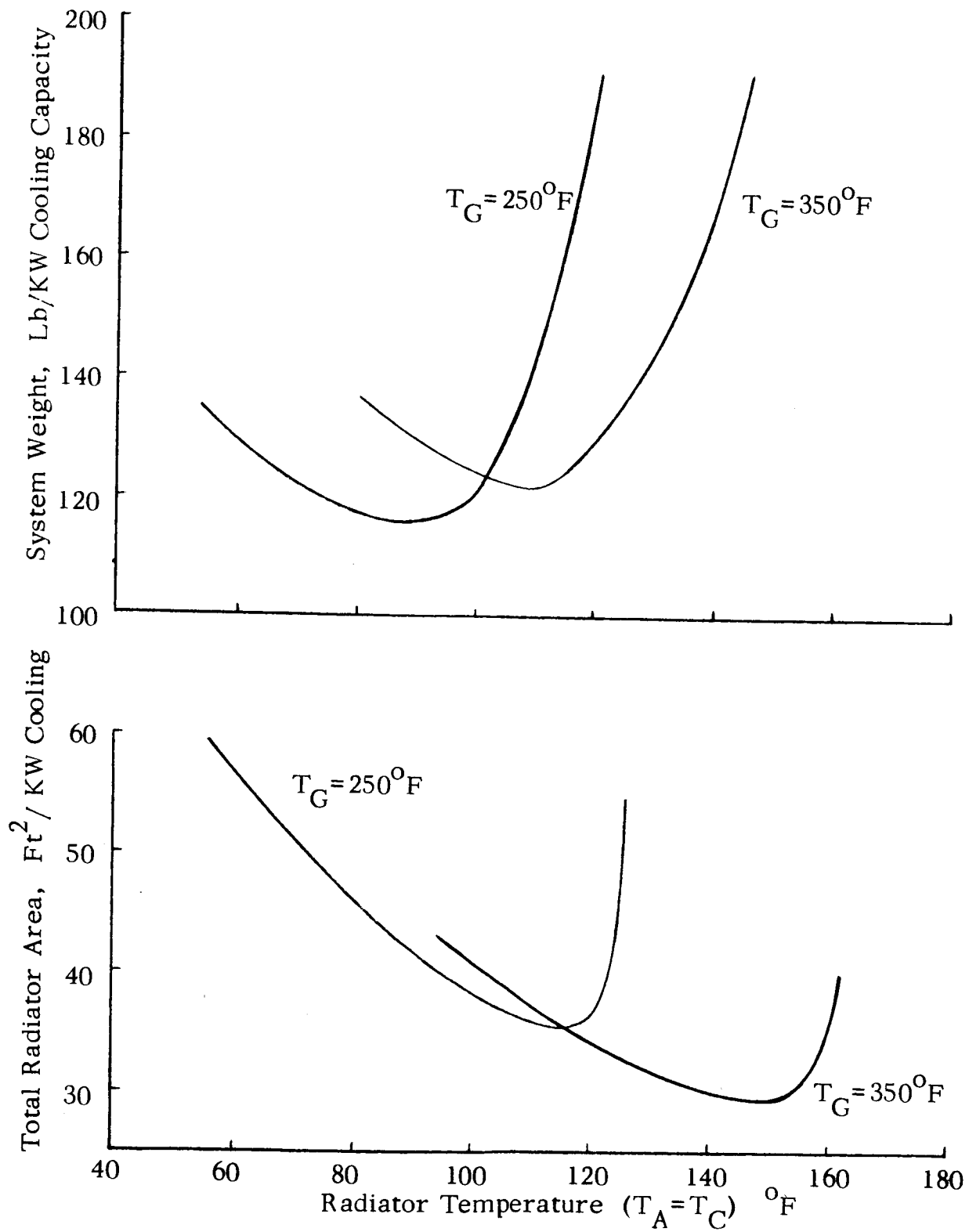


Fig. 5.5 Portable Thermal Control System Weight and Radiator Area

Table 5.2
PORTABLE THERMAL CONTROL SYSTEM DESIGN

<u>Component</u>	<u>Temperature</u>	<u>Weight</u>
Generator	350 ^o F	5.4 lbs.
Condenser	110 ^o F	15.8 lbs.
Absorber	110 ^o F	11.7 lbs.
Evaporator	40 ^o F	1.2 lbs.
Recuperator	--	1.1 lbs.
Sub-Cooler	--	0.7 lbs.
Pump	--	0.4 lbs.
Heat Source	--	40.7 lbs.
Power Weight Penalty	--	7.3 lbs.
Miscellaneous	--	<u>4.7</u> lbs.
System Total		89.0 lbs.

$$Q_c = 63 \text{ Btu/min}$$

$$T_c = 110^\circ\text{F}$$

$$Q_G = 66 \text{ Btu/min}$$

$$T_G = 350^\circ\text{F}$$

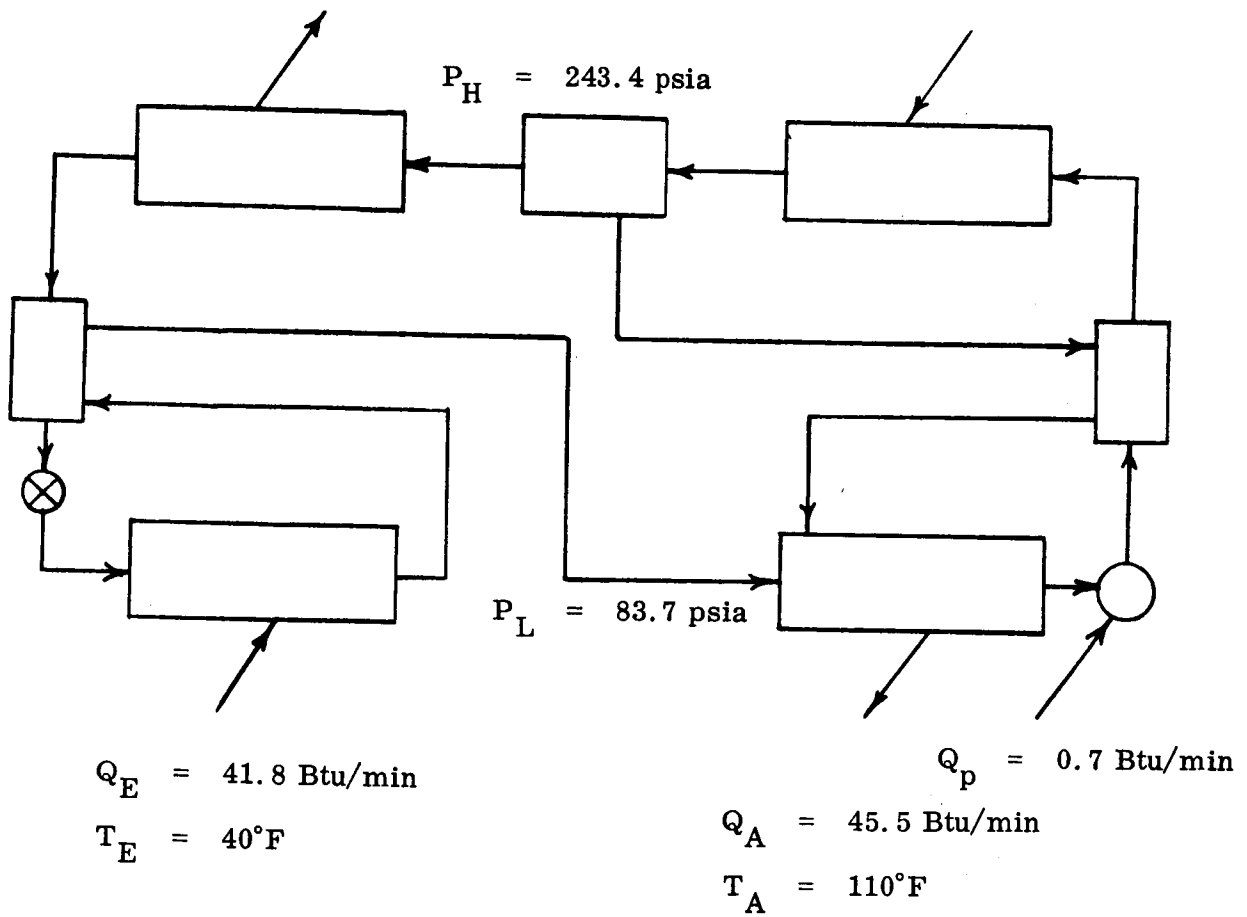


Figure 5.6 Portable Thermal Control System Operating Parameters

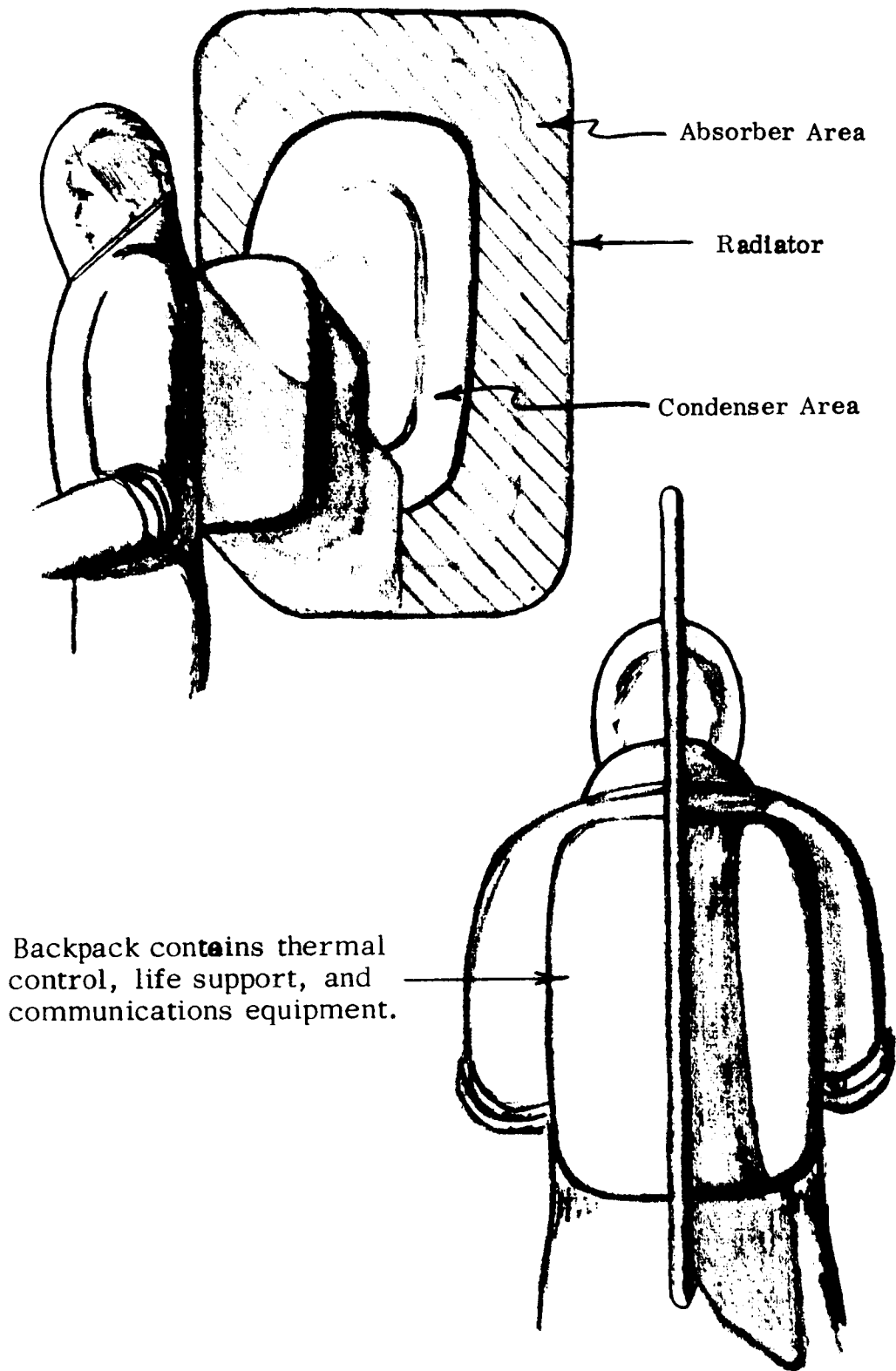


Figure 5.7 General Arrangement -- Portable Thermal Control System

Section 6
CONCLUSIONS AND RECOMMENDATIONS

Contract NASW-1372 was originally directed toward determining the feasibility of using electrohydrodynamic (EHD) forces to augment the operation of gravity dependent components of the vapor absorption refrigerator and thereby permit operation of the refrigerator in weightless environments. The fact that the vapor absorption system is driven primarily by thermal power and that waste heat is normally available on space vehicles which could be used to drive the system was the primary reason for initiating the study.

During the course of the study the possibility of using methods other than EHD for augmentation of the component operations became evident. The conclusion of this study is that the optimum (minimum weight, maximum reliability) system would use the following critical component designs:

1. Condenser -- condensing radiator with uniform, small diameter tubes
2. Evaporator -- twisted tape in tube to induce centrifugal forces on the liquid
3. Absorber -- ejector principle with the ejector tubes integrated directly with the radiator
4. Vapor generator -- twisted tape as in the evaporator
5. Liquid/vapor separator -- wick "sock" type device

Component weights were determined approximately for typical component designs covering a wide range of operating parameters. Systems were designed and their weights determined on the basis of the component weights. Weights of semi-passive and vapor compression refrigerator systems were determined for system cooling capacities matching the capacity of the vapor absorption system designs.

Comparison of the weights of semi-passive, vapor compression, and vapor absorption systems indicated a definite advantage of the vapor absorption system over the other competing systems.

The cooling requirements for space applications (lightweight, gravity independent, heat driven) were recognized as also being the requirements for cooling

systems for a wide variety of applications not related to space missions. Typical examples are airborne, mobile, and portable (backpack) systems.

The results of this report indicating feasibility in conjunction with the wide interest and applicability of such a system, if developed, strongly support the suggestion to fabricate and test a complete, operational vapor absorption refrigerator. It is recommended that a laboratory breadboard refrigerator be assembled, using the components specified above, and that this breadboard model be tested in all orientations in 1 g. Having demonstrated such gravity independence, an operational system could be constructed for space operation and ground tested.

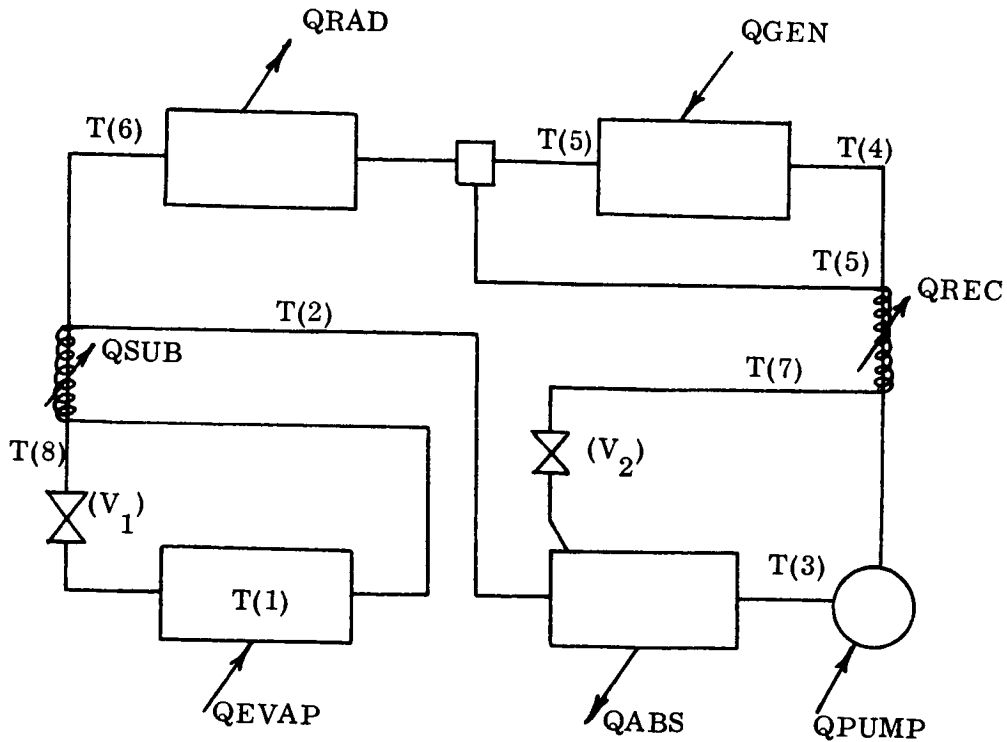
REFERENCES

1. Freon Technical Bulletin B-2, Published by E. I. duPont de Nemours.
2. Eiseman, B. J., "A Comparison of Fluoralkane Absorption Refrigerants," ASHRAE Journal 1, 45, No. 12 (December 1959).
3. Roberson, J. P., et al., "Vapor Pressure of Ammonia and Methylamines in Solutions for Absorption Refrigeration Systems," Presented at ASHRAE Semiannual Meeting, Houston, Texas (January 24-27, 1966).
4. Feldmanis, C. J., "Performance of Boiling and Condensing Equipment under Simulated Outer Space Conditions," ASD-TDR-63-862, Wright-Patterson Air Force Base, Ohio (November 1965).
5. Ginwala, Kymus, "Engineering Study of Vapor Cycle Cooling Equipment for Zero-Gravity Environment," WADD Technical Report 60-776, Wright-Patterson Air Force Base, Ohio (January 1961).
6. Honea, F. I., Bacha, C. P., and Watanabe, D., "Temperature Control Systems for Space Vehicles," Aeronautical Systems Division Technical Documentary Report No. ASD-TDR-62-493, Part I, Wright-Patterson Air Force Base, Ohio (May 1963).
7. Rohsenow, W. M., and Choi, H., Heat, Mass, and Momentum Transfer, Prentice-Hall, Inc., New Jersey (1961) p. 192.
8. Eckert, E. R. G., and Drake, R. M., Jr., Heat and Mass Transfer, McGraw-Hill Book Company, Inc., New York (1959).
9. McAdams, W. H., Heat Transmission, McGraw-Hill Book Company, Inc., New York (1954).
10. Costello, C. J. and Redeker, E. R., "Boiling Heat Transfer and Maximum Heat Flux for a Surface with Coolant Supplied by Capillary Wicking," Chemical Engineering Progress Series, Heat Transfer Houston, No. 41, Vol. 59 (1963).
11. Langston, L. S., Sherman, A., and Hilton, B. H., "Vapor Chamber Fin Studies," National Aeronautics and Space Administration Contract NAS3-7622, First Quarterly Report NASA CR-54882 (September 1965), Second Quarterly Report NASA CR-54922 (January 1966), Third Quarterly Report NASA CR-54989 (April 1966).
12. Reynolds, J. M., "Stability of an Electrostatically Supported Fluid Column," The Physics of Fluids, 8, 1 (January 1965) 161-170.
13. Melcher, J. R., Field Coupled Surface Waves, MIT Press, Cambridge, Massachusetts (1963).
14. Malkus, W. V. R., and Veronis, G., "Surface Electroconvection," The Physics of Fluids, 4, 1 (January 1961), 13-23.
15. Brown, G. A., and Miguel, J., "An Analytical and Experimental Investigation of a Condensing Ejector with a Condensable Vapor," AIAA Paper 64-469 (1964).

16. Denhigh, K. G., Principles of Chemical Equilibrium, Cambridge University Press, (1961) p. 238.
17. Colburn, A. P., and Schoenborn, E. M., Trans. AIChE, 41, (1945), p. 421.
18. Mastrangelo, S. V. R., "Solubility of Some Chlorofluorohydrocarbons in DME-TEG," ASHRAE Journal 1, 64 No. 10 (October 1959).
19. Mackay, Donald B., Design of Space Power Plants, Prentice-Hall, Inc., Englewood Cliffs, New Jersey (1963).
20. Mackay, D. B., and Bacha, C. P., "Space Radiator Analysis and Design: Parts I & II," Air Force Systems Command, Wright-Patterson Air Force Base, Ohio, ASD-TR-61-30 (Part I, 1961, Part II, 1962).
21. Goetzel, C. G., Rittenhouse, J. B., and Singletary, J. B., Space Materials Handbook, Addison-Wesley Publishing Company, Inc., Reading, Massachusetts (1965).
22. Whipple, F. L., "On Meteoroids and Penetration," Interplanetary Missions Conference, Los Angeles (January 1963).
23. Kays, W., and London, A. L., Compact Heat Exchangers, 2nd Edition, McGraw-Hill (1964).
24. Shaffer, A., "Analytical Methods for Space Vehicle Atmospheric Control Processes," ASD Technical Report 61-162, Part I, Wright-Patterson Air Force Base, Ohio (December 1961).
25. "Source Data for Promethium-147," Isochem, Incorporated, Richland, Washington.
26. Reynolds, J. M., Choi, H. Y., Mela, R. L., and Hurwitz, M., "Design Study of a Liquid Oxygen Converter for Use in Weightless Environments," AMRL-TDR-63-42, Wright-Patterson Air Force Base, Ohio (1963).
27. Woods, R. W., and Erlanson, E. P., "Thermal Integration of Electric Power and Life Support Systems for Manned Space Stations," NASA-CR-543, (September 1966).
28. Hanson, K. L., "Thermal Integration of Electrical Power and Life Support Systems for Manned Space Stations," NASA-CR-316 (November 1965).
29. Nauman, R. J., "Pegasus Satellite Measurements of Meteoroid Penetration (Feb. , 16-July 20, 1965)," NASA Technical Memorandum x-1192, George C. Marshall Space Flight Center, Huntsville, Alabama, (December, 1965).

APPENDIX A

A.1 Cycle Analysis



The program listed below calculates the cycle performance for a system using Freon 22 and DME-TEG. The relevant points of the program are listed below.

1. The refrigerant vapor enthalpies (HVHI and HVLO) were calculated from an equation derived by fitting a curve to the Mollier chart of F-22. This defined the enthalpy of vapor as a function of pressure and temperature.

2. The liquid refrigerant enthalpy was assumed to be essentially unaffected by the pressure, and equal to the enthalpy of saturated liquid at the system temperature.

3. The specific heat of the solvent was assumed constant within our temperature range and the solvent enthalpy is therefore directly proportional to the system temperature.

4. Heats of mixing were assumed to be small compared to latent heats, and enthalpies of the liquid mixture are therefore proportional to the composition of the liquid.

5. It was assumed that pressure drops due to fluid flow were small except through the throttle valves V_1 and V_2 . The high pressure (PHI) is therefore the refrigerant vapor pressure at the condenser temperature, while the low pressure (PLO) is the refrigerant pressure at the evaporator temperature.

6. An absorber efficiency (ETAA) was defined as:

$$ETAA = \frac{XA - XG}{XA - XGE},$$

where XA and XG are the refrigerant mole fractions in the strong and in the weak solutions respectively. XGE is the equilibrium refrigerant mole fraction under the pressure and at the temperature of the generator. ETAA was assumed to be = 0.8.

7. A generator efficiency (ETAG) was defined as:

$$ETAG = \frac{XA - XG}{XAE - XG}.$$

Here XAE is the equilibrium refrigerant mole fraction under the pressure and at the temperature of the absorber. ETAG was also assumed to be = 0.8.

8. No solvent carryover occurs.

In the particular program listed below, the radiator configuration was such that both absorber and condenser radiated from both sides of their structure.

The final printouts are for QEVAP = 1 KW.

```
00000      DIMENSION T(10),HL(10),HVLO(10),HVHI(10),HAB(10)
00001 C TEMPERATURES IN DEGREES RANKINE
00010      READ:T(1),T(2),T(3),T(4),T(5),T(6),T(7)
00011 C REFRIGERANT-SOLVENT P-T-X DATA
00020      D1=13.856
00021      D2=4810.
00022      D3=4970.
00023      D4=4720.
00024      D5=2.
00030      FWR=86.5
00031      FWA=222.2
```

```

00040      RHOR=74.4
00041      RHOA=62.
00042      DELX=0.02
00043      DELT4=5.
00044      ETAA=0.8
00045      ETAG=0.8
00046      CE=72.
00047      SPHTA=0.447
00051 C EVAPORATOR COOLING CAPACITY IN BTU/MINUTE
00060      QEVAP=57.0
00061 C ENTHALPY CALCULATIONS
00070      PLO=EXPF(-D2/T(1)+D1)
00080      PHI=EXPF(-D2/T(6)+D1)
00090      DO 30 N=1,7
00100      IF(T(N)-664.8) 10,10,20
00110 10    HL(N)=0.316*(T(N)-420.)-0.000383*(T(N)-420.)**2+
00111 1      2.5/(10.**6)*(T(N)-420.)**3
00120      GO TO 30
00130 20    HL(N)=.1542*(T(N)-420.0)+101.5-0.1*PHI*(T(N)/420.)**-2.67
00140 30    CONTINUE
00150      DO 40 N=1,2
00160      HVLO(N)=.154*(T(N)-420.)+101.5-0.1*PLO*(T(N)/420.)**-2.67
00170 40    CONTINUE
00180      HVHI(5)=.154*(T(5)-420.)+101.5-0.1*PHI*(T(5)/420.)**-2.67
00190      DO 50 N=3,7
00200      HAB(N)=SPHTA*(T(N)-420.0)
00210 50    CONTINUE
00211 C PERFORMANCE SEQUENCE
00220      WRL=QEVAP/(HVLO(1)-HL(1))
00230      HL(8)=HL(6)-HVLO(2)+HVLO(1)
00240      WRV=WRL*(HL(8)-HL(1))/(HVLO(1)-HL(8))
00250      X=1.0
00260 60    P=EXPF(((D5-1.)*D4*(1.-X)**3-D3*(1.-X)**2-D2)/T(3)+D1)*X
00270      IF (P-PLO) 75,75,70
00280 70    X=X-DELX
00290      GO TO 60
00300 75    XAE=X
00310      X=0.0
00320 80    P=EXPF(((D5-1.)*D4*(1.-X)**3-D3*(1.-X)**2-D2)/T(5)+D1)*X
00330      IF (P-PHI) 85,90,90
00340 85    X=X+DELX
00350      GO TO 80
00360 90    XGE=X
00370      XA=(ETAG*XGE+ETAA/(1.-ETAA)*XAE)/(ETAG+ETAA/(1.-ETAA))
00380      XG=(ETAA*XAE+ETAG/(1.-ETAG)*XGE)/(ETAA+ETAG/(1.-ETAG))
00390      IF(XA-XG) 251,251,95
00400 95    WRC=(WRL+WRV)*(1.0-XA)*XG/(XA-XG)
00410      WAB=FWA*WRC*(1.0-XG)/(FWR*XG)
00420 C Q VALUES
00421 97    QABS=(WRL+WRV)*HVLO(2)+WRC*HL(7)-(WRL+WRV+WRC)*HL(3)+
00422
00423 1      WAB*(HAB(7)-HAB(3))
00430      QREC=WRC*(HL(5)-HL(7))+WAB*(HAB(5)-HAB(7))

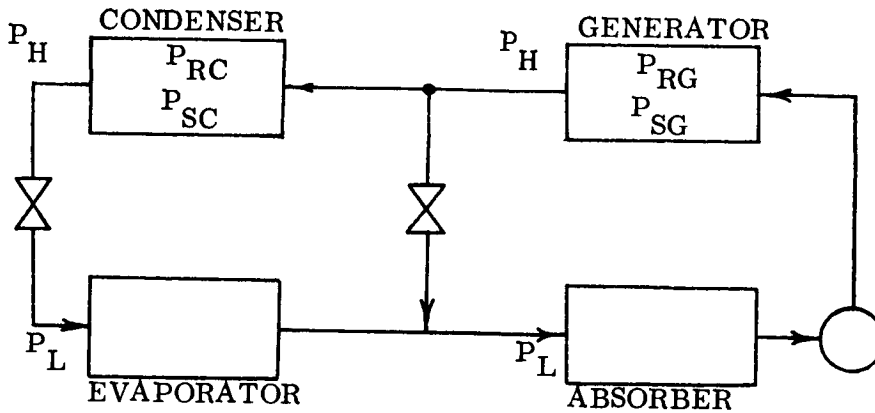
```

```

00440 100  HAB(4)=HAB(3)+(QREC-(WRL+WRV+WRC)*(HL(4)-HL(3)))/WAB
00450      Y=HAB(4)/SPHTA +420.0
00460      IF(Y-T(4)) 110,120,120
00470 110  T(4)=T(4)-DELTA
00471      IF(T(4)-664.8) 112,112,114
00480 112  HL(4)=0.316*(T(4)-420.0)-0.000383*(T(4)-420.0)**2+
00481      1 2.5/(10.**6)*(T(4)-420.0)**3
00482      GO TO 100
00485 114  HL(4)=.154*(T(4)-420.0)+101.5-0.1*PHI*(T(4)/420.0)**-2.67
00490      GO TO 100
00500 120  QGEN=(WRL+WRV)*HVHI(5)+WRC*HL(5)-(WRL+WRV+WRC)*HL(4)+WAB*
00501      1 (HAB(5)-HAB(4))
00510      QCOND=(WRL+WRV)*(HVHI(5)-HL(6))
00520      QSUB=(WRL+WRV)*(HVLO(2)-HVLO(1))
00530      QPUMP=((WRL+WRV+WRC)/RHOR+WAB/RHOA)*0.185*(PHI-PLO)
00531 C SYSTEM MASSES PER UNIT KW COOLING CAPACITY
00540      WE=1.22+0.358
00549 C ABSORBER RADIATING FROM BOTH SIDES
00550      WA=QABS*3412.0/((2.94*10.**-9*T(3)**4-CE)*QEVAP)
00560      WP=0.22+39.5*RHOA*QPUMP/(QEVAP*(PHI-PLO))
00570      WPP=0.0
00575      LMTD=(T(5)-T(4)+T(3)-T(7))/LOGF((T(5)-T(4))/(T(7)-T(3)))
00580      WREC=0.00224*3412.*QREC/(LMTD*QEVAP)
00590      WG=5.01 *QGEN/QEVAP
00599 C CONDENSER RADIATING FROM BOTH SIDES
00600      WC=QCOND*3412./((2.94*10.**-9*T(6)**4-CE)*QEVAP)
00610      WSUB=QSUB*34.12/((T(6)-T(2))*QEVAP)
00619      HOLD=0.1
00620      WTOT=(WE+WA+WP+WREC+WG+WC+WSUB)*(1.+HOLD)+WPP
00621      WLE=0.364*WE
00622      WLREC=1.456*WREC
00623      WLSUB=0.646*WSUB
00624      WTOT=WTOT+WLE+WLREC+WLSUB
00630      PRINT 150,T(1),T(2),T(3),T(4),T(5),T(6),T(7),T(8)
00640 150  FORMAT(15HT VALUES,DEG.R ,/8F8.1 //)
00650      PRINT 200, QEVAP,QABS,QPUMP,QREC,QGEN,QCOND,QSUB
00660 200  FORMAT(16HQ VALUES,BTU/MIN ,/7F8.1 //)
00670      PRINT 250, WE,WA,WP,WPP,WREC,WG,WC,WSUB
00680 250  FORMAT(35HCOMPONENT MASSES IN LBS/KW COOLING ,/8F8.4//)
00690 251  PRINT 260,XA,XG
00700 260  FORMAT(7HXA, XG: ,/2F8.4 //)
00705      PRINT 280, WRL,WRV,WRC,WAB
00706 280  FORMAT(15HWRL,WRV,WRC,WAB ,/4F10.5 //)
00708      PRINT 290, WLE,WLREC,WLSUB
00709 290  FORMAT(30HLIQUID MASSES: WLE,WLREC,WLSUB ,/3F8.4 //)
00710
00711 300  PRINT 310, WTOT
00720 310  FORMAT(32HTHE TOTAL REFRIGERATOR WEIGHT IS ,F10.2)
00730 320  END

```

A.2 Penalties Caused by Solvent Carryover



Let the vapor pressures of the pure refrigerant and solvent at the generator temperature be P_{RG}^0 and P_{SG}^0 respectively. For ideal solutions (for the sake of simplicity), the partial pressures of refrigerant (P_{RG}) and of solvent (P_{SG}) in the generator are:

$$P_{RG} = P_{RG}^0 X_G$$

$$P_{SG} = P_{SG}^0 (1 - X_G)$$

where

$$P_{RG} + P_{SG} = P_H$$

= total pressure on the high pressure side (generator, condenser side)

and so the mole fraction of refrigerant vapor leaving the generator is

$$Y_G = \frac{P_{RG}}{P_H} .$$

Leaving the condenser, all vapors have been condensed and so the mole fractions of refrigerant and solvent are equal to their mole fractions in the vapor leaving the generator. The mole fraction of refrigerant in the condenser liquid, X_C , is then

$$X_C = Y_G = \frac{P_{RG}}{P_H} .$$

The mole fraction of solvent is

$$(1 - X_C) = \frac{P_{SG}}{P_H}$$

$$= \frac{P_{SG}^0 (1 - X_G)}{P_{RG}^0 X_G + P_{SG}^0 (1 - X_G)}$$

The presence of solvent in the liquid entering the evaporator creates a boiling point elevation at the constant total system pressure. This could reduce the effectiveness of the evaporator and require larger refrigerant flow rates through the system than originally estimated.

As an example, take a system using F-22 + DME-TEG as refrigerant and solvent. If the generator is made to operate at 250°F and $X_G = 0.2$, then at this temperature

$$P_{SG}^0 \cong 10 \text{ mm Hg}$$

and

$$P_{RG}^0 \cong 50,000 \text{ mm Hg}.$$

The solvent mole fraction in the condenser liquid is then equal to

$$1 - X_C = \frac{10 \times 0.8}{50,000 \times 0.2 + 10 \times 0.8}$$

$$\cong 0.0008.$$

If a 5°F elevation in boiling point is considered allowable, then at an evaporator temperature level of 40°F, this is equivalent to a change in vapor pressure of the pure refrigerant from 82.5 psia to about 85 psia. In order to calculate the fraction refrigerant evaporated under these conditions, use is made of the fact that the total pressure in the evaporator is constant and approximately equal to the refrigerant vapor pressure (solvent vapor pressure is very low at this relatively low temperature); and so

$$P_L = (P_{RE}^0 X_E)_{in}$$

$$= (P_{RE}^0 X_E)_{out} ;$$

i. e. ,

$$(82.5 X_E)_{in} = (85 X_E)_{out} .$$

Since

$$(X_E)_{in} = X_C = 0.992 ,$$

then

$$(X_E)_{out} = \frac{82.5}{85.0} \times 0.9992 = 0.970 ;$$

and so moles of refrigerant not evaporated per mole of refrigerant introduced in liquid

$$\begin{aligned} &= \left(\frac{0.0008}{0.9992} \times \left(\frac{0.970}{0.030} \right) \right) \\ &= 0.0258 . \end{aligned}$$

A 2.6 per cent increase in flow rate through the system is necessary to maintain the nominal cooling capacity of the refrigerator system, owing to the vaporization of solvent in the generator. Had the refrigerant vapor pressure been lower, or the solvent vapor pressure higher, still larger flow rates would have been necessary. For example, using the F-113 + DME-TEG system at the same temperatures as those used above, the moles refrigerant not vaporized per mole refrigerant introduced into the evaporator would be = 0.05.

If the system F-22 + (some solvent with vapor pressure of 50 mms Hg pressure at 250°F) is used, the fraction of refrigerant not vaporized per unit weight of liquid refrigerant introduced into the evaporator is 0.114. Thus, it is extremely important to choose a solvent with low vapor pressure.

APPENDIX B

B.1 Experimental Determination of Vapor-Liquid Equilibrium

P-T-X data was determined in the apparatus shown in Fig. B-1 . This consisted of a stainless steel cell of approximately 150 cc capacity to which was connected a pressure gauge (0 - 400 psig). The gauge and part of the tubing connecting it to the cell was filled with low vapor pressure oil in order to avoid any transfer of refrigerant into the gauge. A mercury leg was used to separate this oil from the vapor space of the cell.

One part of a "quick-connect" valve was fitted onto the cell to allow the introduction of refrigerant into the system. A small tube fitted with the counter-part of the "quick-connect" was used to transfer known weights of refrigerant from the cylinder to the cell.

The test procedure was as follows:

1. With the cover removed, a known weight of solvent was introduced into the cell. The cover was then tightened in position.
2. The transfer tube was filled with refrigerant and carefully weighed. This tube was then connected to the cell by means of the "quick-connect" valve.
3. After the contents of the tube were discharged into the cell, the tube was disconnected and carefully reweighed. The weight of refrigerant introduced was then obtained by difference.
4. The cell and its contents were placed in a constant temperature bath and left until temperature and pressure readings remained constant. These were then recorded.
5. The temperature of the bath was then changed systematically and the steady state pressure recorded for each temperature.

Correlation of Data

1. The pressure readings were corrected for the air remaining inside the cell.

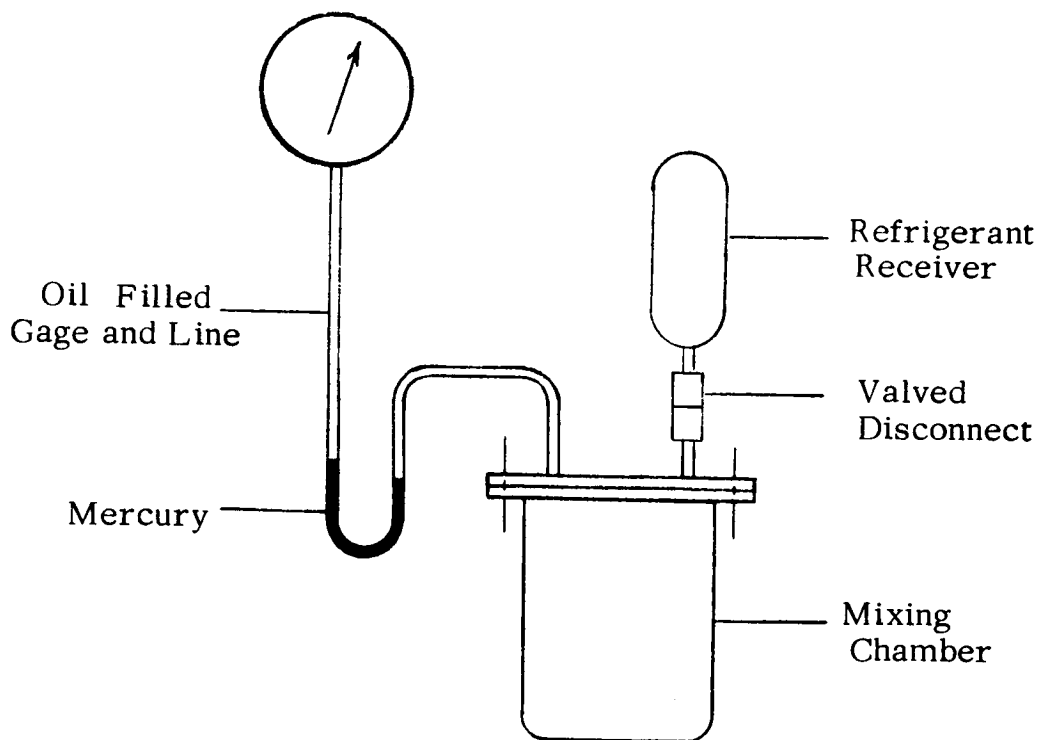


Figure B.1 PTx Apparatus

$$P = \text{True vapor pressure (psia)} = \text{pressure reading (psig)} - \left(\frac{T - T^0}{T^0} \right) \times 14.7$$

where T and T⁰ are the test temperature and room temperature respectively.

2. Refrigerant concentration in the liquid was corrected for the quantity of refrigerant in the vapor.

$$\left(\frac{M_L}{M} \right) = \left(\frac{M_T}{M} \right) - \frac{V \times 273 \times P}{22400 \times T \times 14.7}$$

where M_L and M_T are the weight of refrigerant in the liquid and the total weight of refrigerant introduced, respectively.

M is the refrigerant molecular weight,

V is the volume of the vapor space in cc,

P is the refrigerant vapor pressure, and

T is the test temperature.

3. The mole fraction of refrigerant in the liquid was calculated.

$$X = \frac{(m_L/M)}{(m_L/M) + (m_A/M_A)}$$

where m_A is the weight of absorbent in the system and M_A is its molecular weight.

4. Activity coefficients were calculated:

$$\alpha = \frac{P}{P_X^0}$$

where P⁰ is the pure refrigerant vapor pressure at the test temperature T.

5. For a given refrigerant-absorbent system, the Margules relation was chosen to relate the activity coefficients to the refrigerant mole fractions.¹⁶

$$\text{Log } \alpha = A(1 - X)^3 + B(1 - X)^2$$

where A and B are empirical constants.

The effect of temperature was taken to be of the form

$$T \log \alpha = \text{constant}$$

at constant composition, following the suggestion of Colburn and Schoenborn.¹⁷

The values of

$$\frac{T \log \alpha}{(1 - X)^2}$$

were plotted against $(1 - X)$, and the best straight line drawn through the data.

The pressure of the system at any temperature and any concentration could then be calculated using these data together with the Clausius-Clapeyron relationship.

Results

1. F-22 + DME-TEG

A plot of

$$\frac{-T \log \alpha}{(1 - X)^2}$$

against $(1 - X)$ (see Fig. B-2) in conjunction with the Clausius-Clapeyron relation, yielded the following equation relating the pressure to the system temperature and refrigerant mole fraction.

$$P = X \cdot \exp \left(\frac{4720 (1 - X)^3 - 4970 (1 - X)^2 - 4810 + 13.856}{T} \right)$$

where T is in $^{\circ}\text{R}$ and P is in psia.

2. F-22 + decane

This system most probably follows Raoult's Law, and the system pressure is therefore given by

$$P = X \cdot \exp \left(\frac{-4810}{T} + 13.856 \right)$$

3. F-113 + DME-TEG

This system was also found to follow Raoult's Law. The P-T-X relationship is then given by:

$$P = X \cdot \exp \left(\frac{-6150}{T} + 13.28 \right)$$

4. F-21 + DME-TEG¹⁸

A plot of

$$\frac{-T \log \alpha}{(1 - X)^2}$$

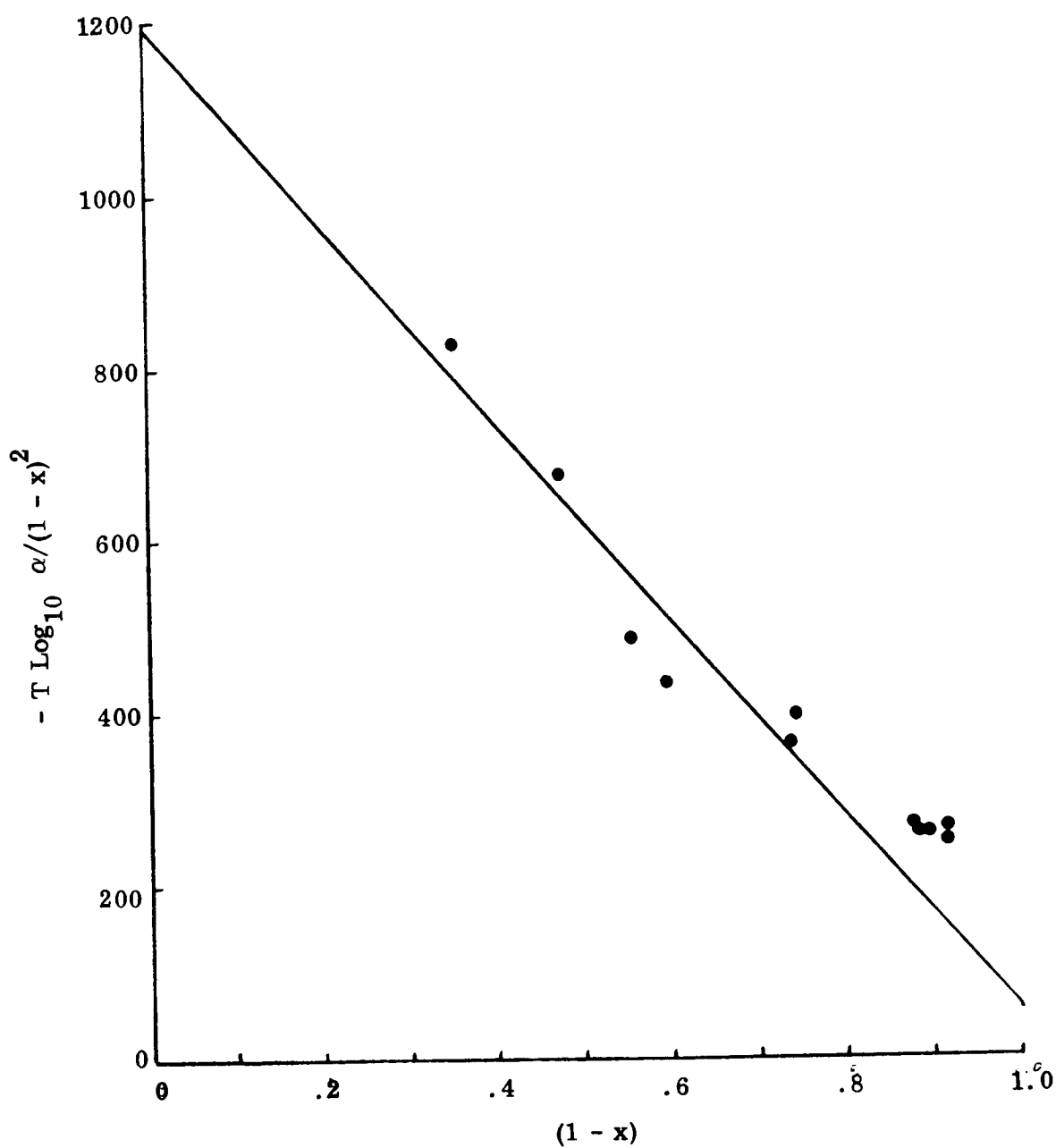


Fig. B.2 Activity Coefficient Correlation -- F 22 & DME-TEG

against $(1 - X)$ for this system is shown in Fig. B-3 . The best fit from this data, in conjunction with the Clausius-Clapeyron relation of F-21 yields the following relation:

$$P = X \cdot \exp \left(\frac{5300[(1 - X)^3 - (1 - X)^2] - 5250}{T} + 13.07 \right) .$$

P is in psia while T is in $^{\circ}$ R.

5. F-22 + decane

This system followed Raoult's Law and hence

$$P = X \cdot \exp \left(\frac{-5250}{T} + 13.07 \right) .$$

6. F-21 + Chlorodecane

The P-T-X relation for this pair is given by:

$$P = X \cdot \exp \left(\frac{-560(1 - X)^3 - 5250}{T} + 13.07 \right) .$$

The activity coefficient relationship is shown in Fig. B-4 .

7. Ammonia - TEG³

The P-T-X relationship for this system was determined by Roberson et al.³

Rearranging their data yields the following:

$$P = X \cdot \exp \left(\frac{3320(1 - X)^3 - 4150(1 - X)^2 - 2390}{T} + 7.05 \right) .$$

B.2 Viscosity

The viscosities of DME-TEG and TEG were determined under a wide range of temperatures. These are plotted in Fig. B-5 .

The viscosity measurement was made by means of a standard Cannon-Fenske viscometer. The viscosity of TEG is considerably higher than that of DME-TEG. The latter is therefore preferable since pressure drops are smaller when it is used. Heat transfer is also expected to be better with the lower-viscosity fluid.

The densities of DME-TEG and TEG at 20° C were determined and found to be = 1.01 and 1.10 gms/cc respectively. A coefficient of thermal expansion

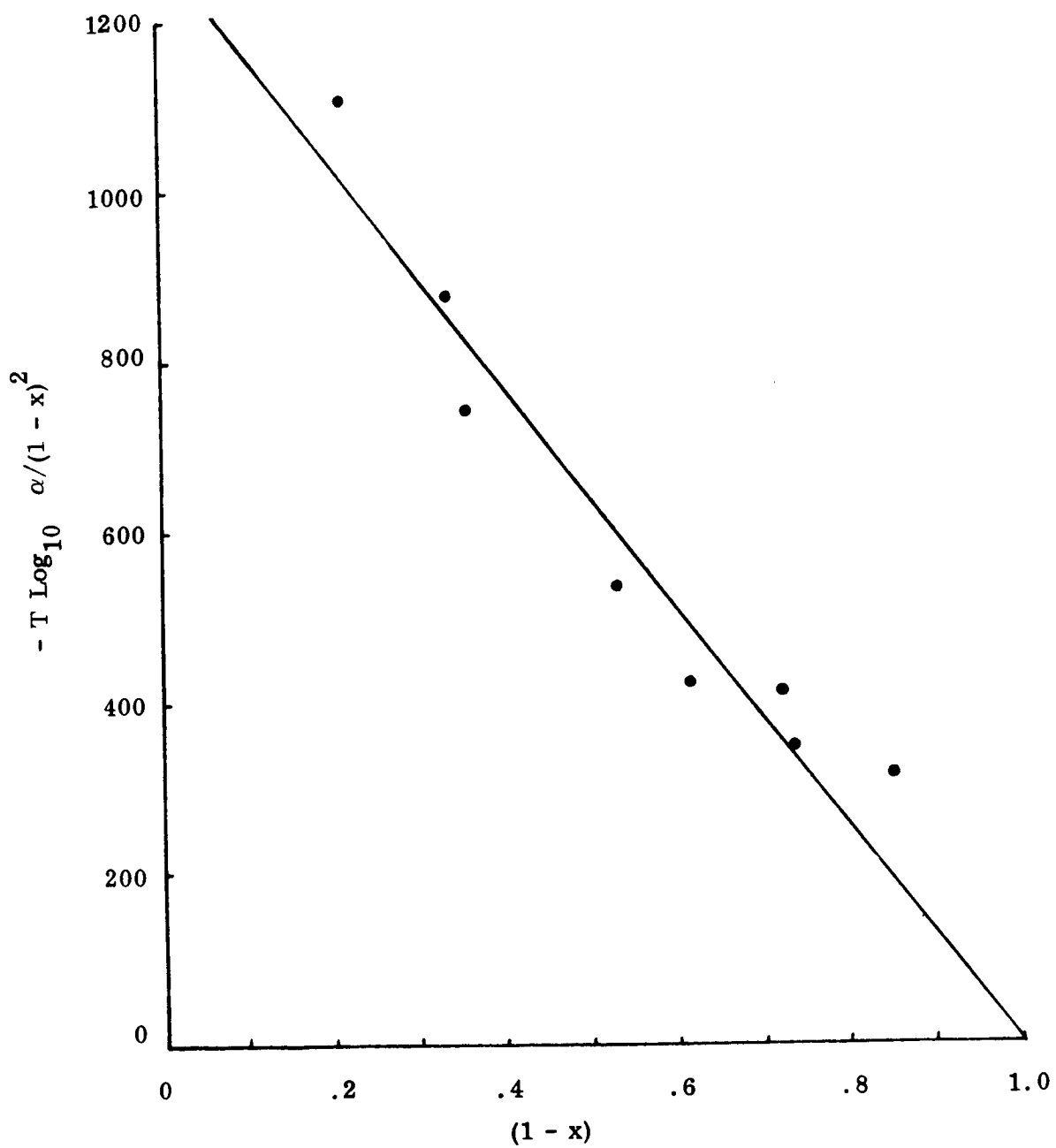


Fig. B.3. Activity Coefficient Correlation -- F 21 & DME-TEG

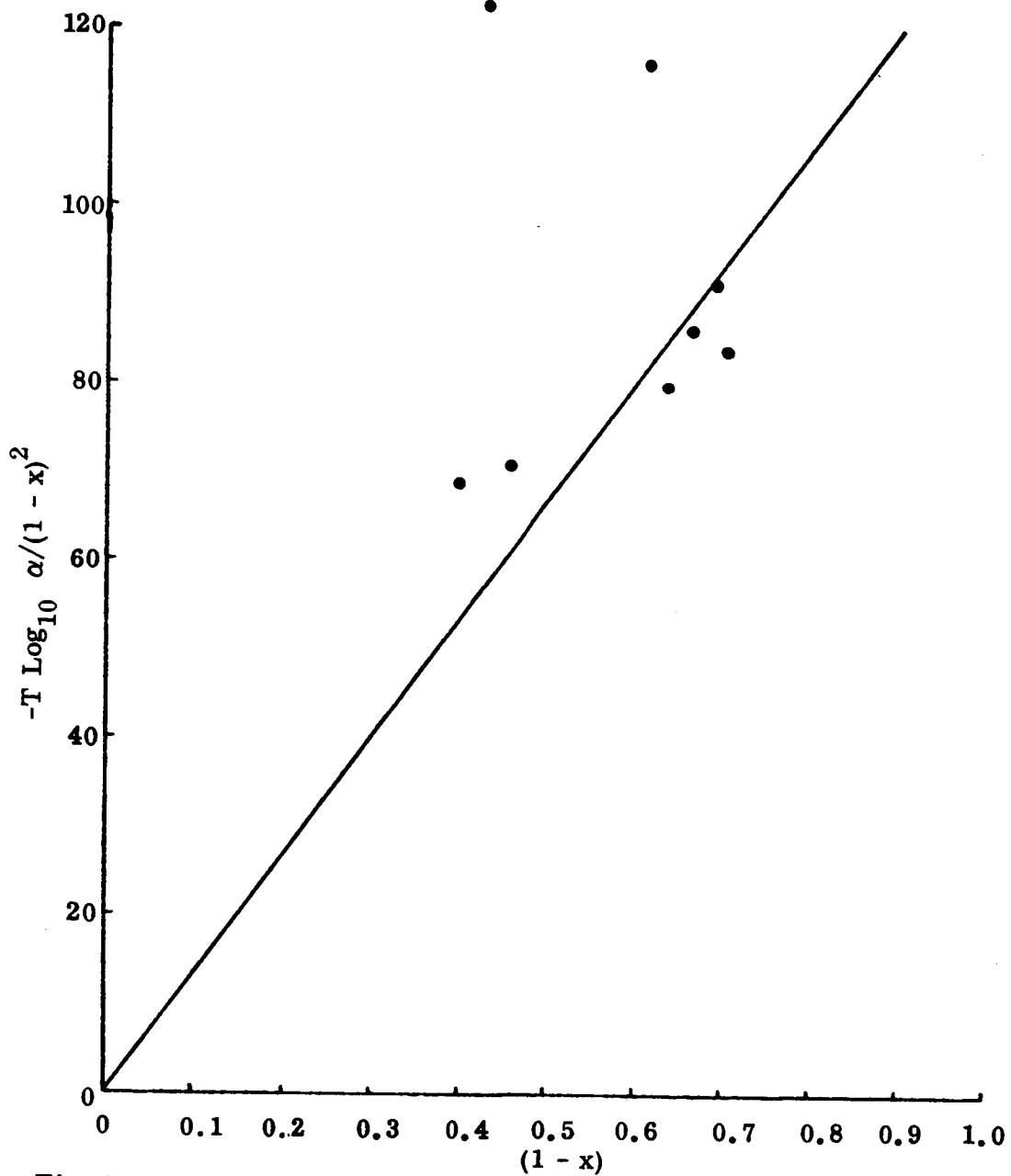


Fig. B.4 Activity Coefficient Correlation -- F21 & Chlorodecane

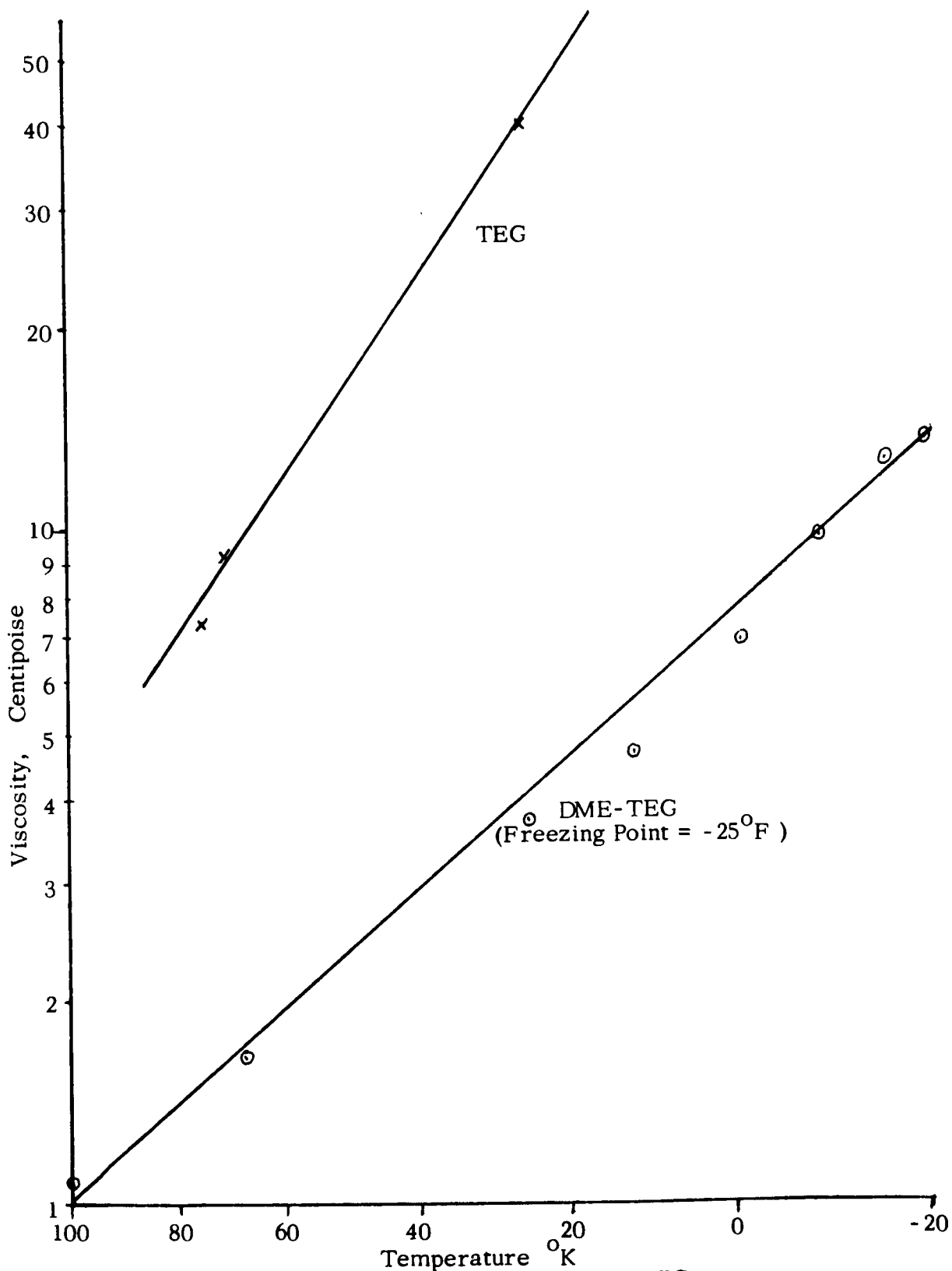


Figure B.5 Viscosity of DME-TEG and TEG

of $10^{-3}/^{\circ}\text{C}$ was assumed for the calculation of the densities at the various temperatures. This was necessary to estimate the viscosity from the experimental data.

Appendix C
COMPONENT DESIGNS AND WEIGHT ANALYSES

It is the purpose of this appendix to determine the relationship between the operating parameters and the weights of components of a general design. The relationships so determined are to be the common basis for the comparison of various refrigeration systems assembled from these components. The wide operating range and variety of design possibilities prevent the development of a relationship which will give the optimum case for each application. However, the relationships should be typical over a large part of the range, and where all the systems compared are based on the same component relations, the results of the comparisons should be valid in their sense if not in their absolute magnitude.

The components discussed in the following sections are summarized in Table C.1.

C.1 Radiators

The design of radiators for space applications is concerned with two major factors:

a. Heat Transfer

- Heat transfer fluid to radiator tube wall
- Conduction from tube to fin surface
- Radiation from fin surface
- Absorption of incident radiation from the environment

b. Construction

- Structural materials
- Surface coatings
- Meteoroid protection

The heat transfer aspects of space radiator design (for both the uniform fluid temperature and the changing fluid temperature cases) have been presented in considerable detail by Mackay.^{19,20} To attempt to present a complete radiator analysis covering the range of parameters expected for the systems being considered would greatly increase the complexity of the discussion with little increase in understanding. A more meaningful approach for the present study is to combine

Table C.1
COMPONENT SELECTION

Section	Component Type	SYSTEM		
		Semi-Passive	Vapor Compression	Vapor Absorption
C.1	Radiator	Circulated liquid	Condenser	Condenser Absorber
C.2	Heat Exchanger	Gas-liquid	Evaporator	Evaporator
				Vapor generator
				Recuperator
				Sub-cooler
C.3	Separator	N. A.	N. A.	EHD separator
				Wick separator
C.4	Pump or Compressor	Liquid circulating pump	Vapor compressor	Liquid pressure pump
C.5	High-Voltage Power Supply	N. A.	N. A.	AC Separator supply
				DC Absorber supply
C.6	Power Weight Penalty	Electrical	Electrical	Electrical
				Thermal

N. A. - not applicable

the fluid to tube-wall and conduction heat transfer factors into an assumed typical radiator effectiveness factor. For uniform temperature radiators (such as the condenser and, essentially, the absorber) an effectiveness of 0.95 will be used. For radiators having a temperature change from the inlet to the outlet, an effectiveness of 0.80 will be used.

The radiator performance can now be related to the design and operational parameters by the equation

$$\frac{q_R}{A_R} = \eta C_\epsilon T_R^4 - C_\alpha \quad (C.1)$$

where q_R/A_R is the net heat rejection rate per unit radiator area, η is the radiator effectiveness, $C_\epsilon = \sigma\epsilon_{IR}$ is the radiation constant for infrared radiation, T_R is the log-mean radiator temperature, and C_α is the absorption constant for incident solar or environmental radiation.

Using LMSC silicate paint (Ref. 21, pg. 523), $C_\epsilon = 0.153 \times 10^{-8} \text{ Btu/hr ft}^2 \text{ } ^\circ\text{R}^4$, $C_\alpha = 45 \text{ Btu/hr ft}^2$ for an orbital environment with the radiator facing the sun, $C_\alpha = 130 \text{ Btu/hr ft}^2$ for a lunar environment with the radiator facing the sun and with the horizon at 20° elevation.

The thickness of armor required for protection of the radiator tubes from meteoroid penetration is seen from the following equation from Whipple²²

$$t_m = 2(a) \left(\frac{6}{\pi}\right)^{1/3} \left(\frac{1}{\rho_m}\right)^{1/3} \left(\frac{\rho_m}{\rho_R}\right)^{1/2} \left(\frac{\bar{V}}{C_R}\right)^{2/3} \left[\frac{\alpha (NT) L (ID) \tau}{- \ln (P_o)} \right]^{1/3\beta} \quad (C.2)$$

where t_m is the armor thickness required, (a) is the penetration factor (= 1.5), ρ_m is the meteoroid density (= 0.44 gm/cc), ρ_R is the tube and armor density (= .098 lb/in³), \bar{V} is the average meteoroid velocity (= 30 km/sec), C_R is the sonic velocity of the target (= $\sqrt{Eg/\rho_R}$), E is Young's modulus (= 10^7 psi), g is the gravitational constant, NT is the number of tubes, L is the tube length, ID is the tube inner diameter, τ is the mission time, P_o is the probability of no penetration, and α and β are empirical meteoroid flux distribution parameters (see Fig. C.1) ($\alpha = 2.76 \times 10^{-10}$, $\beta = 1.34$). More current data on meteoroid penetration has resulted from the Pegasus program (29) but there is no reported correlation of this data on the basis of meteoroid mass presently available.

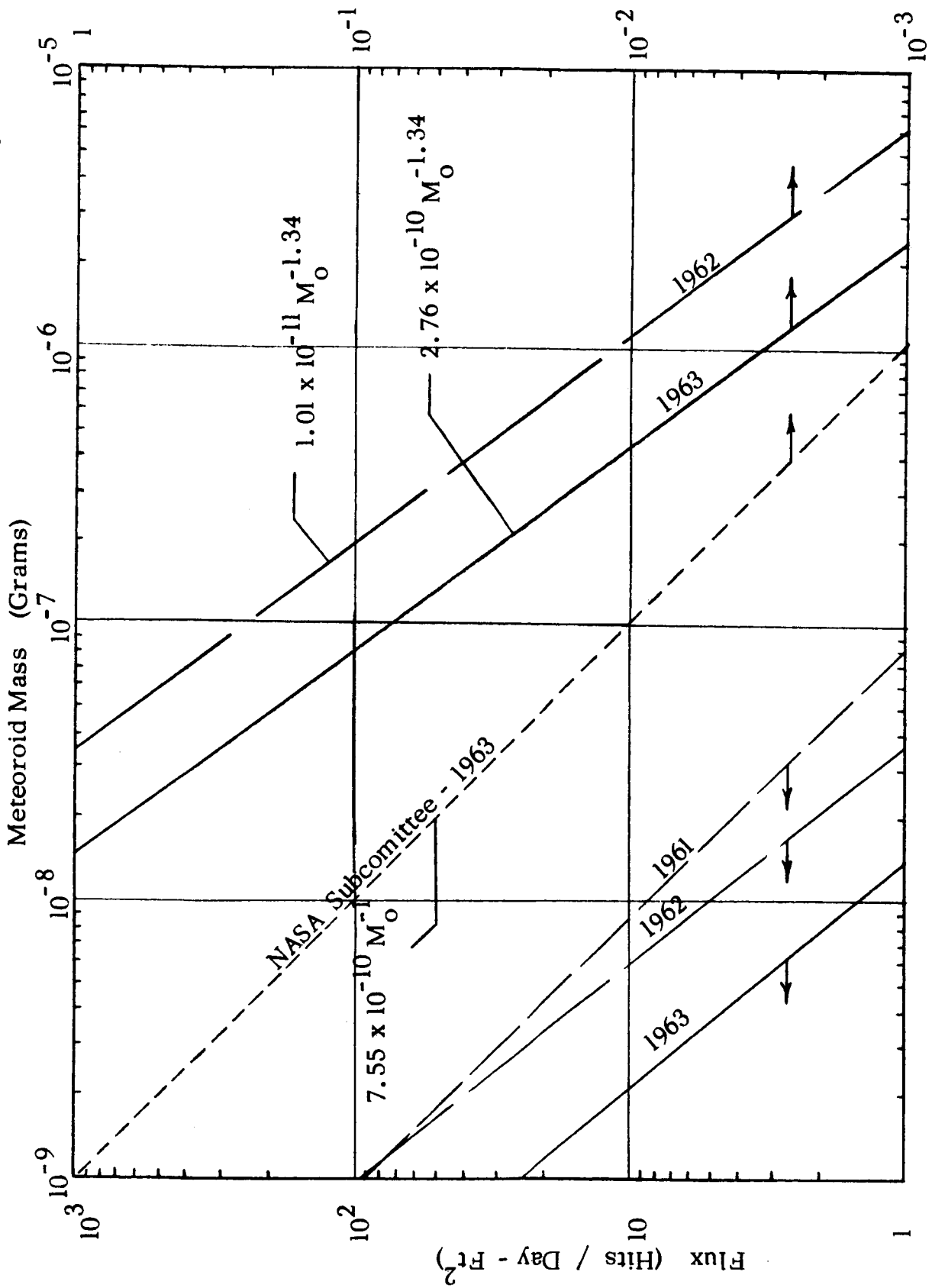


Figure C.1 Meteoroid Flux Distribution

As an example of the meteoroid protection requirements for a typical application, the armor required for 99.9% probability of no penetration on a 5-foot square radiator having 0.080 inch ID tubes on 6-inch spacing for a mission duration of 40 days would be on the order of 1 centimeter thickness.

The weight of a typical radiator can now be determined. Assuming aluminum construction with 0.020 inch fin thickness, 0.080 inch ID, 1/4 inch wall tubes spaced 6 inches apart, the weight per unit area is about 0.85 lb/ft². To account for support structure and headers a radiator weight of 1 lb/ft² of radiator surface area will be used.

Based upon the heat transfer and weight relations, the specific weights of typical radiators for lunar and orbital applications are given in Fig. C.2.

C.2 Heat Exchangers

The analytical design procedures for compact heat exchangers are developed in a number of available reports, notably Kays and London²³ and Shaffer²⁴. The heat exchanger designs used in this study were those reported by Shaffer²⁴.

Typical heat transfer coefficients were assumed (see Rohsenow and Choi⁷, page 102) as follows:

	Typical h ($\frac{\text{Btu}}{\text{hr ft}^2 \text{ } ^\circ\text{F}}$)
Flowing gas	10
Flowing liquid	200
Boiling liquid	1000
Condensing liquid	750

The overall heat transfer coefficient is given by Shaffer as:

$$\frac{1}{UA} = \frac{1}{\epsilon h_1 A_1} + \frac{1}{\epsilon h_2 A_2} \quad (\text{C.3})$$

where (UA) is the overall heat transfer coefficient (Btu/hr °F ft³) (where ft³ is the volume of the exchanger core), ϵ is the exchanger effectiveness (taken equal to 0.85), and A is the exchanger surface area per unit volume of exchanger core (the subscripts refer to sides 1 and 2 of the exchanger).

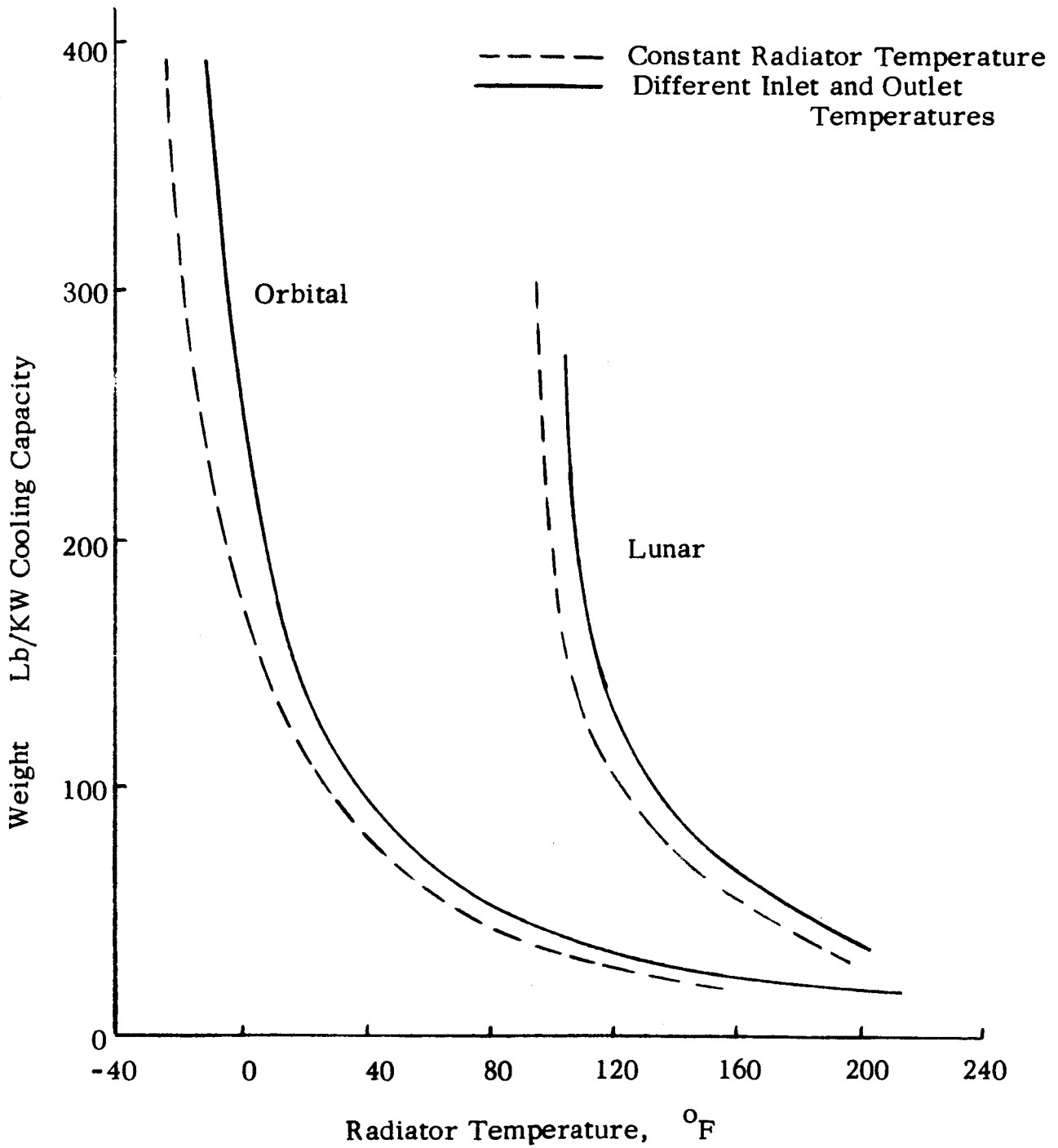


Figure C.2 Radiator Weights

The core volume requirement is given by:

$$V_c = \frac{q}{UA\Delta T} \quad (C.4)$$

where V_c is the core volume, q is the required heat transfer rate, and ΔT is the temperature difference between the hot and cold fluids.

The weight of the heat exchanger (including the header weight) is given by the equation:

$$W = 1.34 \rho_c V_c^{0.882} \quad (C.5)$$

where ρ_c is the core weight density. Heat exchanger core weight and surface area densities which have been obtained in compact heat exchangers for aircraft applications were reported by Shaffer²⁴ (page 326) as:

Type of Surface	Core Weight Density (lb/ft ³ of core vol.)	Surface Area Density (ft ² /ft ³ of core vol.)		Appli- cations
		Side 1	Side 2	
Finned tube (Al.)	19.2	46.7	597	Liquid to gas
Shell and tube (Al.)	34.1	280	313	Liquid to liquid

On the basis of the above relations and data, the weights of the various heat exchangers required are as shown in Fig. C.3.

C.3 Liquid/Vapor Separator

Two general types of liquid/vapor separators were examined in considerable detail, electrohydrodynamic (EHD) separators (described and analyzed in Appendix D) and "wick type" surface tension separators (presented in Appendix G). Whereas the EHD separators can only be made to operate dependably in low-gravity environments while the wick type separators can be made to operate in any orientation in one-g, the wick type separator was chosen for use in the vapor absorption refrigeration system. A weight analysis of the wick type separator is presented in Appendix G.

C.4 Pumps and Compressors

The weights of pumps and compressors used in this study were taken from the report by Honea, et al.⁶ The pump weight relation was linearized resulting in the relation:

$$\text{Pump Weight} = 0.22 + 0.692 W_L \quad (\text{C. 6})$$

where W_L = liquid pumped in lbs/minute. The compressor weights used are shown in Fig. C.4.

C.5 High-Voltage Power Supply

The power supplies required by the EHD augmented components typically operate at less than 2 KV at 400 to 1000 cps and are rated at less than 50 watts (more commonly in the area of 5 to 10 watts). The power supply in every instance is a relatively insignificant item as far as system weight is concerned.

A simple linearized estimation of power supply weight was used in the study.

$$\text{Power Supply Weight} = 100 \text{ lb/KW} \quad (\text{C. 7})$$

C.6 Power Weight Penalty

The weight penalty relations for electrical power were taken from Honea, et al,⁶ page 222.

$$\text{Solar Cell Power Penalty} = 430 \text{ lb/KW}_e \quad (\text{C. 8})$$

$$\text{Fuel Cell Power Penalty} = 185 \text{ lb/KW}_e + 0.82 \text{ lb/KW hr} \quad (\text{C. 9})$$

(for fuel)

Thermal power was, in most cases, assumed available as waste heat from other systems on the mission vehicle. No weight penalty was associated with this waste heat.

For applications where waste heat was not available, a Promethium-147²⁵ nuclear heat source was assumed. The nuclear source was selected after examining a number of fueled systems, the results of which are tabulated below.

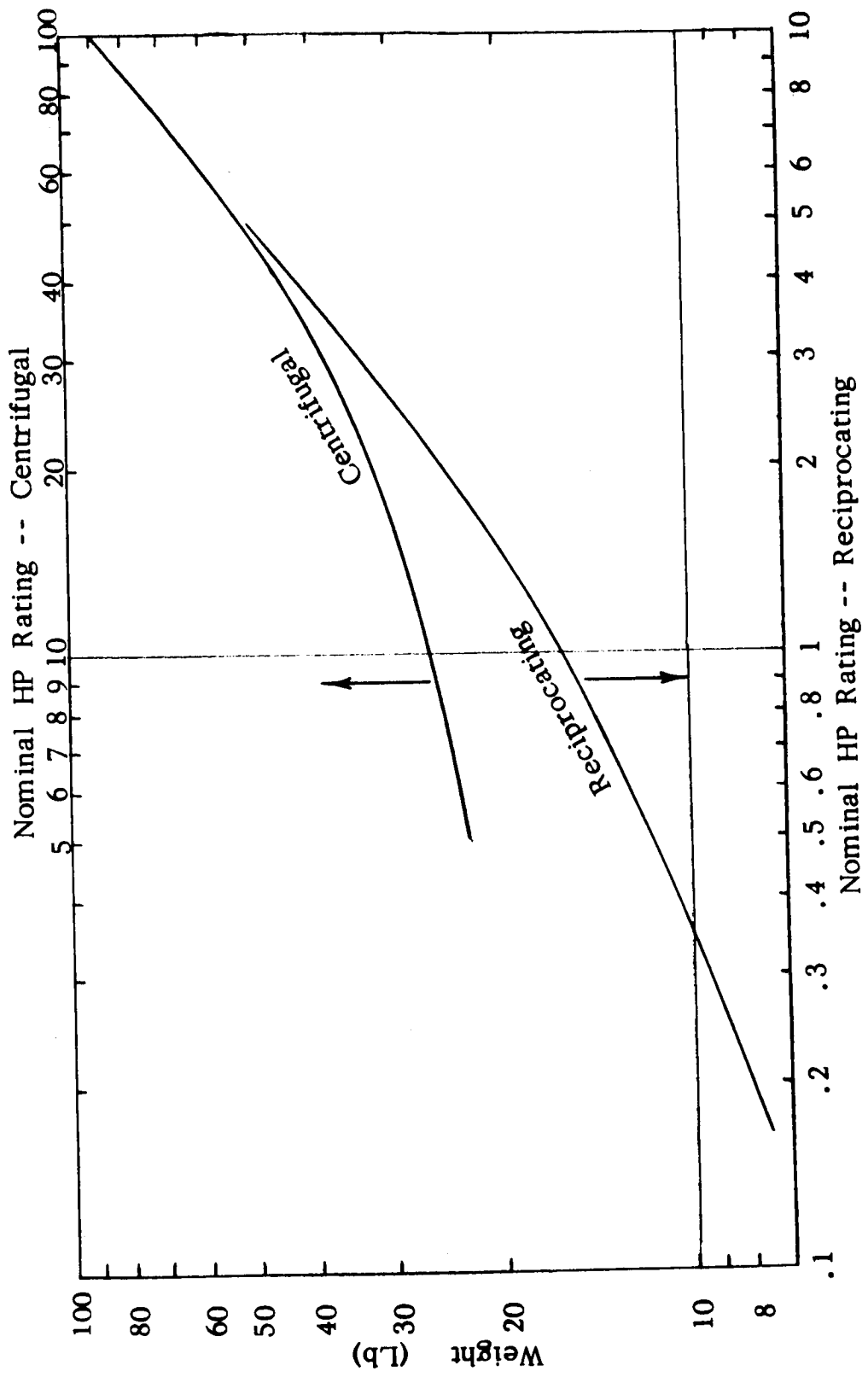


Figure C.4. Compressor Weights

Thermal Power Sources

<u>Source</u>	<u>Heat Rate</u>	<u>Weight Penalty*</u>
● $H_2 + O_2$ Combustion	$6200 \frac{\text{Btu}}{\text{lb. of reactants}}$	0.55 lb/hr.
● Hydrocarbon fuel + O_2 Combustion	$4300 \frac{\text{Btu}}{\text{lb. of reactants}}$	0.80 lb/hr.
● $H_2O_2 \rightarrow H_2O + O_2$	$1250 \frac{\text{Btu}}{\text{lb of } H_2O_2}$	2.73 lb/hr.
● Hydrazine Decomposition	$1500 \frac{\text{Btu}}{\text{lb of } N_2H_4}$	2.28 lb/hr.
● Hydrazine + O_2 Combustion	$4180 \frac{\text{Btu}}{\text{lb. of reactants}}$	0.82 lb/hr.
● Promethium 147		6.6 lb. (no time dependence)

* Weight penalty is fuel weight only for a 1 KW heat source. Burner and tankage weight or shield weight for the nuclear source not included.

In addition to the weight of the actual nuclear element, a 1-inch thick shield of uranium is required to maintain the radiation within an acceptable level. The thermal power weight penalty is given approximately by the relation:

$$\text{Thermal Weight Penalty} = 6.6 Q + 31.6 Q^{2/3} \quad \text{lb.} \quad (\text{C. 10})$$

where Q is the heating rate in kilowatts and the element is assumed to be a cylinder with the height equal to the diameter.

Appendix D

ANALYSIS AND TESTS OF
AN ELECTROHYDRODYNAMIC LIQUID/VAPOR SEPARATOR

Two electrohydrodynamic (EHD) separator concepts are analyzed; the linear-E case where the separation force increases in the direction of liquid collection, and the linear-E² case where the separation force is constant.

Linear-E Case

Referring to the sketch below, a force balance on the droplet results in the relation:

$$\text{Electrical force } (F_e) + \text{Buoyancy force } (F_b) + \text{Drag force } (F_d) + \text{Inertial force } (F_i) = 0$$

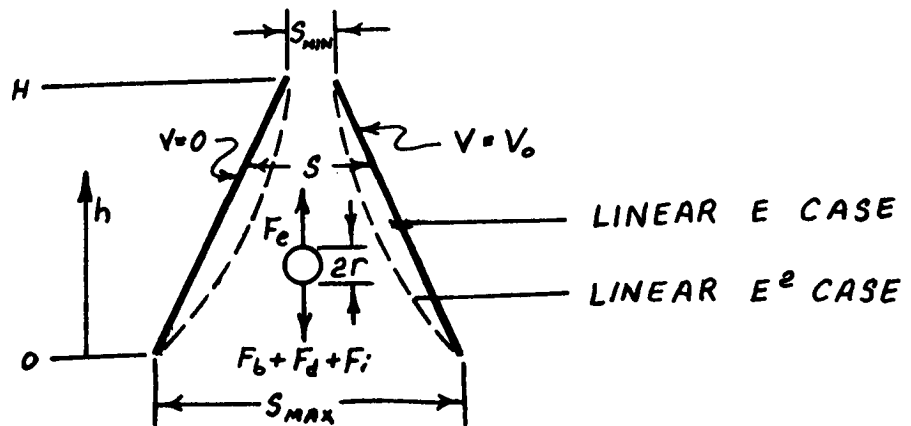
where:

$$F_e = \left(\frac{4}{3} \pi r^3 \right) \epsilon_0 \frac{3K_V (K_L - K_V)}{2(K_L + 2K_V)} \nabla (E^2) \quad (\text{Ref. 26})$$

$$F_b = - \left(\frac{4}{3} \pi r^3 \right) (\rho_L - \rho_V) g^*$$

$$F_d = -6 \pi r \mu \frac{dh}{dt}$$

$$F_i = - \left(\frac{4}{3} \pi r^3 \right) \rho_L \frac{d^2 h}{dt^2}$$



The electric field can, for small angles between the plates ($\frac{S_{\max} - S_{\min}}{H} < 0.3$), be approximated by

$$E = (E_{\max} - E_{\min}) h^* + E_{\min}$$

where $h^* = \frac{h}{H}$. The gradient of E^2 is then:

$$\nabla (E^2) = \frac{2}{H} \left(\frac{V_o}{S_{\max}} \right)^2 \left[(Re - 1) + (Re - 1)^2 h^* \right]$$

where

$$E_{\min} = V_o / S_{\max}$$

$$E_{\max} = V_o / S_{\min}$$

$$Re = S_{\max} / S_{\min}$$

With suitable substitutions, the differential equation of motion for the liquid drop-let is:

$$\frac{d^2 h^*}{dt^2} + A \frac{dh^*}{dt} + B h^* + C = 0$$

where:

$$A = \frac{6\pi r \mu}{\rho_L \left(\frac{4}{3} \pi r^3 \right)}$$

$$B = - \frac{\epsilon_o}{\rho_L} \frac{3K_V(K_L - K_V)}{(K_L + 2K_V)} \left(\frac{V_o}{S_{\max}} \right)^2 \frac{(Re - 1)^2}{H^2}$$

$$C = \left(1 - \frac{\rho_V}{\rho_L} \right) \frac{g}{H} - \frac{\epsilon_o}{\rho_L} \frac{3K_V(K_L - K_V)}{(K_L + 2K_V)} \left(\frac{V_o}{S_{\max}} \right)^2 \frac{(Re - 1)}{H^2}$$

A solution of this equation of motion is:

$$h^* = a(e^{bt} - 1)$$

where $a = C/B$, $b = -\frac{A}{2} + \sqrt{\left(\frac{A}{2}\right)^2 - B}$

The separation time (τ) is the time required for $h^* = 1$. Thus:

$$\tau_{\text{linear-E}} = \frac{1}{b} \ln \left(\frac{1}{a} + 1 \right)$$

Linear-E² Case

The force balance and the force equations for the linear-E² case are the same as for the linear-E case. Here, however, the electric field is described by:

$$E^2 = (E_{\max}^2 - E_{\min}^{-2}) h^* + E_{\min}^2$$

the gradient of which is:

$$\nabla (E^2) = \left(\frac{V_o}{S_{\max}} \right)^2 \frac{(Re^2 - 1)}{H}$$

which is a constant for all h^* . The differential equation of motion is:

$$\frac{d^2 h^*}{dt^2} + A' \frac{dh^*}{dt} + B' = 0$$

where:

$$A' = \frac{6\pi r \mu}{\rho_L \left(\frac{4}{3} \pi r^3 \right)} = A$$

$$B' = \left(1 - \frac{\rho_V}{\rho_L} \right) \frac{g^*}{H} - \frac{\epsilon_o}{\rho_L} \frac{3K_V(K_L - K_V)}{2(K_L + 2K_V)} \left(\frac{V_o}{S_{\max}} \right)^2 \frac{(Re^2 - 1)}{H^2}$$

The solution to this equation is:

$$h^* = a' e^{-At} + b' + C' t$$

where:

$$a' = -B/A^2$$

$$b' = -a' = B/A^2$$

$$C' = -B/A$$

The collection time for the linear- E^2 case is given by:

$$e^{-A\tau} + A\tau = 1 - A^2/B$$

Worked Examples

Representative separation times for liquid droplets of various diameters and under various adverse accelerations were determined for the linear-E and linear- E^2 systems. The system conditions used in these sample calculations were:

$$\rho_V/\rho_L = 0.03$$

$$g^* = 0 \text{ to } 10^{-2} g_0 = 0 \text{ to } 9.8 \times 10^{-2} \frac{\text{m}}{\text{sec}^2}$$

$$\rho_L = 10^3 \text{ Kg/m}^3$$

$$K_V = 1$$

$$K_L = 3$$

$$V_0 = 0 \text{ to } 50 \text{ KV}$$

$$S_{\text{max}} = 0.03 \text{ m}$$

$$H = 0.1$$

$$\text{Re} = 3$$

$$\begin{aligned} \epsilon_0 &= 8.85 \times 10^{-12} \text{ F/m} \\ \mu &= 0.014 \text{ centipoise} = 1.4 \times 10^{-5} \frac{\text{Kg}}{\text{m-sec}} \\ 2r &= 1 \text{ mm and } 0.1 \text{ mm} \end{aligned}$$

The results of these sample calculations are shown in Figs. D.1 and D.2 for the linear-E and linear-E² cases, respectively.

The conclusion drawn from a comparison of the two cases is that the collection times are comparable for the two cases. The linear-E² system has the advantage, however, of 30% lower threshold voltage required for separation under an adverse acceleration.

Liquid-Liquid Analog Tests

A two-dimensional model of a linear-E case separator was constructed as shown in the Figure D.3. The analog fluids used were silicone oil, simulating the vapor, and corn oil, simulating the liquid. The relative densities of the two analog liquids were adjusted to be representative of an adverse acceleration in the upward direction on the corn oil of from 10⁻³ to 10⁻² g₀. The other conditions for the test were:

$$\begin{aligned} \rho_V / \rho_L &= 1.001 \text{ to } 1.01 \text{ (simulating } 10^{-3} \text{ to } 10^{-2} \text{ g}_0) \\ g^* &= -1g_0 = -9.8 \text{ m/sec}^2 \\ \rho_L &= 0.92 \text{ g/cc} = 920 \text{ Kg/m}^3 \\ K_V &= 2.5 \\ K_L &= 3.1 \\ V_0 &= 0 \text{ to } 20 \text{ KV} \\ S_{\text{max}} &= 0.8175 \text{ in} = 2.075 \times 10^{-2} \text{ m} \end{aligned}$$

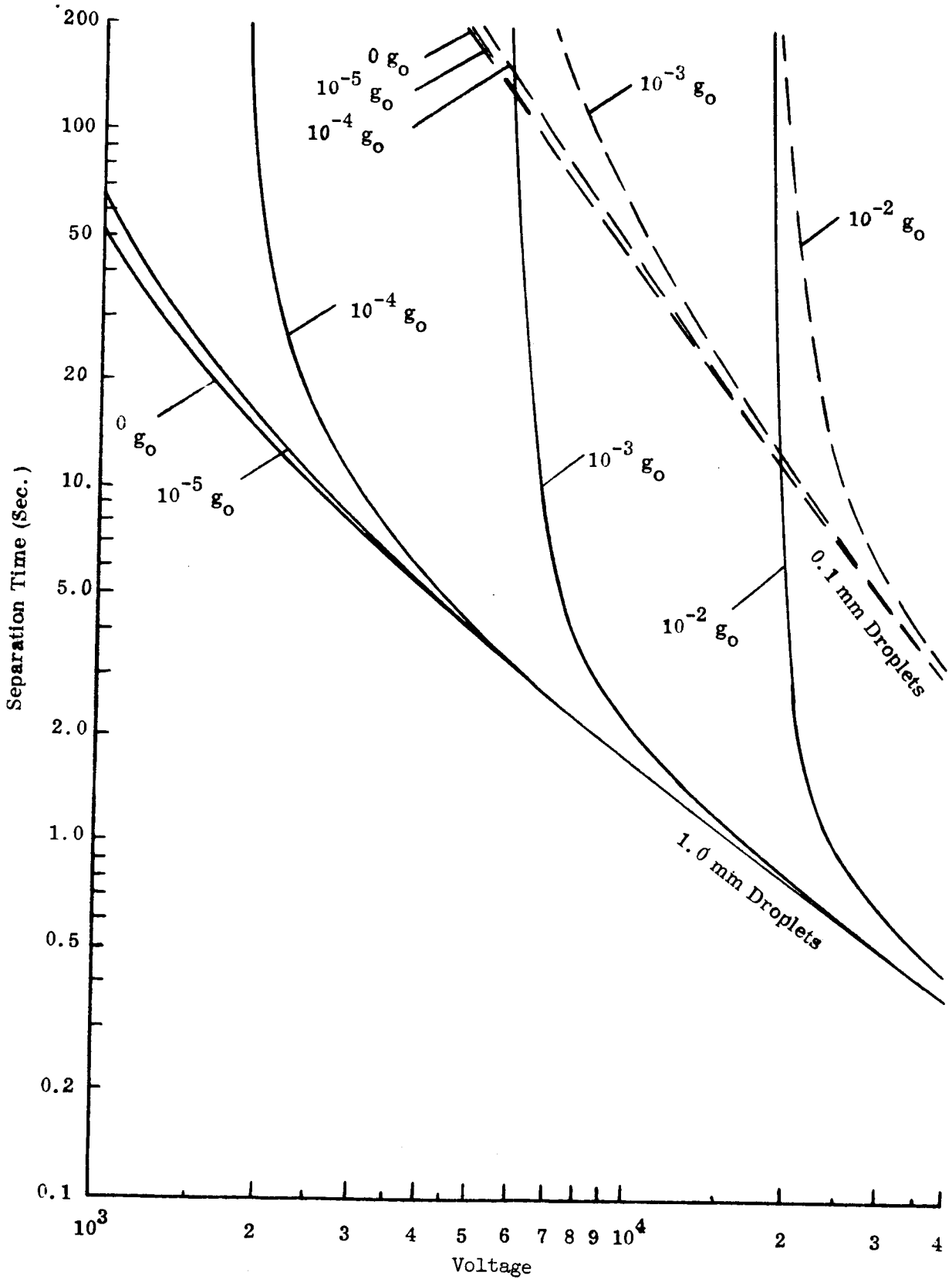


Fig. D.1. Separation Time Linear-E Device

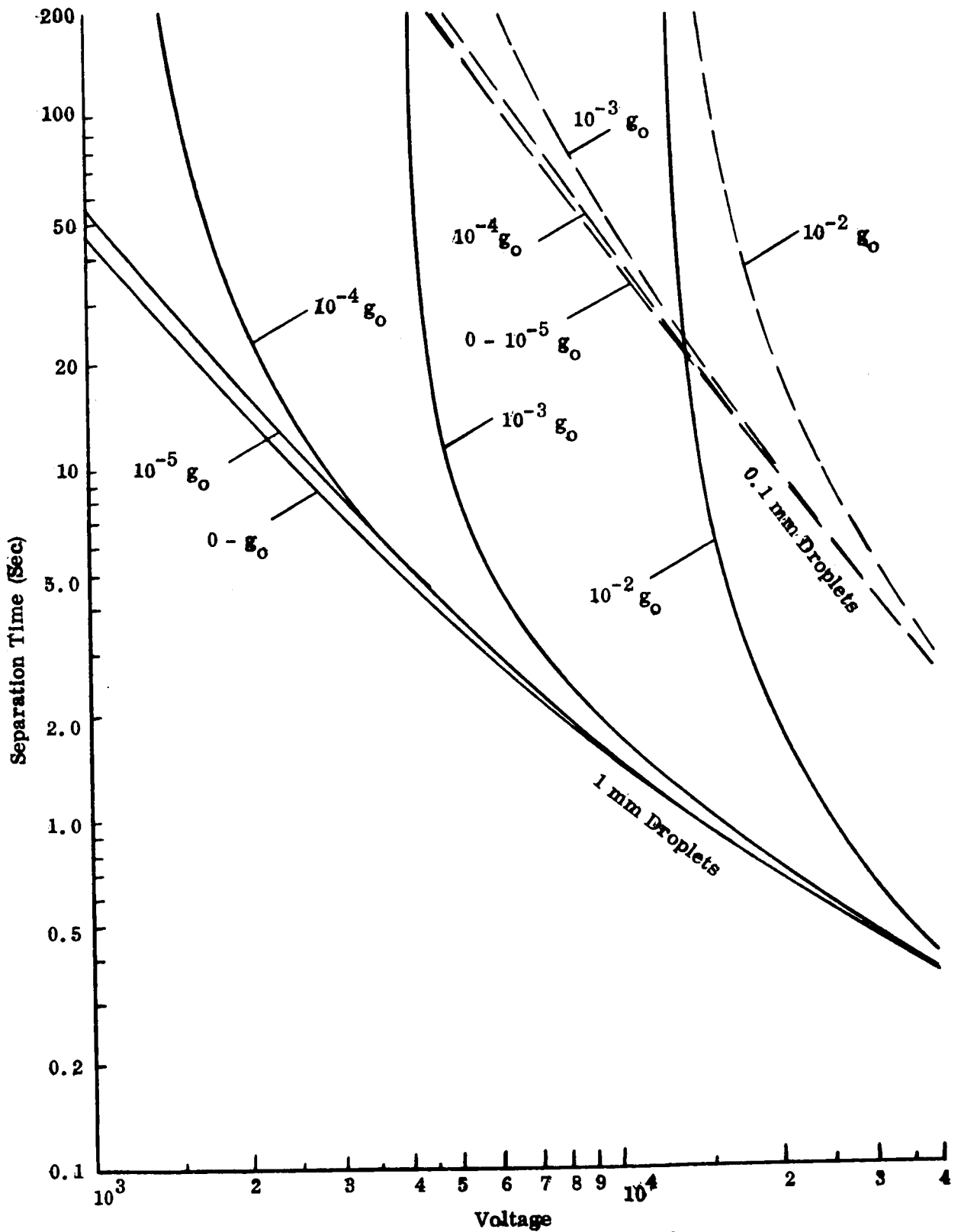


Fig. D.2. Separation Time Linear- E^2 System

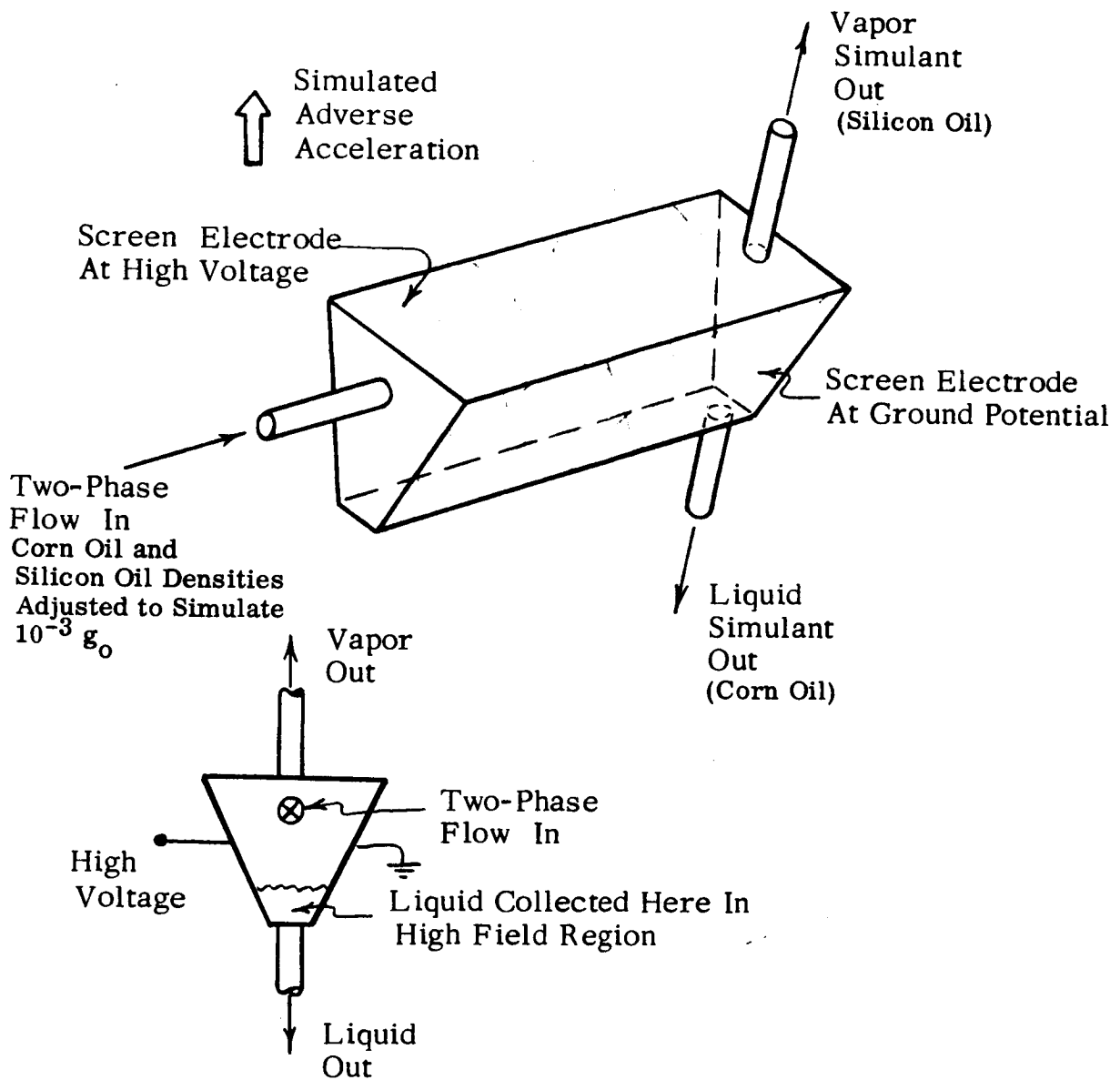


Figure D.3 Analog Model of EHD Separator

$$H = 1.125 \text{ in} = 2.855 \times 10^{-2} \text{ m}$$

$$Re = 1.858$$

$$\epsilon_0 = 8.85 \times 10^{-12} \text{ F/m}$$

$$\mu = 5.43 \text{ centipoise} = 5.43 \times 10^{-3} \text{ Kg/m-sec}$$

$$2r = 1 \text{ mm to } 4 \text{ mm}$$

Figure D.4 shows the analytical and experimental results of the separation time for the analog separator for 2mm droplets. The experimental results are within a factor of two of the theoretical separation times.

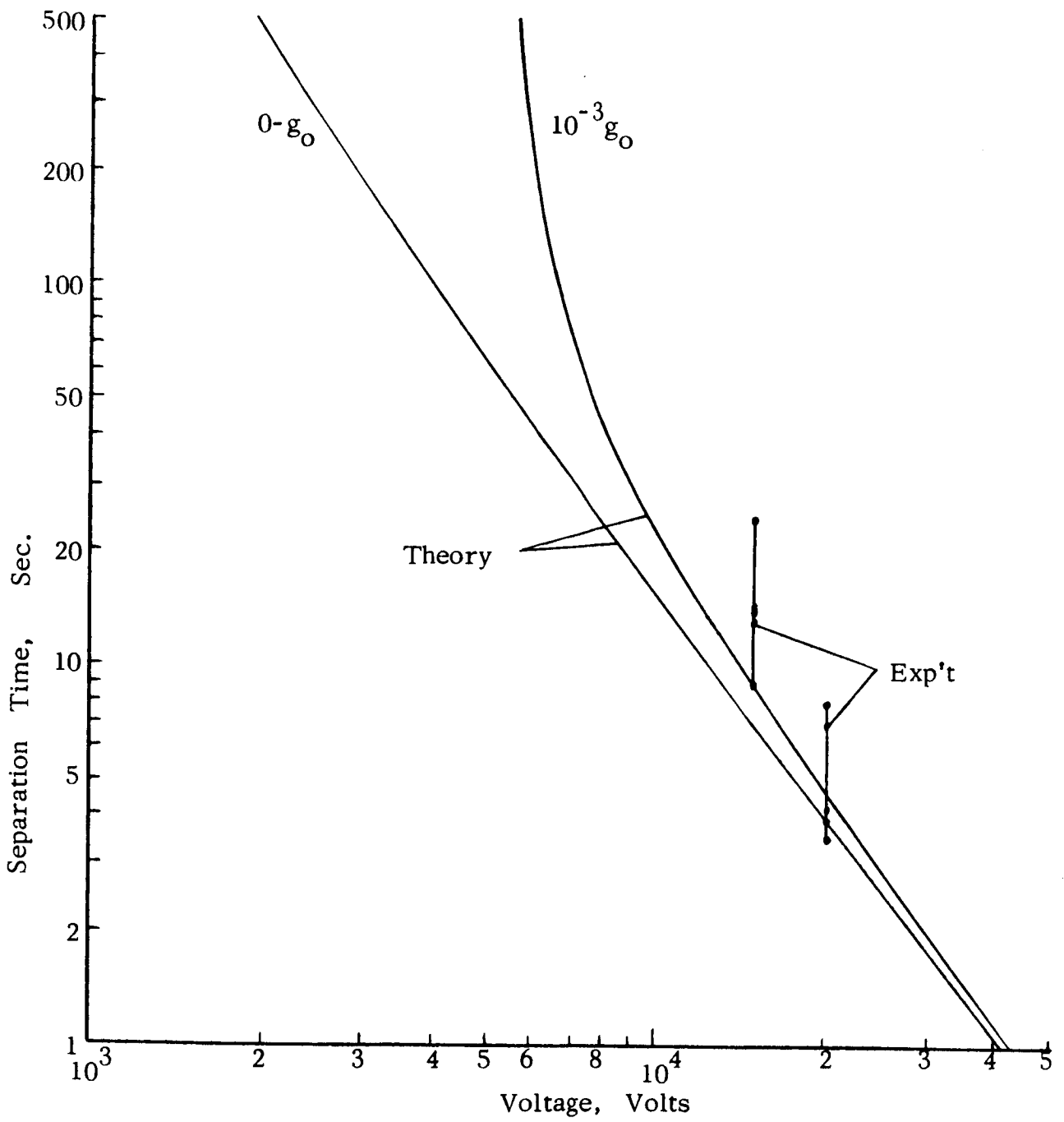


Figure D.4 Analog Separator Test Results

Appendix E
SEMI-PASSIVE SYSTEMS

The semi-passive system designs were developed essentially after the procedure reported by Woods and Erlanson,²⁷ pages 40-42. To ensure consistency between the semi-passive system designs and those of the vapor compression and vapor absorption systems, the component weights as determined in Section 3 and Appendix C were used wherever possible.

Pressure drops in the radiators were assumed to be as reported by Hanson.²⁸ His pressure drops were replotted as a function of the liquid flow rates for direct use. These pressure drops were found to be approximately given by

$$\Delta P = 27.3M + 14 \text{ psi} \quad (\text{E.1})$$

where M is the rate of liquid circulated in lbs/second.

Assuming the finned-tube dimensions and the heat transfer coefficient as in Ref. 27, the pressure drop in the heat exchanger is given by:

$$\Delta P = 136M \quad (\text{E.2})$$

The pressure drop in the interconnecting piping is assumed constant at 15 psi. The weights of the semi-passive systems as a function of cooling load and radiator temperature are shown in Figs. E.1 and E.2, respectively.

In obtaining the weights for this figure, 10 per cent of the radiator weight was added on to the system weight to take care of liquid hold-up and other miscellaneous system items.

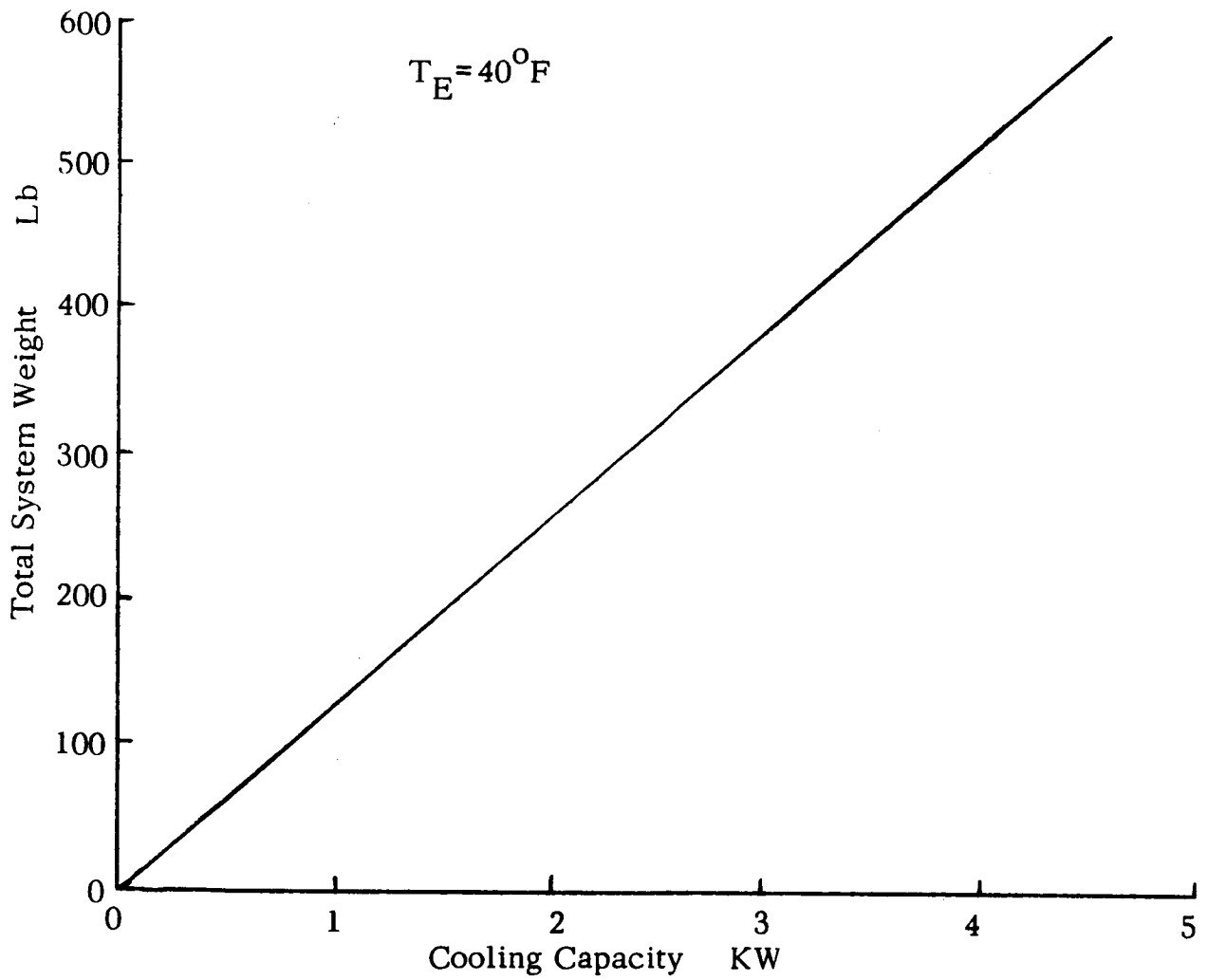


Figure E.1 Semi-Passive System Weight
(vs. Cooling Capacity)

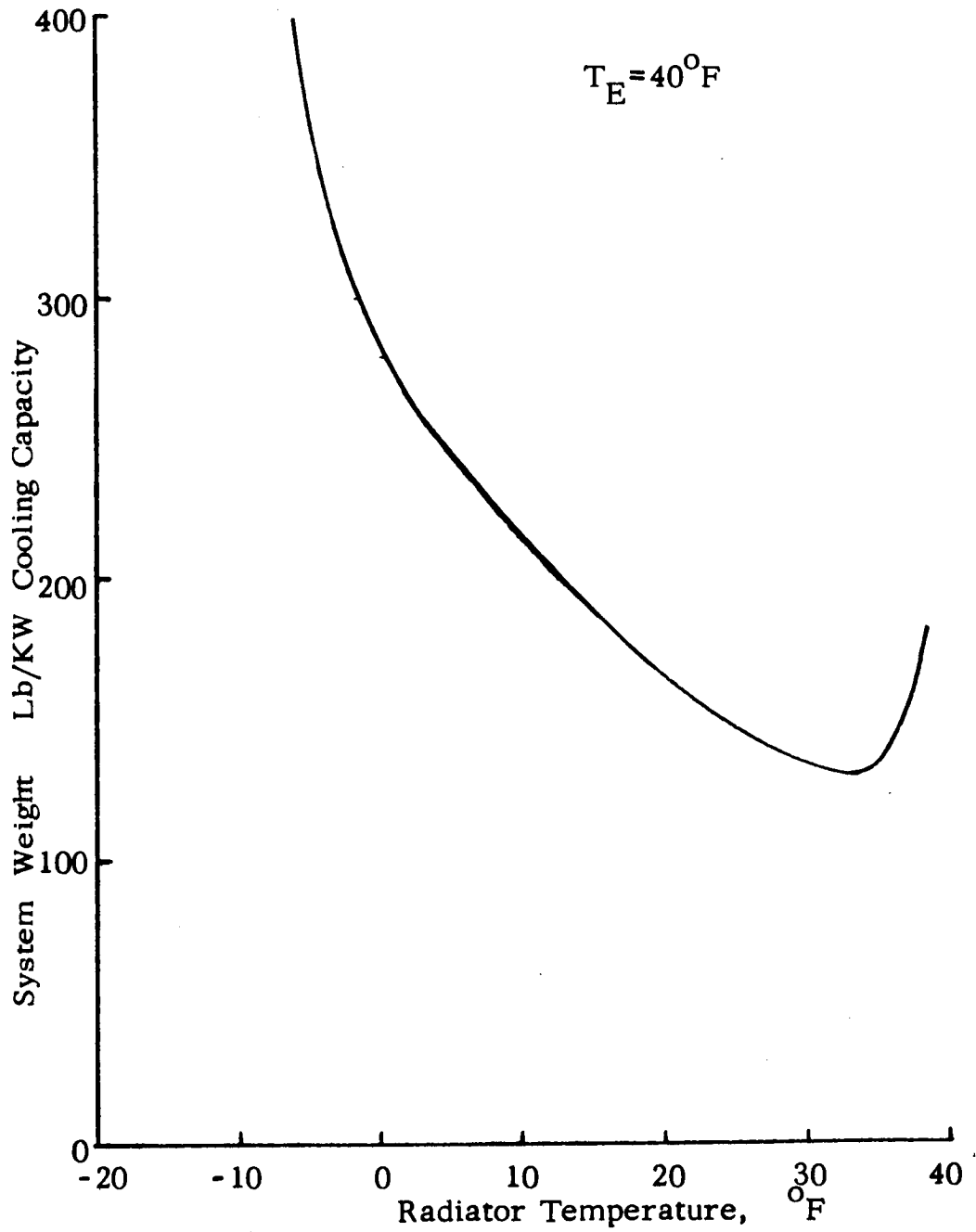


Figure E.2 Semi-Passive System Weight (vs. Radiator Temperature)

Appendix F
VAPOR COMPRESSION SYSTEMS

An ideal refrigerator removing heat from a source at temperature T_1 and rejecting it to a sink at temperature T_2 requires (according to the second law of thermodynamics) a minimum amount of work of:

$$W = Q \frac{T_2 - T_1}{T_1} \quad (\text{F.1})$$

where Q is the quantity of heat removed from the source. The heat rejected to the sink at T_2 is the sum of $Q + W$.

Because of inefficiencies in the motor and compressor of a vapor compression system the actual work which must be supplied is:

$$W' = \frac{W}{\eta} \quad (\text{F.2})$$

where η is the motor/compressor efficiency.

Assuming component weights as presented in Section 3 and Appendix C and $\eta = 0.5$, the vapor compression system weights are shown in Figs. F.1 and F.2 as functions of cooling capacity and radiator temperature, respectively.

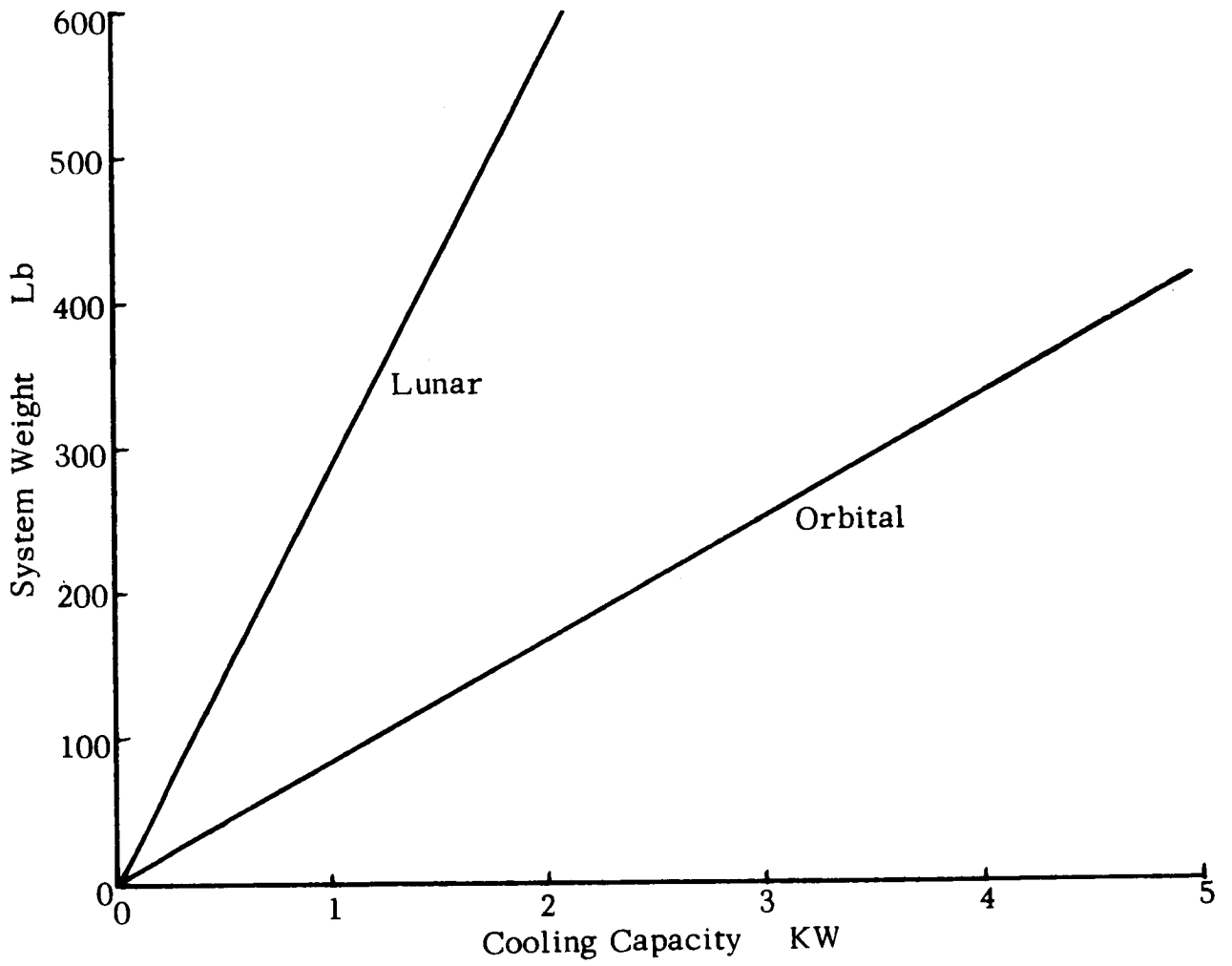


Figure F.1 Vapor Compression System Weights
(vs. Cooling Capacity)

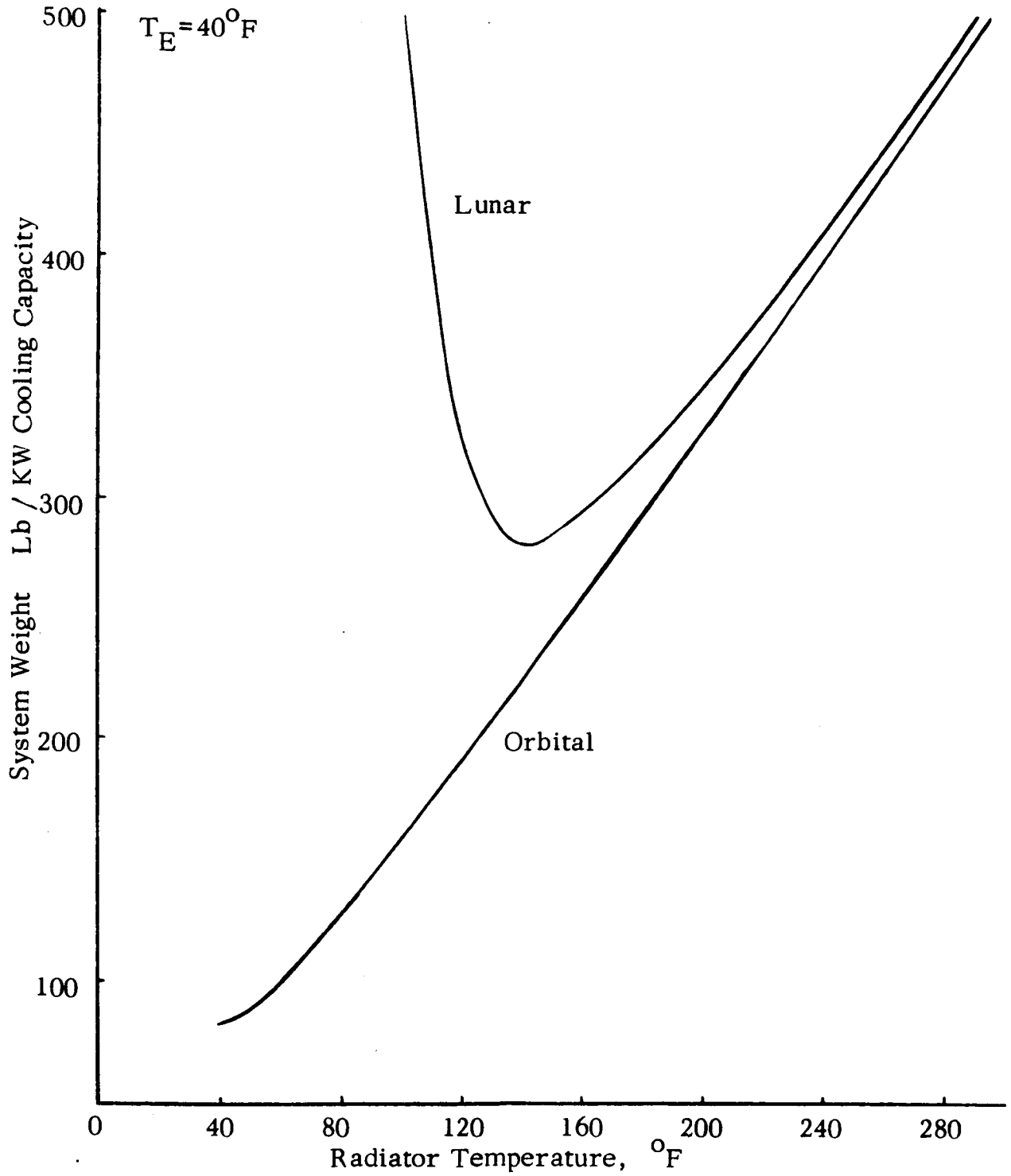


Figure F.2 Vapor Compression System Weights (vs. Radiator Temperature)

Appendix G

WICK-TYPE LIQUID/VAPOR SEPARATOR

G. 1 Introduction

Two general classes of liquid/vapor separators using surface tension forces to perform the separation were considered. In one class of device two-phase flow (liquid and vapor) is passed through a wick material. The vapor readily passes through the wick, but the liquid is held in the wick by surface tension forces. Single-phase liquid can be drawn from the wick by actively sucking it out. In the second class of device the wick is saturated by a single-phase liquid solution. By the addition of heat, vapor is generated within the wick. The vapor can pass out of the wick while the liquid is held by surface tension and withdrawn as above.

The first class of device, where the vapor generation and liquid/vapor separation are performed independently, has several advantages over the second, where vapor generation and liquid/vapor separation are performed together. These are:

- a. The heat transfer coefficient for boiling off a wick covered surface is much lower than that for a plain surface. As a result, much higher wall temperatures are required for the same vapor generation rate per unit area.
- b. The separate vapor generator can be integrated with the heat source, thereby eliminating a separate heat transfer loop to bring the heat from the heat source to the vapor generator.

The investigation of the first class of device was concentrated upon as the more preferable design.

A number of investigators including Langston⁽¹¹⁾ at Pratt & Whitney, Jeffries* at General Electric, and Ginwala⁽⁵⁾ at Northern Research and Engineering have studied

*Mr. Neal Jeffries, General Electric, Cincinnati, Ohio, personal communication.

the problem associated with long term operation of wick devices. Ginwala reported that after an initial period (8 to 10 hrs) of apparently stable operation, the wick had a tendency to plug up. This phenomenon has generally been attributed to noncondensable vapor coming out of solution. The vapor bubbles become trapped in the wicking matrix and eventually block off the flow passage. Langston⁽¹¹⁾ and Jeffries* indicate that careful degassing of the fluids and the use of metallic (as opposed to natural fiber) wicks eliminate the plugging problem.

The approach selected for the investigation of the separator designs was to demonstrate the operation of models which closely represent the actual device design. Fundamental tests of more general nature, such as the capillary rise height and friction factor tests on various wick materials, are beyond the scope of the present study. Success or failure of any particular test is based solely upon the observations (assuming balanced flow conditions have been set) of:

- a. Flooding of the wick, the result of the wick plugging up.
- b. Liquid entrainment in the vapor stream.
- c. Vapor pull-through into the liquid withdrawal line.

An analysis of the primary modes of failure of the wick separator was conducted in order to determine approximate operating limits as a function of geometry. On the basis of these design limits an estimate of the separator weight as a function of the liquid and vapor flow rates was established.

G.2 Laboratory Demonstrations

One configuration of a wick type liquid/vapor separator is shown in Figure G. 1. The design is functionally similar to the "sock" demister used on the outlet of an open air-cycle cooling system.

A two-dimensional model of the design of Figure G. 1 was constructed as shown in Figures G. 2, G. 3, G. 4 and G. 5. The wick used in the model was made up of ten sheets of stainless-steel screen with the dimensions and properties as given in the following table.

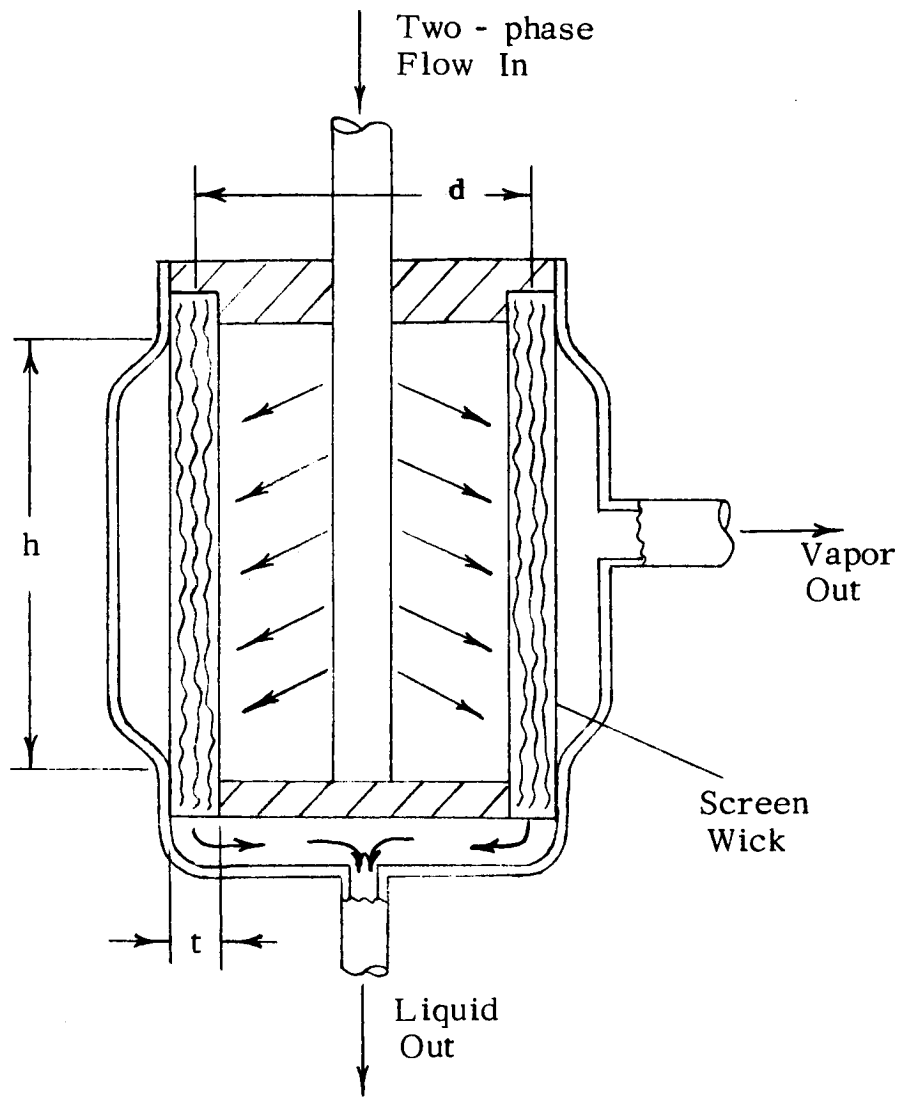


Figure G.1. Wick Separator

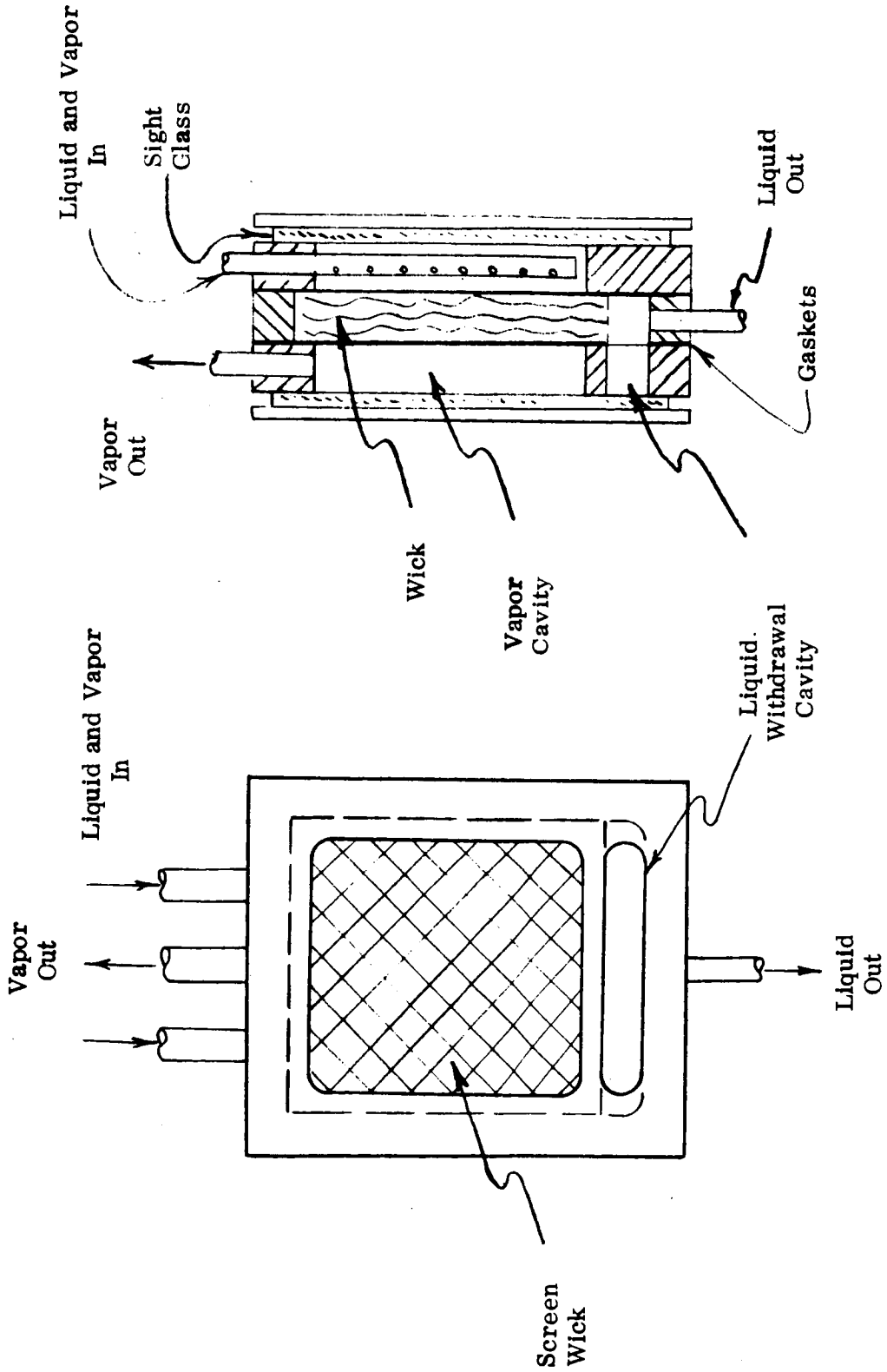


Figure G. 2. Separator Model Schematic

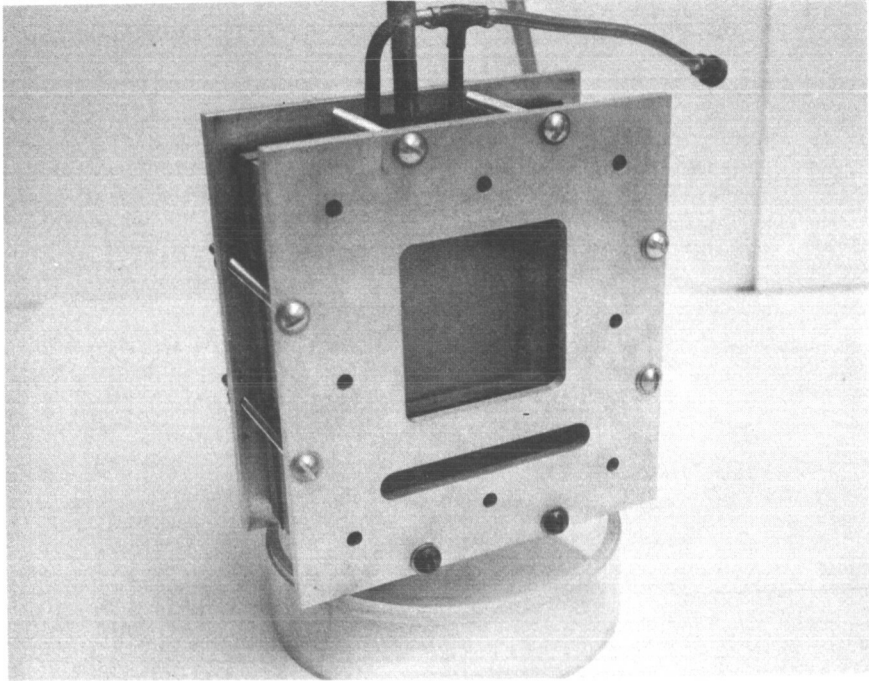


Fig. G.3 Separator Model

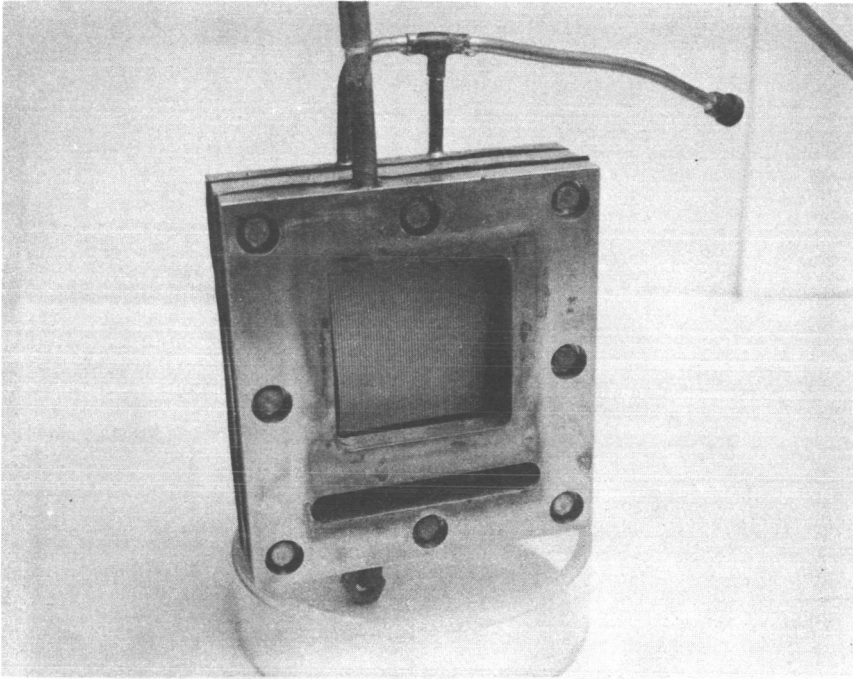


Fig. G.4 Wick Assembly

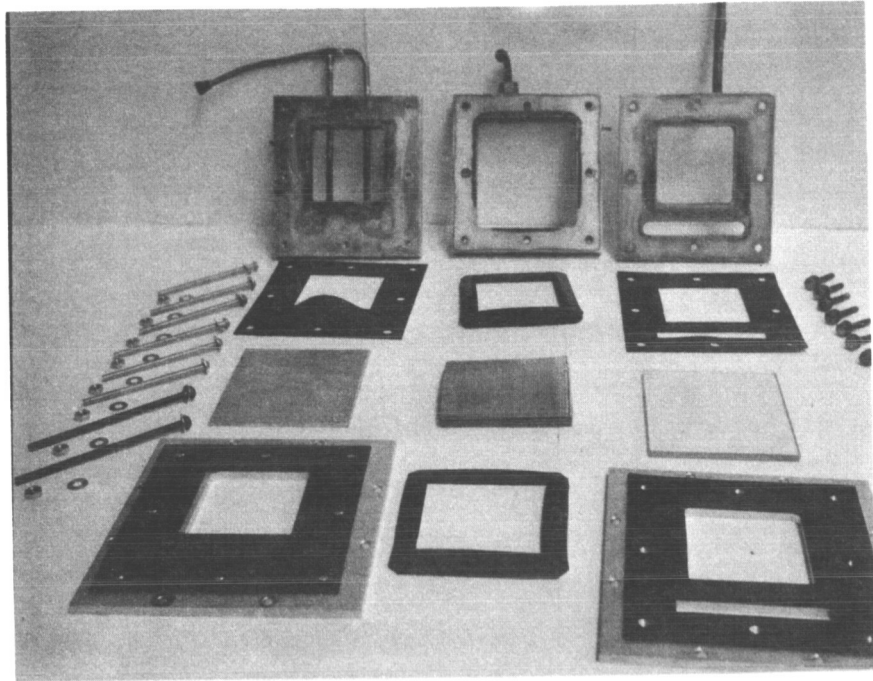


Fig. G.5 Model Components

Wick Properties

Material	18-8 stainless steel
Weave	Twill Dutch single weave
Mesh	20 x 250
Wire Diameters	0.010" and 0.0082"
Openings	84 micron
Void Fraction	0.65 (estimated)
Manufacturer	Newark Wire Cloth Company Newark, New Jersey

The ten sheets of screen wicking were stacked and firmly compressed as shown in Figure G. 2. The wick was tightly sealed by rubber gasketing around its periphery, both front and back.

The two-phase fluid flow was sprayed at one face of the wick from a double row of nozzles. A manifold cavity was provided for withdrawal of the liquid from the wick. Glass face-plates permit observation of the inlet spray, the liquid withdrawal cavity, and the vapor withdrawal cavity.

The separator model was assembled into a circulation loop shown schematically in Figure G. 6. The model, flow meters, and flow control valves were mounted on a test panel as shown in Figures G. 7 and G. 8. The boiler consists of a coil of copper tubing immersed in a constant temperature water bath. The liquid and vapor flows from the separator are cooled or condensed in similar copper coils immersed in a water-cooled temperature bath.

Prior to filling the apparatus with liquid it was evacuated with a mechanical vacuum pump to remove virtually all the air. The loop was then back-filled with Freon 113. The initial Freon charge was circulated for a time (approximately 2 hrs) to thoroughly clean the tubing, valves, pumps, and model. The loop was then re-evacuated and filled with an initial charge of 500 ml of dimethyl ether of tetra-ethylene glycol and 500 ml of Freon 113.

Circulation was started and the boiler temperature bath then turned on. As the bath temperature increased and more vapor was generated constant re-adjustment was required to maintain and balance the flows. Approximately an hour of operation

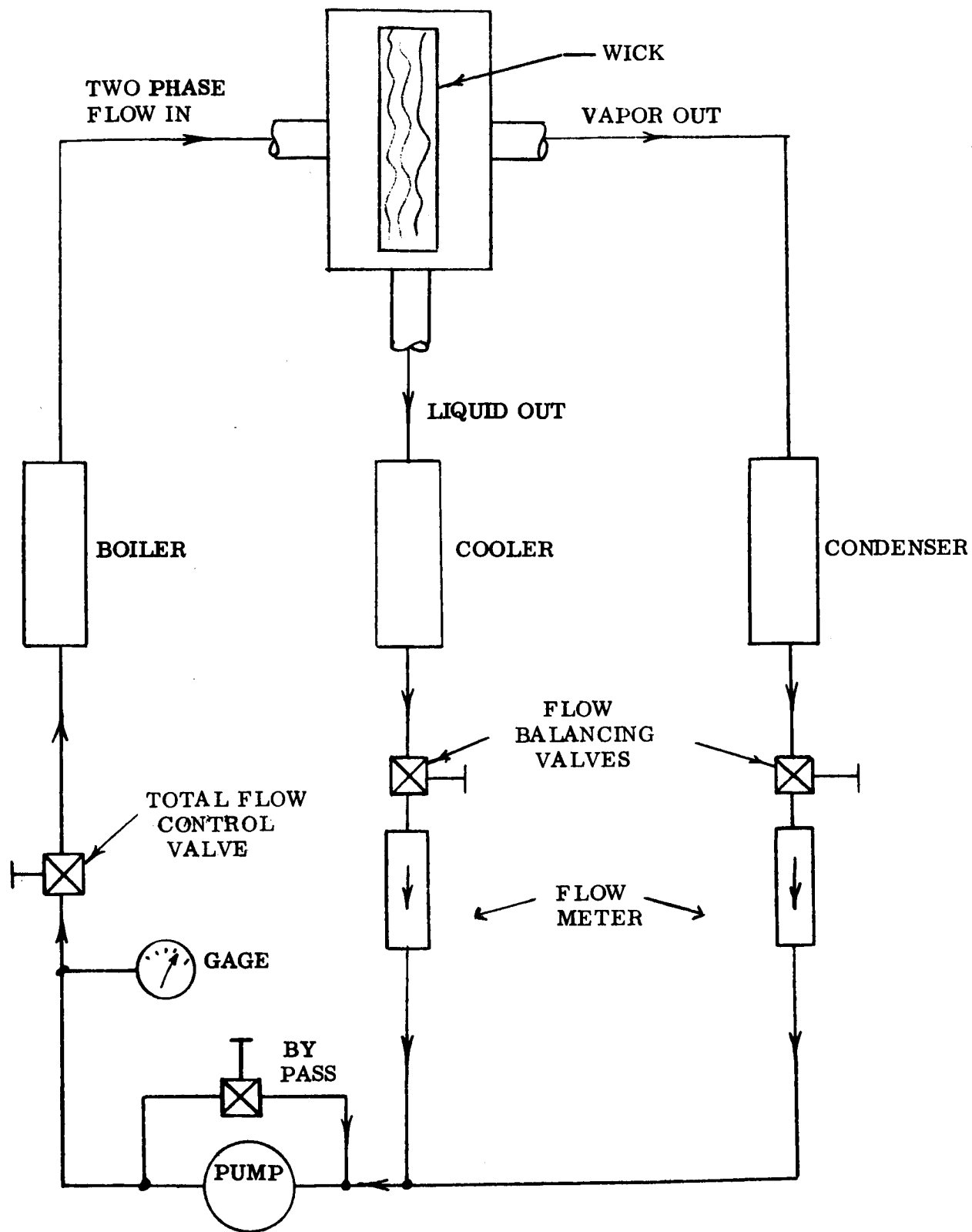


Fig. G. 6 Wick Separator Test Apparatus

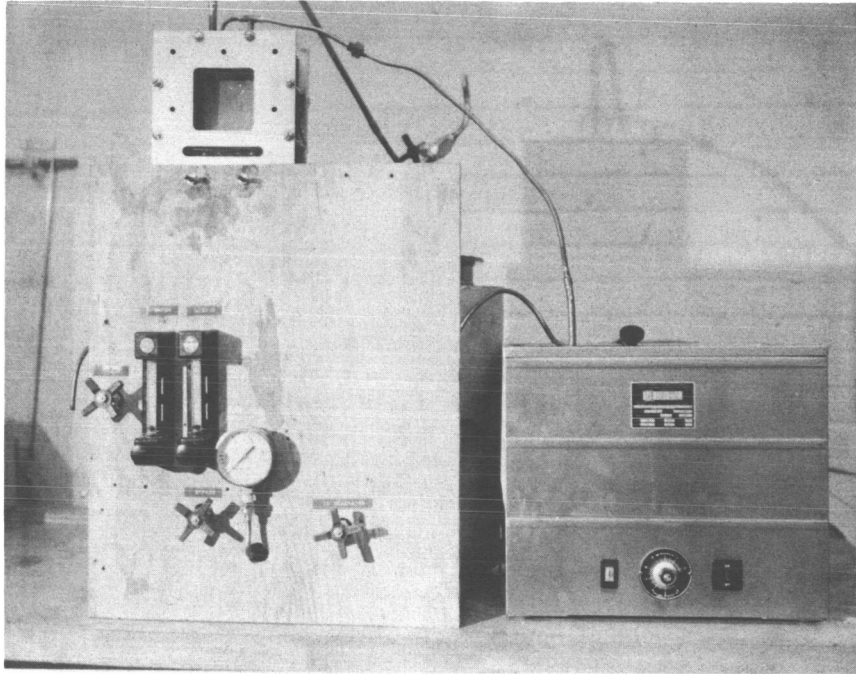


Fig. G.7 Experiment Apparatus (Front View)

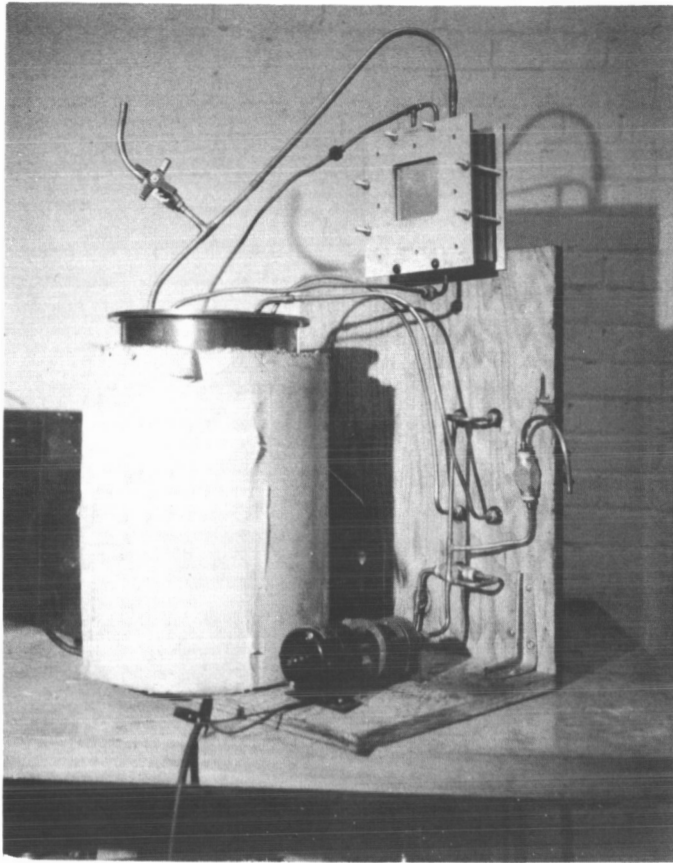


Fig. G. 8. Experiment Apparatus - Rear View

(continuously adjusting the flows) was required to establish a stable, balanced flow situation. Stability was assumed when no control adjustments were required in a one-hour period. From this time on no control adjustments were made for the duration of the test and data was recorded starting retro-actively from the beginning of the one-hour flow stability test period.

Failure of the model was to be determined visually. Plugging of the wick would appear as a decrease in liquid flow rate followed by a flooding of the model as the liquid accumulated. Vapor pull-through would appear as a draining of the liquid manifold cavity. Liquid entrainment would be seen as liquid on the sight glass or as accumulation of liquid in the bottom of the vapor cavity.

The results of two series of tests are shown in Figure G.9. Other than the drop in liquid flow rate early in Run #2-25 the flow rates were absolutely constant. The test was terminated after 17 hours due to a dangerously over-heated pump motor. Run #3-1 shows a similarly constant flow rate through the 40 th hour. At hour 42 the front sight glass cracked. The slow leakage of Freon gradually deteriorated the operation and the test was terminated after 45 hours as shown. In spite of the problems encountered requiring early termination of the tests the results obtained following complete degassing of the system are in agreement with the results reported by Langston⁽¹¹⁾.

G.3 Failure Analysis

Langston, et al⁽¹¹⁾, reported, in their "Vapor Chamber Fin Studies," an extensive evaluation of the properties and performance of wicking materials. The three characteristics they have used to describe and compare the various wick materials are:

- a. Permeability -- pressure drop as a function of flow rate.
- b. Capillary Rise-- equilibrium rise height.
- c. Burnout -- maximum nucleate boiling heat flux.

The first two of these characteristics are of importance for the liquid/vapor separator.

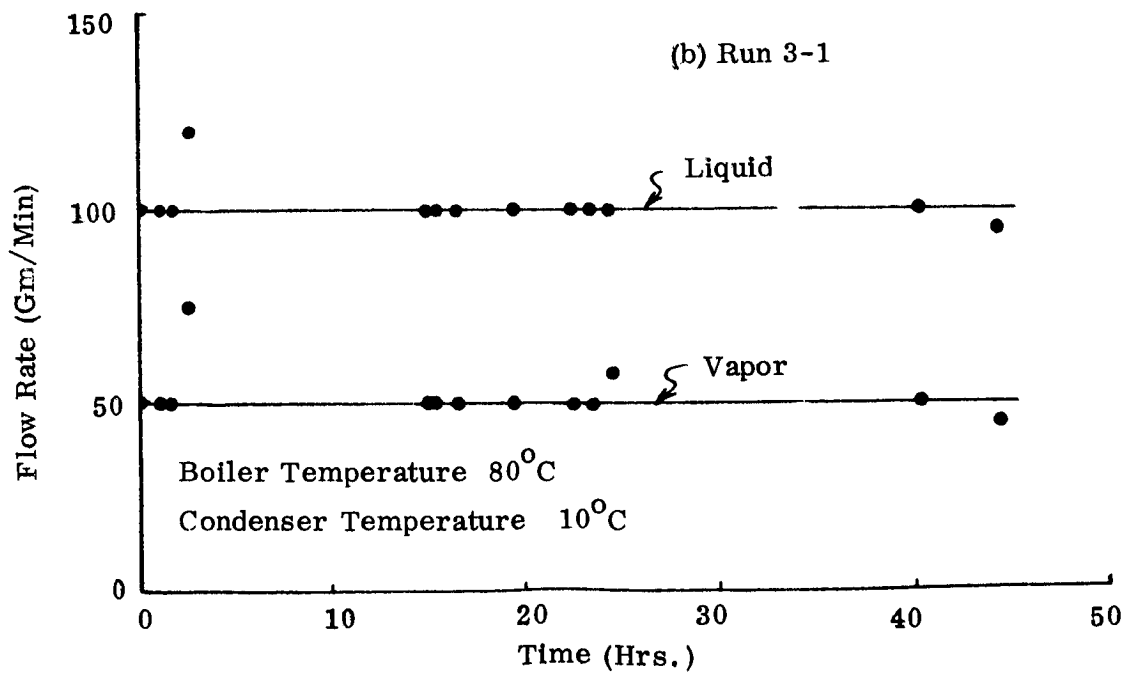
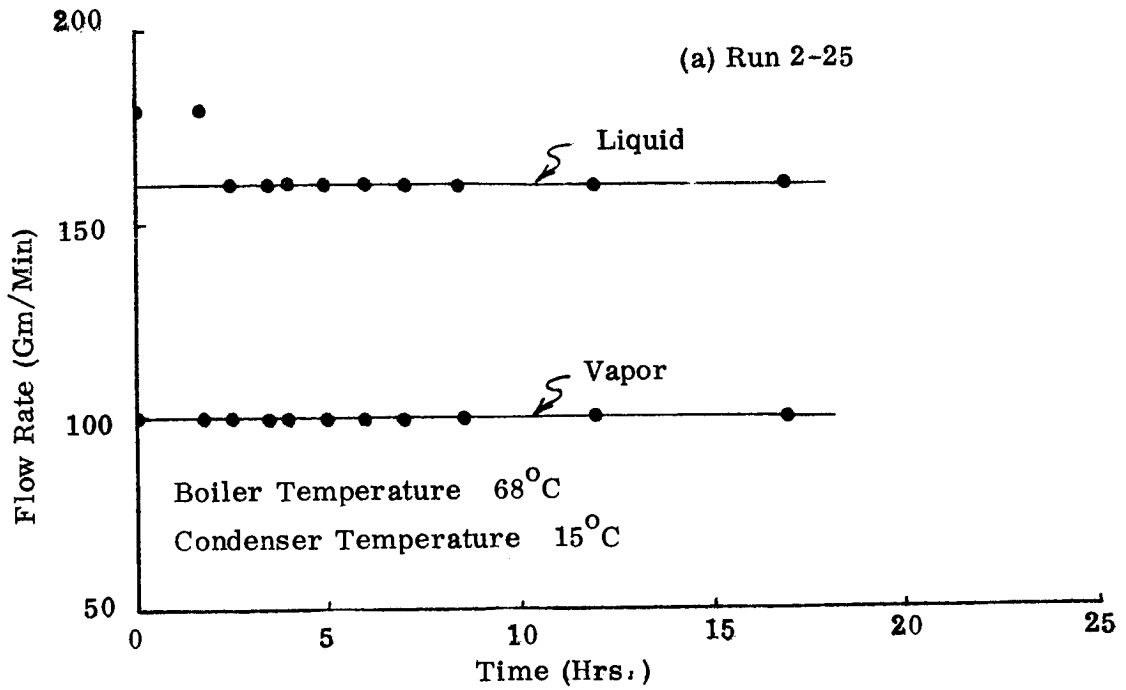


Fig. G.9 Wick Separator Test Results

From Langston⁽¹¹⁾ the pressure drop (ΔP) for flow through a wick of length h is given by:

$$\Delta P = K \mu u h \quad (G. 1)$$

where K is an empirically determined friction factor for the particular wick, μ is the fluid viscosity, and u is the average fluid velocity. The velocity (u) is determined by the equation:

$$u = \frac{\dot{m}}{\rho A F_{AR}} = \frac{\dot{m}}{\rho A [1 - (1 - \epsilon)^{2/3}]} \quad (G. 2)$$

where \dot{m} is the mass flow rate, ρ is the density of the fluid, A is the total cross-section of the wick, F_{AR} is the "flow area ratio", and ϵ is the void volume fraction.

The wick separator, shown schematically in Fig. G.1, has two modes of failure (assuming steady state operation).

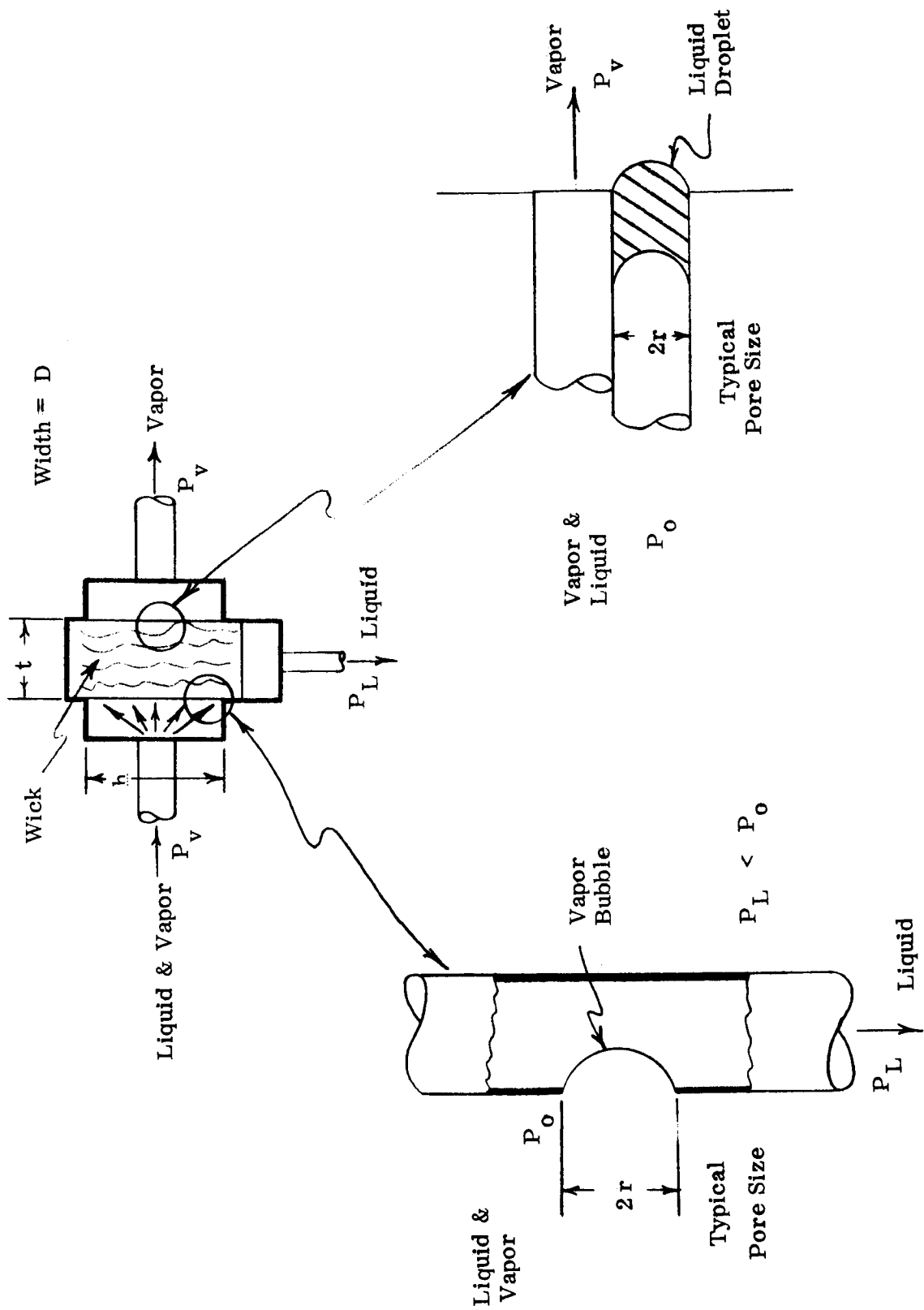
- a. Vapor can be drawn into the liquid withdrawal line.
- b. Liquid can be entrained in the vapor flow.

Vapor pull-through will occur when the pressure drop required to withdraw the liquid from the wick is greater than the pressure difference that can be supported by surface tension for the particular pore diameter of the wick. This situation is illustrated in Figure G. 10 (a). Assume that the liquid droplets are uniformly dispersed in the two-phase flow entering the separator and that the flow is evenly distributed over the face of the wick. A linear liquid velocity gradient will occur in the wick increasing toward the liquid withdrawal part. The pressure drop required to withdraw the liquid is given by:

$$\Delta P = \frac{1}{2} \frac{K \mu \dot{m}_L h}{\rho A [1 - (1 - \epsilon)^{2/3}]} \quad (G. 3)$$

where \dot{m}_L is the liquid mass flow rate, and the pressure difference that can be supported by surface tension is given by the equation:

$$\Delta P = \frac{2\sigma}{r} \quad (G. 4)$$



(b) Liquid Entrainment Model

(a) Vapor Pull-Through Model

Fig. G.10. Failure Modes

where σ is the surface tension of the liquid and r is the typical pore radius. Combining (G. 3) and (G. 4) results in the design limiting relation:

$$\frac{\dot{m}_L h}{Dt} \leq \frac{4 \sigma \rho_L [1 - (1 - \epsilon)^{2/3}]}{K \mu_L r} \quad (\text{G. 5})$$

Similarly liquid entrainment will occur if the pressure drop from the two-phase inlet to the vapor outlet is greater than can be supported by the surface tension of a droplet in a pore of the wick. The limiting relation for liquid entrainment is:

$$\frac{\dot{m}_V t}{Dh} \leq \frac{2 \sigma \rho_V [1 - (1 - \epsilon)^{2/3}]}{K \mu_V r} \quad (\text{G. 6})$$

For a separator fabricated from the stainless steel screen described above and operated using Freon-22 and dimethyl ether of tetraethylene glycol the parameters and properties are:

$$\begin{aligned} \sigma &= 35 \text{ dyne/cm} \\ \rho_L &= 60 \text{ lb/ft}^3 \\ \rho_V &= 2 \text{ lb/ft}^3 \\ \mu_L &= 1 \text{ centipoise} \\ \mu_V &= 0.013 \text{ centipoise} \\ K &\approx 12 \times 10^9 \text{ ft}^{-2} \\ \epsilon &\approx 0.65 \\ r &\approx 45 \text{ microns} \end{aligned}$$

The two design conditions (G. 5 and G. 6) become:

$$\begin{aligned} \frac{\dot{m}_L h}{Dt} &\leq 0.0388 \text{ lb/min-in} \\ \frac{\dot{m}_V t}{Dh} &\leq 0.0499 \end{aligned} \quad (\text{G. 7})$$

G.4 Weight Analysis

The separator weight analysis is based on a cylindrical configuration as shown in Figure G.1. The limiting flow relations are derived from Equations (G.5) and (G.6), and are:

$$\frac{\dot{m}_L h}{D't} \leq 0.122 \text{ lb/min-in}$$
$$\frac{\dot{m}_V t}{D'h} \leq 0.154 \text{ lb/min-in} \quad (\text{G.8})$$

The equal sign applies at the limit of breakdown, and therefore in order to operate within a safe limit, flow rates below the limiting ones should be used. Assuming a safe flow rate to be 80% that of the limiting one, the above relations may be rewritten as:

and

$$\frac{\dot{m}_L h}{D't} = 0.1$$
$$\frac{\dot{m}_V t}{D'h} = 0.12 \quad (\text{G.8'})$$

By combining these two equations in order to eliminate D, one obtains

$$\frac{h}{t} = \frac{\dot{m}_V}{1.2 \dot{m}_L}^{1/2} \quad (\text{G.9a})$$

Eliminating (h/t), one gets:

$$D' = \frac{\dot{m}_L \dot{m}_V}{0.012}^{1/2} \quad (\text{G.9b})$$

The above two equations therefore define the required diameter and height-to-thickness ratio for a given combination of flow rates.

Assuming an average density of the wick of 0.15 lb/in³ based on the dimensions D', h and t, and assuming an extra 20% for the hardware, the wick weights may be calculated. The wick weight, W, is given by

$$\begin{aligned}
 W &= 0.565 D'th \\
 &= 0.565 (\dot{m}_L \dot{m}_V / 0.012)^{1/2} th \quad (G. 10)
 \end{aligned}$$

For structural purposes, a minimum value of t and h should be set. These may be assumed to be

$$\begin{aligned}
 h_{\min} &= 1 \text{ inch} \\
 t_{\min} &= 0.25 \text{ inch} \quad (G. 11)
 \end{aligned}$$

The wick weights may now be calculated for various \dot{m}_L 's and \dot{m}_V 's, provided that the values of h and t used are consistent with equations (G. 9a) and (G. 11). Within the flow rates of interest (\dot{m}_V and \dot{m}_L between 0.5 and 10 lbs/min), the critical limitation is that on h . Substituting for $h = 1''$ and equating (G. 9a) in equation (G. 10), separator weight is found to be independent of the vapor flow rate and is given by:

$$\begin{aligned}
 W &= 5.65 \dot{m}_L h_{\min}^2 \\
 &= 5.65 \dot{m}_L \quad (G. 12)
 \end{aligned}$$

These weights are shown plotted on Figure G. 11.

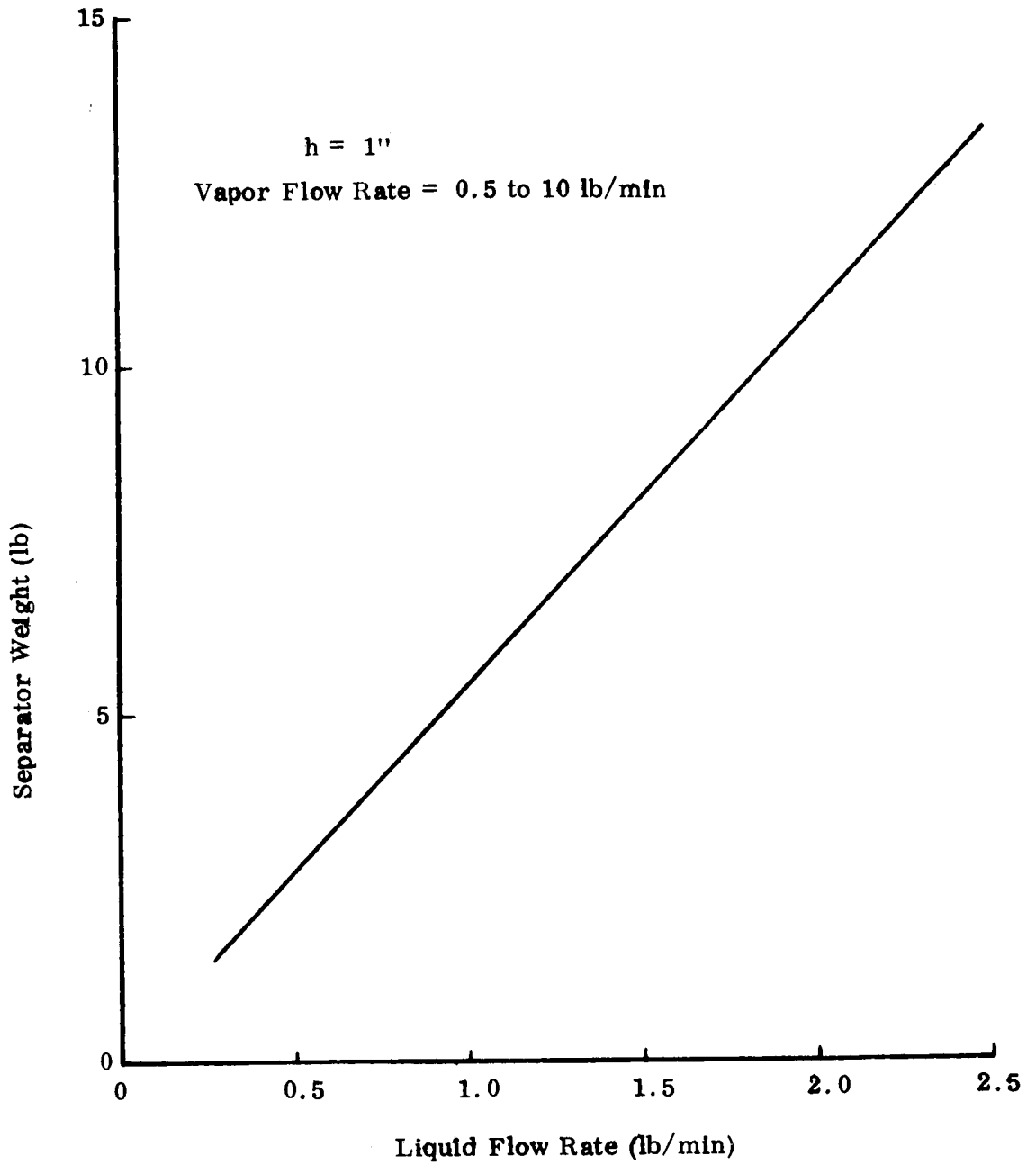


Fig. G.11. Wick Separator Weight